



Norwegian University of  
Science and Technology

# Process Modeling of a Biorefinery for Integrated Production of Ethanol and Furfural in HYSYS

**Lars Moen Strømsnes**

Chemical Engineering and Biotechnology

Submission date: June 2016

Supervisor: Størker Moe, IKP

Co-supervisor: Magne Hillestad, IKP

Norwegian University of Science and Technology  
Department of Chemical Engineering



# Preface

This thesis is written as part of the Master's of Science in Chemical Engineering at the Norwegian University of Science and Technology (NTNU). The work presented here was carried out during the period from January 2016 to June 2016 at the Department of Chemical Engineering.

I would like to thank my main supervisor Associate Professor **Størker Moe** for providing an interesting and challenging topic for my thesis. His guidance and insight has been of great value for the progress towards the work presented here.

I would also like to thank my co-supervisor Professor **Magne Hillestad** for his technical assistance and support on modeling and simulation.

## Declaration of Compliance

I hereby declare that this thesis is an independent work according to the exam regulations of the Norwegian University of Science and Technology (NTNU).

Lars Moen Strømsnes

Trondheim, June 10, 2016.



# Abstract

Existing bioethanol production relies heavily on the use of corn and sugarcane as feedstocks. A prerequisite for increased consumption of bioethanol is the transition from the current use of corn and sugarcane to lignocellulosic biomass. This includes the use of wood, straws and agricultural residue such as sugarcane bagasse and corn stover, which do not compete directly with food production. Cellulosic ethanol also offers increased reduction in greenhouse gas emissions over both current bioethanol and petroleum based fuels.

A biorefinery utilizing corn stover as feedstock has been designed and implemented in HYSYS. The model is based on the process for biochemical conversion of lignocellulosic biomass to ethanol designed by the U.S. National Renewable Energy Laboratory (NREL). The Marcotullio process for the production of furfural from aqueous xylose is integrated by selectively fractionating the feedstock into hemicellulose and cellulose. The model also includes a steam boiler cycle for co-generation of heat and electricity from residual solid material, and the biorefinery is found to be energy self-sufficient.

The performance of the biorefinery is comparable to the NREL and Marcotullio processes. The combined conversion of useful carbohydrates into ethanol and furfural is found to be 81.1%, which corresponds to 47% of the total energy content in the corn stover feedstock. The heating demand is slightly increased compared to the NREL process, and generation of electricity is reduced.



# Sammendrag

Eksisterende produksjon av bioetanol er i stor grad basert på bruk av mais og sukkerrør som råstoff. En forutsetning for fortsatt økt bruk av bioetanol er å gå over til bruk av lignocellulose som råmaterial til fordel for dagens bruk av mais og sukkerrør. Dette inkluderer for eksempel bruk av tre og avfall fra skogsvirksomhet, ulike typer gress og strå og landbruksavfall, som ikke konkurrerer direkte med matproduksjon. Spesielt avfall fra mais- og sukkerproduksjon er foreslått som aktuelle råstoff. Hovedfordelen med bioetanol laget fra slike råstoff er redusert utslipp av drivhusgasser sammenlignet både med eksisterende produksjon av bioetanol og petroleumsbaserte drivstoff spesielt.

Et bioraffineri med avfall fra maisproduksjon som råstoff er blitt utviklet og modellert i HYSYS. Modellen er basert på en prosess for biokjemisk prosessering av lignocellulose til bioetanol, utviklet og publisert av U.S. National Renewable Energy Laboratory (NREL). Produksjon av furfural fra xylose basert på en prosess utviklet og patentert av Marcotullio er inkludert ved hjelp av selektiv fraksjonering av råstoffet til hemicellulose og cellulose. Modellen inkluderer også et eget anlegg for kraftvarmeproduksjon ved forbrenning av uutnyttede rester av råstoffet.

Modellen viser tilsvarende ytelse sammenlignet med prosessene foreslått av NREL og Marcotullio. Den kombinerte omgjøringen av nyttige karbohydrater i råstoffet til enten etanol eller furfural er 81.1%, som tilsvarer 47% av energiinnholdet i råstoffet. Bioraffineriet har et noe høyere varmebehov sammenlignet med prosessen foreslått av NREL, noe som reduserer den totale produksjonen av elektrisitet.





# Table of Contents

1. Introduction .....	1
1.1 Motivation .....	1
1.2 Objectives .....	2
1.3 Structure.....	2
2. Theory .....	5
2.1 Lignocellulosic Material.....	5
2.2 Lignocellulosic Biorefinery .....	6
2.3 Processing of Lignocellulosic Material .....	8
2.3.1 Pretreatment .....	8
2.3.2 Acid Hydrolysis of Lignocellulose .....	9
2.3.3 Enzymatic Hydrolysis of Cellulose.....	11
2.3.4 Fermentation.....	12
2.3.5 Washing.....	12
3. Current Technology.....	15
3.1 Corn Stover.....	15
3.2 Ethanol Production .....	16
3.3 Furfural Production.....	17
3.4 Proposed Integrated Furfural and Ethanol Production .....	18
3.4.1 Marcotullio Process.....	19
4. Process Basis .....	21
4.1 Process description .....	21
4.1.1 Pretreatment and Conditioning.....	21
4.1.2 Enzymatic Hydrolysis and Fermentation .....	22
4.1.3 Ethanol Recovery .....	22
4.1.4 Furfural Production and Recovery .....	22

4.1.5	Wastewater Treatment and Steam Boiler.....	22
4.2	Design Basis .....	23
4.3	Report Conventions .....	24
5.	HYSYS Setup.....	25
5.1	Component List .....	25
5.1.1	Hypotheticals.....	25
5.1.2	Modeling of Corn Stover.....	26
5.2	Reaction Sets .....	27
5.3	Choosing Property Package.....	28
5.4	Estimating Binary Coefficients .....	29
6.	HYSYS Process Implementation .....	33
6.1	Area 100: Pretreatment and Conditioning.....	33
6.2	Area 200: Enzymatic Hydrolysis and Fermentation.....	38
6.3	Area 300: Ethanol Recovery.....	41
6.4	Area 400: Furfural Production and Recovery.....	44
6.5	Area 500: Wastewater Treatment and Steam Boiler .....	48
7.	Heat Integration.....	53
7.1	Alternative Heat Integration .....	55
8.	Analysis and Discussion.....	57
8.1	Carbon and Energy Balance .....	57
8.2	Ethanol Recovery Performance .....	59
8.3	Furfural Production and Recovery Performance .....	59
8.4	Heat Recovery and Electricity Production .....	63
8.5	Process Optimization .....	65
8.5.1	Area 400 Column Integration.....	65
8.5.2	COL-401 Vapour Draw Composition .....	67
8.5.3	COL-300 Vapour Draw Composition .....	68

8.5.4	Steam Boiler Cycle Pressure .....	68
8.6	Market Considerations.....	69
9.	Conclusion.....	73
	References .....	75



# List of Figures

- 2.1** Schematic representation of the physical structure of lignocellulosic material in its natural form (left) and the goal of pretreatment (right). Cellulose (black); Hemicellulose (green); Lignin (pink). Adapted from [15].
- 2.2** Schematic overview of possible reactions during acid hydrolysis of lignocellulose.
- 2.3** Simple kinetic model of acid catalyzed hydrolysis of sugar polymers to monomers and decomposition products.
- 2.4** Kinetic model of hydrolysis of cellulose to glucose, which degrades into 5-HMF.
- 2.5** Schematic representation of a single washing stage.  $V$  is the wash filtrate,  $L$  is the slurry containing solid material, and  $x$  and  $y$  is the concentration of dissolved matter in wash filtrate and liquid slurry respectively. Adapted from [21].
- 2.6** Washing yield for a single stage washing unit, as a function of liquid weight ratio and efficiency, taken from [21].
- 3.1** U.S. Corn Consumption, 2015 [26].
- 3.2** Global fuel ethanol production by country/region and year [29].
- 3.3** Block diagram of the NREL ethanol process.
- 3.4** Schematic of a modern Chinese furfural plant, taken from [4].
- 3.5** Simplified process flow diagram of the Marcotullio process with a production rate of 2.8 ton/h 95 wt% furfural [4].
- 4.1** Block diagram of a process for integrated production of furfural with ethanol.
- 5.1** XY plot of the binary mixture of furfural and water at 1.0 atm. Composition is given in wt%.
- 5.2** T-XY plot of the binary mixture of furfural and water at 1.0 atm. Composition is given in wt%.
- 5.3** XY plot of the binary mixture of ethanol and water at 1.0 atm. Composition is given in wt%.
- 5.4** LLE plot of the tertiary mixture of water, furfural and acetic acid at 1.0 atm and 20.0 C. Composition is given in wt%.

- 6.1** Process flow diagram of the first part of pretreatment.
- 6.2** Process flow diagram of the second part of pretreatment.
- 6.3** Process flow diagram of the enzymatic hydrolysis and fermentation.
- 6.4** Process flow diagram of the ethanol recovery process.
- 6.5** Process flow diagram of the furfural production process.
- 6.6** Process flow diagram of the furfural recovery process.
- 6.7** Process flow diagram of the steam boiler process.
  
- 8.1** Total flow of furfural in vapour and liquid phase as a function of column tray number.
- 8.2** Installed reboiler heat exchanger area and compressor duty as a function of outlet pressure in the compressor [COMP-400]. Purchase cost of reboiler and compressor is included. The vertical line indicates the design pressure.
- 8.3** Installed reboiler heat exchanger area and compressor duty as a function of outlet pressure in the compressor [COMP-401]. Purchase cost of reboiler and compressor is included. The vertical line indicates the design pressure.
- 8.4** Column recycle inlet, reboiler heat deficit and overall plant electricity surplus as a function of varying composition in the column vapour draw. The vertical line indicates the design composition.
- 8.5** Reboiler duty in beer column and rectification column as a function of varying composition in the beer column vapour draw. The vertical line indicates the design composition.
- 8.6** Produced electricity in the two steam turbines in the steam boiler cycle as a function of the cycle pressure in the boiler.
- 8.7** Ethanol and furfural production rate as a function of pretreatment washing yield.

# List of Tables

- 4.1** Corn stover feedstock composition on dry-weight basis.
- 5.1** Overview of all hypothetical components used, and information about basic properties.
- 5.2** Overview of kinetic parameters used in the acid catalyzed formation and decomposition of glucose and xylose [17,37].
- 6.1** Pretreatment reactor operating conditions.
- 6.2** Oligomer conversion tank operating conditions.
- 6.3** Reaction conversion after pretreatment- and oligomer conversion reactor.
- 6.4** Enzymatic hydrolysis operating conditions.
- 6.5** Seed train reactions and assumed conversions.
- 6.6** Batch fermentation reactions and assumed conversions.
- 6.7** Design specifications and operating conditions of ethanol distillation columns.
- 6.8** Design specifications and operating conditions of furfural distillation columns.
- 7.1** Heating requirements for the plant. Start and end temperatures for the stream to be heated are given. These are set equal for the reboilers.
- 7.2** Cooling requirements for the plant. Start and end temperatures for the stream to be cooled are given. These are set equal for the condenser.
- 8.1** Overall Carbon Mole Balance.
- 8.2** Lower heating value (LHV) of corn stover feedstock and products. Excess electricity is also included.
- 8.3** Comparison of data for ethanol recovery. The data is given as specific values relative to the given ethanol production rate, for easy comparison. Data for comparison is taken from [23].
- 8.4** Comparison of main performance data for production and recovery of furfural. The data are given as specific values relative to the given furfural production rate, for easy comparison. The COL-401 Recycle Factor described the ratio of the recycle stream into the azeotropic distillation column relative to the main feed into the same column. Data for comparison are taken from [4].

**8.5** Steam boiler cycle performance data, and data from the NREL ethanol plant for comparison [23]. The amount of wastewater, and the produced methane from anaerobic digestion, is also included. These are given as absolute values, while the rest are given as specific values relative to the boiler duty.

**8.6** Overall electricity production and consumption for the plant.

**8.7** Overview of main feedstock costs and products revenue [27, 31, 35, 44].



# 1. Introduction

## 1.1 Motivation

The current environmental situation, with accelerating global warming caused by increasing CO<sub>2</sub>-emissions, is considered one of the largest challenges of the world today. A change from today's excessive use of non-renewable resources such as oil and gas, to an economy including higher utilization of renewable resources is considered an important part of the solution. Lignocellulosic biomass can be utilized both for biofuels, such as bioethanol, bioenergy and biobased chemicals [1]. Today, first generation feedstocks such as sugarcane or corn are utilized to some extent, mainly in the production of ethanol. Lignocellulosic biomass such as wood, designated energy crops and agriculture residue is considered a better option for producing fuel ethanol, as it do not compete with food production. The potential reduction in greenhouse gases is also larger for second generation biofuels such as cellulosic ethanol. Estimates show that fueling vehicles with cellulosic ethanol reduces emissions with up to 95% compared to conventional fuels [2]. Introduction of cellulosic ethanol is therefore considered a prerequisite for increasing use of bioethanol.

The current production of cellulosic ethanol is mainly at a research or pilot scale. A few industrial-scale plants also exist, but it has proven hard to compete with the existing corn milling and sugarcane industry. The major obstacle is the increased cost of obtaining fermentable sugars from lignocellulosic material, compared with either starch from corn or raw sugar from sugarcane.

A possible solution is to achieve a better utilization of the lignocellulosic feedstock. Agricultural residue such as sugarcane bagasse and corn stover contains considerable amounts of xylose. In current cellulosic ethanol plants, xylose is fermented along with glucose to produce ethanol. Xylose however is suitable for making other value adding chemicals, which could give such plants the necessary economical advantage. One of these chemicals is furfural, which is proposed as a future renewable platform chemical for production of biofuels and biochemical. Current production of furfural is based on relatively old and inefficient technology. High cost of production combined with poor yields have reduced its competitiveness with petroleum based products.

Several studies have indicated that an integrated production of furfural in biorefineries could both reduce energy consumption and increase production yields [3]. Integrated production of furfural with cellulosic ethanol may therefore improve process economy for both processes.

## 1.2 Objectives

The main objective for this thesis is to implement a working model of an integrated process for furfural and ethanol in the process simulation software HYSYS. The model is based on the process for biochemical conversion of lignocellulosic biomass to ethanol, proposed by the U.S. National Renewable Energy Laboratory (NREL). The implementation of the integrated furfural production is based on the innovative process proposed by Marcotullio. [4]

The following subjects are investigated in this thesis:

1. Modeling of the corn stover feedstock as a solid material in HYSYS, including the creation of necessary hypothetical components.
2. Implementation of kinetic reactions for the feedstock pretreatment and the furfural production.
3. Investigate the use of residual solid material for co-generation of heat and electricity, and if the plant is self-sufficient in energy.
4. Compare the plant performance to NREL and Marcotullio, with emphasis on changes in heating demand.

## 1.3 Structure

The thesis consists of nine chapters including this introduction.

### *Chapter 2 Theory*

Contains an introduction to lignocellulosic materials, biorefineries and processes that are important for lignocellulosic material.

### *Chapter 3 Current Technology*

Overview of current processes for production of fuel ethanol and furfural. Also discussed processes for integrated production of furfural.

### *Chapter 4 Process Basis*

Introduction and outline of the process studied in this work, including the various process areas. Also defines the design basis for the process.

### *Chapter 5 HYSYS Setup*

Description of the HYSYS setup, including component list and reaction sets. Discussion of property package and estimation of binary coefficients.

### *Chapter 6 HYSYS Process Implementation*

Thorough description of each process area, and how they are implemented in HYSYS.

### *Chapter 7 Heat Integration*

Discussion of the process heat integration, and opportunities for further integration. Overview of heating and cooling demand is included.

### *Chapter 8 Analysis and Discussion*

Analysis of the plant performance, including comparison of performance of specific plant areas compared to the NREL and Marcotullio designs. Some important design parameters are also discussed.

### *Chapter 9 Conclusion*

Summary of the process performance and energy requirements, and recommendations for further work on the developed model.



## 2. Theory

### 2.1 Lignocellulosic Material

Lignocellulosic material is a generic classification of biomass derived from both non-woody and woody plants. The definition of the term is somewhat unclear, but strictly speaking, it is a mixture of cellulose, hemicellulose and lignin, which together constitutes the largest fraction of all plant cell walls [5]. Some definitions also include plant oils, protein and ash, which are the main non-cell wall constituents [6, 7]. The variety of macroscopic appearance and structure of lignocellulosic materials is extensive, and although the chemical composition also varies, some trends are observed. In general, the largest polymeric fraction is cellulose, in the range of 35-55%. The next largest fraction is hemicellulose, in the range of 20-35%, and then follows lignin, with about 15-30%.

Cellulose is a polysaccharide made up of D-glucopyranose units, linked together by  $\beta$ -(1-4)-glucosidic bonds, the smallest repeating unit being cellubiose [8]. It is a strictly linear molecule with a high average degree of polymerization, up to 10,000 and above for some species. Cellulose chains are able to form both intra- and inter-molecular hydrogen bonds, and easily forms aggregates (microfibrils), which is the smallest structural component in cellulose fibers [9]. Cellulose fibers consist of regions of varying crystallinity. For most species, the degree of crystallinity is 50% or more, rendering it insoluble in most solvents [10].

Hemicellulose is a group of polysaccharides made up of different sugar units, such as D-glucopyranose, D-xylopyranose, D-galactopyranose, L-arabinofuranose, D-mannopyranose and minor amounts of other sugars [8]. The *DP* of hemicelluloses are much smaller than for cellulose, with an average of about 100-200. Most hemicellulose polymers usually consist of a combination of different sugar types, and are often named by the sugar content, for example arabinogalactan, glucomannan or galactoglucomannan. Because of its branched structure, its physical structure is purely amorphous. This makes it more soluble than cellulose, and generally reacts faster.

Lignin is a group of highly amorphous, highly complex, and mainly aromatic polymers. Lignins are polymerized from three different monomers, often referred to as monolignols. These are *p*-coumaryl alcohol, conifer alcohol and sinapyl alcohol. The tree monomers are bound together via C-C and C-O-C linkages, forming a three dimensional structure, or *web* [8]. It also forms bonds with hemicellulose chains. The interaction between hemicellulose and

cellulose, together with the crystalline nature of cellulose makes lignocellulosics a type of natural composite material. The composite structure gives all plant material a natural resistance to pest, diseases and chemical modification, known as *recalcitrance* [11].

All biomass also contain varying amounts of extractives and ash. Extractives is a group of low molecular mass compounds that can be extracted by either polar or non-polar solvents. Such compounds are often a combination of fats, fatty alcohols, fatty acids and esters. The extractives- and ash content varies not only between different species, but are also affected by location, time of harvesting and age.

## 2.2 Lignocellulosic Biorefinery

The research on utilizing renewable resources for the production of non-food products has gained increased attention since the early 1990s. This has led to the development of new integrated processes, biomass conversion technology and biorefinery technology [1].

Alongside this development, the term “biorefinery” was established during the 90s. Today, the U.S. Department of Energy (DOE) defines a biorefinery as “...and overall concept of a processing plant where biomass feedstocks are converted and extracted into a spectrum of valuable products”. Similarly, the American National Renewable Energy Laboratory (NREL) has published the following definition: “A biorefinery is a facility that integrates biomass conversion processes and equipment to produce fuels, power, and chemicals from biomass” [1]. An important aspect in this regard is the adaptability of the plant with respect to production technology and products. A biorefinery must be able to use a mix of biomass feedstocks to produce a variety of products, using several different processing technologies. Such a biorefinery is often recognized as a phase III-biorefinery.

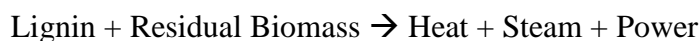
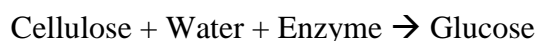
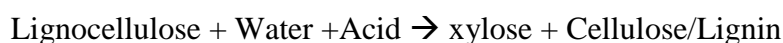
A phase I-biorefinery uses only one feedstock to produce a fixed amount of a specific product and co-products. An example of this is the dry-milling of grain to produce ethanol and feed. A phase II-biorefinery also uses one feedstock, but has the ability to produce a variety of valuable products, based on market demand. An example of this is the wet-milling, which produces starch, corn syrup, ethanol, corn oil, corn gluten and meal [1].

Complex biorefinery systems are often classified into four categories:

- The lignocellulosic feedstock (LCF) biorefinery, which uses nature-dry raw materials, such as cellulose containing biomass, waste etc.
- The whole crop biorefinery, which uses raw materials such as cereals or corn.

- The green biorefineries, which uses nature-wet biomasses such as grass, alfalfa, clover and immature cereals.
- The two platform biorefineries, combining the use of sugar and syngas as platforms for processing.

Of these, the LCF biorefinery technology will most probably be used for large-scale industrial biorefineries [1]. The general idea is to *fractionate* the feedstock into its major constituents, i.e. Cellulose, hemicellulose and lignin. Cellulose, hemicellulose and lignin can then be further processes into fuel, chemicals, materials, heat or power. An approach that has received a lot of attention, and that is partially implemented at a pilot/commercial scale, is the use of chemicals or enzymes to depolymerize the feedstock into fermentable sugars and lignin. Sugars can be fermented into a variety of products, but the main motivation has been the production of fuel ethanol [12]. The basic process is:



Despite extensive research and development, it has proven hard to establish a profitable process with ethanol as the sole product [12]. This may in part be explained by the recalcitrant nature of lignocellulosic material, making it harder to chemically process than feedstocks used in competing processes, for example corn grain. It is also difficult to introduce new technology in a large scale market that is based on well established- and developed technology. A solution that has been considered is using the xylose fraction to produce higher-value chemicals, such as furfural/furfural-derivatives. Competing industry use feedstocks that lack a pentose-fraction, which could make this solution a competitive advantage. The present market of furfural is limited, but it is considered a highly versatile intermediate chemical. It is proposed as one of several *platform-chemicals*, the building blocks of future biorefinery value-chains. There exists several proposed processes for the co-production of furfural, for example the biofine process, which produces furfural and levulinic acid [13]. Several studies indicates that large scale industrial biorefineries producing ethanol and furfural can be economically viable [12, 14].

## 2.3 Processing of Lignocellulosic Material

### 2.3.1 Pretreatment

Pretreatment is the process of altering the physical structure of lignocellulose, as indicated in figure 2.1.

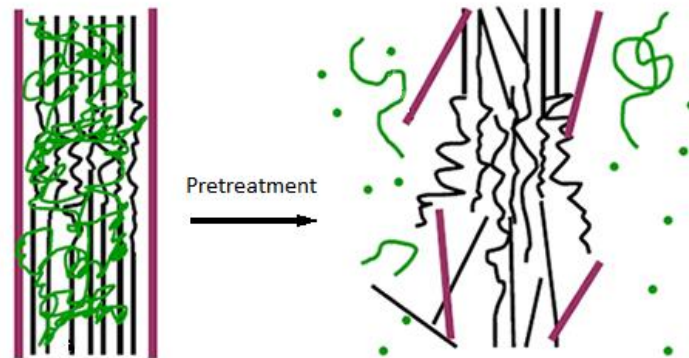


**Figure 2.1:** Schematic representation of the physical structure of lignocellulosic material in its natural form (left) and the goal of pretreatment (right). Cellulose (black); Hemicellulose (green); Lignin (pink). Adapted from [15].

The goal is to break the protecting seal that lignin forms, and to disrupt the crystalline structure of cellulose, making it more accessible for further treatment. Pretreatment can be chemical, physical or a combination of both [16].

Physical pretreatment involves mechanical processing such as chipping, grinding and milling, to reduce both particle/chip size of the raw material, and the crystallinity of cellulose. If done to a high extent, it is often seen as a separate form of treatment. It is often used in combination with other forms of treatment, to help speed up the process. Steam explosion is often considered a physical treatment, as it do not involve any use of chemicals, except water [15]. The raw material is exposed to steam at high pressure and temperature, degrading both hemicellulose and lignin. The pressure is then rapidly decreased, causing high mechanical stress on the material, causing it to break apart. The process can also include the use of acids and alkali, to increase the degradation of lignin and hemicellulose.

Chemical pretreatment often involves the use of reactive chemicals at elevated temperature and pressure. A range of chemicals has been used for this purpose, such as acids, alkali, ozone, strong oxidizers, organic solvents or even specific microorganisms. The mechanisms at which the chemicals alter the raw material structure varies, but the results are similar for all. Lignin and hemicellulose are degraded, while crystalline cellulose is transformed into an

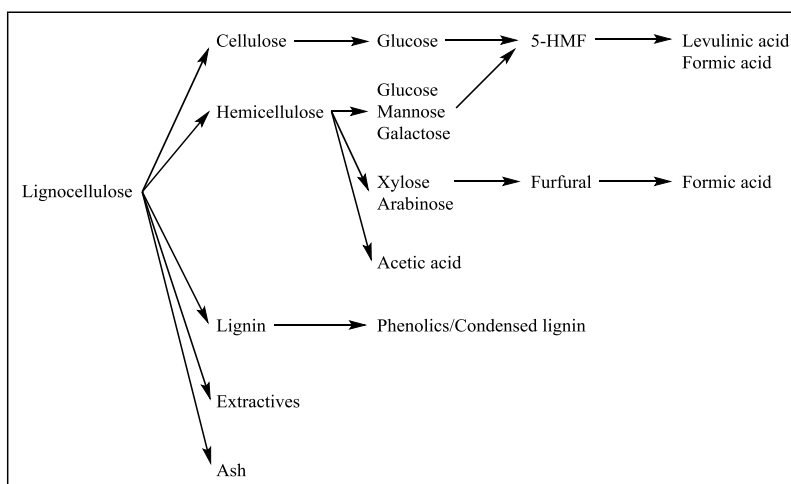


amorphous state. After pretreatment, the raw material structure is more susceptible for further saccharification of cellulose, and what is left of the hemicellulose.

### 2.3.2 Acid Hydrolysis of Lignocellulose

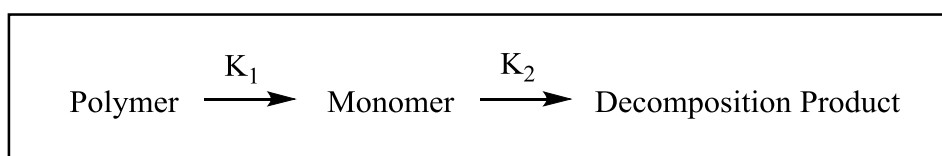
The use of mineral acids such as hydrochloric acid, phosphoric acid and sulfuric acid in particular, is one of the most commonly used methods of hydrolyzing lignocellulosic materials. Sulfuric acid has been used both for pretreatment and as a regular hydrolyzing agent. This is done by using concentrated acid at relatively low temperature (50-150 °C), or by using dilute acid at elevated temperature (150-300 °C). Using concentrated acid as a method for pretreatment or hydrolysis cause a number of difficulties that must be overcome, such as toxicity, corrosion and acid recovery. Dilute sulfuric acid however is easier to handle, and is the preferred choice in industry. Hemicelluloses are easily hydrolysed in dilute acid, while cellulose are more resistant. It has proven hard to get higher yields than 60-70% glucose from cellulose by the use of dilute acid alone [17]. Achieving high yields of glucose also has the effect of degrading hemicellulose monosaccharides into degradation products, such as furfural and 5-Hydroxymethylfurfural (5-HMF). Such compounds are known to have significant inhibitory effects on the fermentation of sugar. An often preferred solution is to use a combination of acid hydrolysis and enzymatic hydrolysis in two stages. The acid hydrolyses the hemicellulose fraction, while at the same time serving as a form of pretreatment for the cellulose fraction. The hemicellulose fraction is solubilized and the cellulose is altered into a more amorphous state, which makes enzymatic hydrolysis in the next stage possible [18].

Figure 2.2 gives an overview of possible reactions during acid hydrolysis of lignocellulose. Cellulose is hydrolysed into glucose, which can further degrade into 5-HMF, which decomposed into levulinic- and formic acid. The hemicelluloses are hydrolysed into their respective monosaccharides. All hemicellulose hexoses will react further in a similar fashion as glucose, while the pentoses react to form furfural, which decomposes into formic acid.



**Figure 2.2:** Schematic overview of possible reactions during acid hydrolysis of lignocellulose.

The study of the formation and decomposition of glucose and xylose has received much attention, and several models have been proposed to describe the kinetics of such reactions. Reactions taking place in acid catalysed hydrolysis of lignocellulose are heterogeneous and complex in nature, and simplifications are often made to describe the system. It is common to describe the process as consecutive (pseudo)homogenous, non-reversible, first-order reactions. The simplest form of this is the model proposed by Saeman (1945), as shown in figure 2.3 [19].



**Figure 2.3:** Simple kinetic model of acid catalyzed hydrolysis of sugar polymers to monomers and decomposition products.

Since it was first proposed, several modifications have been made to adjust for phenomena that later has been observed. For xylan, it is common to distinguish between fast-hydrolysing- and slow-hydrolysing xylan, and for glucan (cellulose), it is common to distinguish between crystalline and amorphous cellulose. It is worth noting that the division of xylan into two fractions is more a question of calculatory convenience, while the division of cellulose is motivated by actual physical differences [20]. A modified version of the cellulose hydrolysis is presented in figure 2.4.

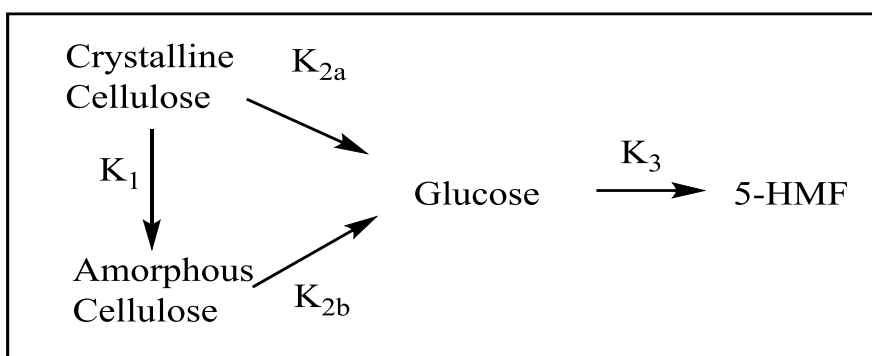


**Figure 2.4:** Kinetic model of hydrolysis of cellulose to glucose, which degrades into 5-HMF.

The direct hydrolysis of crystalline cellulose is slow, while the reaction of amorphous cellulose is rapid. Furthermore, the activation energy of glucose formation is higher than that for glucose degradation [17]. Higher temperature will therefore increase the potential yield of glucose. This is also observed for sugars produced from hemicellulose, especially xylose. It is also worth noting that 5-HMF is unstable under acidic conditions, and will react further into levulinic- and formic acid, as indicated in figure 2.2.

### 2.3.3 Enzymatic Hydrolysis of Cellulose

As mentioned earlier, a solution could be to hydrolyse the cellulose fraction of lignocellulose by enzymes. Cellulose is hydrolysed to glucose by the enzyme complex called *cellulase*, which is excreted by organisms capable of degrading cellulose [18]. The enzyme *complex* consist of two components. Endo- $\beta$ -(1 $\rightarrow$ 4)-glucanase (Cx-cellulase) breaks random bonds in amorphous regions of cellulose molecules, while exo- $\beta$ -(1 $\rightarrow$ 4)-glucanase (cellobiohydrolase) removes cellobiose units from the non-reducing ends of cellulose molecules. To get a complete conversion of cellulose into glucose, a *cellobiase* [ $\beta$ -(1 $\rightarrow$ 4)-glucosidase] must be present [18].

Industrial cellulases normally contain sufficient levels of cellobiase. Enzymatic hydrolysis of hemicelluloses are also possible, but is more complex. Complete utilization of hemicellulose requires a blend of several different hydrolytic enzymes. Commercial cellulases often contain hemicellulase activities, especially for the use on corn stover, where yield approaching 80% are achieved [18]. However, the preferred industrial solution for most lignocellulosic material is to use dilute acid for hemicellulose hydrolysis, and cellulase enzyme for cellulose hydrolysis.

#### 2.3.4 Fermentation

Hydrolysis of lignocellulosic material yields an aqueous mixture of sugars, including glucose, xylose, mannose, arabinose and galactose. The yeast used for industrial production of ethanol, *Saccharomyces Cerevisiae*, is only able to metabolize glucose under anaerobic conditions. Therefore, a lot of work has been done to develop microorganisms capable of metabolizing other sugars in a mixture with glucose. The fermentation reactions are given in equation 2.1 and 2.2.



NREL have studied the use of *Zymomonas mobilis*, as it effectively converts glucose into ethanol with superior ethanol tolerance. Recombinant, integrated strains have been made, able to consume a mixture of glucose, xylose and arabinose, the three largest sugar constituents of corn stover. While all sugars are nearly fully consumed, there is a preferred order of consumption; glucose, then xylose and arabinose last. This represents a challenge for processes where a mixture of different sugars are present, and makes for an reduction of overall utilization of the carbon present in the feedstock.

#### 2.3.5 Washing

Washing is the process of separating liquids containing dissolved matter or chemicals from solids. Washing is an important unit operation in all pulp manufacturing, and a lot of the notation and definitions comes from the field of pulp processing. Washing processes usually consist of different operations, such as dilution, thickening or displacement, often in combination. The goal of all washing is to remove as much dissolved matter using as little wash water as possible.

Washing often includes several washing stages in series to obtain a sufficient washing *yield*,  $Y$ , defined as the amount of dissolved matter removed as a fraction of the incoming amount of dissolved matter. A schematic representation of a single wash stage is shown in figure 2.5

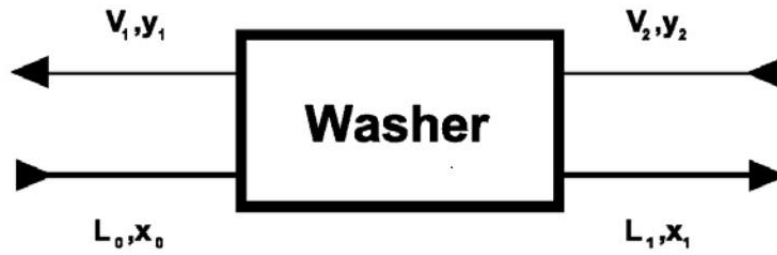


**Figure 2.5:** Schematic representation of a single washing stage.  $V$  is the wash filtrate,  $L$  is the slurry containing solid material, and  $x$  and  $y$  is the concentration of dissolved matter in wash filtrate and liquid slurry respectively. Adapted from [21].

$L$  and  $V$  are often given as the amount of water in both streams relative to the amount of solid material in the slurry to be washed. By doing this, one can define the liquor weight ratio  $W$ , relative wash volume  $R$  and excess wash liquor  $E.W.$

$$W = V_1/L_0 \quad (2.3)$$

$$R = V_2/L_1 \quad (2.4)$$

$$E.W. = V_2 - L_1 \quad (2.5)$$

A single washing stage also have a certain efficiency, and this efficiency is often expressed as the number of series-connected ideal mixing stages needed to give the same washing efficiency as the washing equipment. This number is known as the Nordèn  $E$  value, and can be assigned to any given washing equipment. If  $E$  is known for all stages, The total washing yield for a series of wash equipment is then calculated by equation 2.6.

$$Y = 1 \frac{W-1}{W \prod_i R_i^{E_i-1}} \quad (2.6)$$

$R$  and  $E$  will vary for each equipment unit, while  $W$  is constant. Figure 2.6 shows how  $W$  and the equipment efficiency influences the washing yield of a single unit.

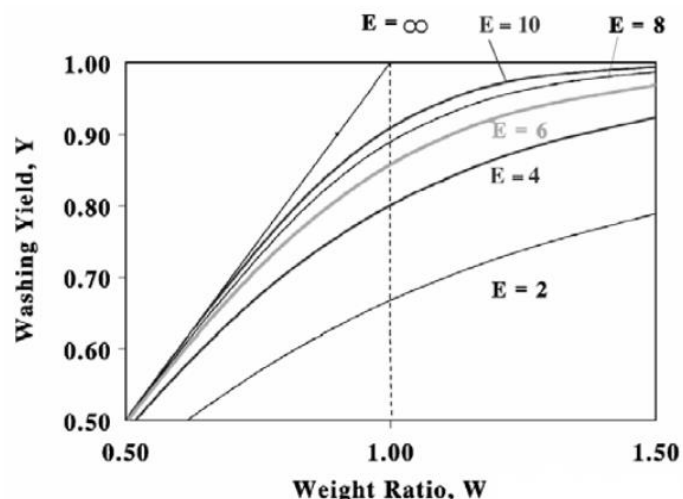


**Figure 2.6:** Washing yield for a single stage washing unit, as a function of liquid weight ratio and efficiency, taken from [21].

With an ideal wash equipment with efficiency approaching infinity, the necessary wash water is at a minimum, equal to the incoming liquid flow. For real equipment, the efficiency will be less than this. The overall yield can be improved by either using more equipment in series, or increasing the amount of wash water.

Solid separation and washing is a well developed technology in the pulping industry. A range of different washing equipment and process configurations exist. Typical yields in pulp washing approaches 99% for cooking liquor recovery, and over 90% for dissolved matter recovery [21]. Typical washing equipment includes different kind of filters and presses, often used in combination to achieve sufficient efficiency [22].

Empirical data on washing efficiency and yields are harder to come by for less typical solids. In this work, corn stover is used as feedstock, and the process involves separation and washing of pretreated biomass. NREL has used a type of pneumatic pressure filter driven by compressed air for the separation of residual lignin [23]. The same filters combined with washing has also been used to separate and wash pretreated corn stover [24]. Wash yields for these filters range from 90% to over 95%, depending on whether washing is used or not.

## 3. Current Technology

### 3.1 Corn Stover

The world corn production in 2014/15 was just over 1000 metric tons annually, with the largest producers being the U.S. (36%) and China (21%) [25]. The U.S. consumption is outlined in figure 3.1.

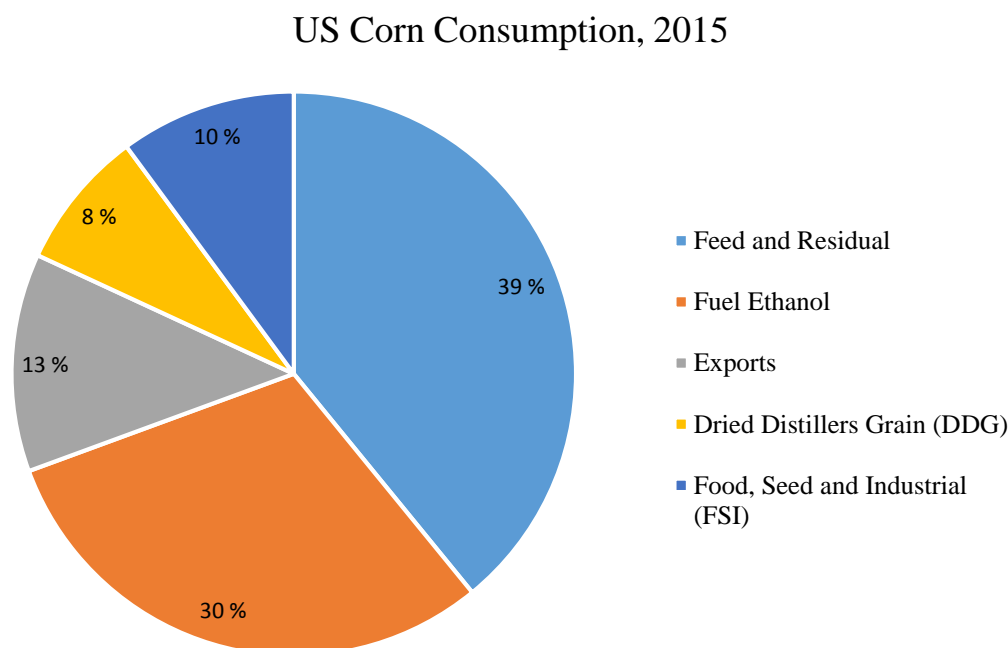


**Figure 3.1:** U.S. Corn Consumption, 2015 [26].

The grain constitutes around 50% of the corn, leaving the other 50% as plant material, mainly stalks, leaves, sheaths and husks. This is known as corn stover, which is used as bedding in crop fields and as feed for cattle production [27]. The last few decades, a lot of research have been done in investigating the use of corn stover and other comparable biomass feedstocks as possible lignocellulosic raw material for cellulosic ethanol production. In the US, there are currently to major pilot/commercial plants producing cellulosic ethanol from corn stover, operated by DuPont and POET DSM, both located in Iowa, US. Other pilot plants, running on other raw materials also exist [28].

Corn stover consist of about 35% cellulose, 24% hemicellulose and 16% lignin, and minor amounts of extractives, ash and protein. The crystallinity of the cellulose fraction is in the range of 60-70%, making it difficult to process into glucose/ethanol [10]. The hemicellulose

fraction mostly contain xylose, making it an excellent feedstock for co-production of ethanol and furfural.

### 3.2 Ethanol Production

The world fuel ethanol production has more than doubled over the last decade. The two largest producers are the U.S. (58%) and Brazil (27%), using corn(starch) and sugarcane(sucrose) as their respective feedstocks.

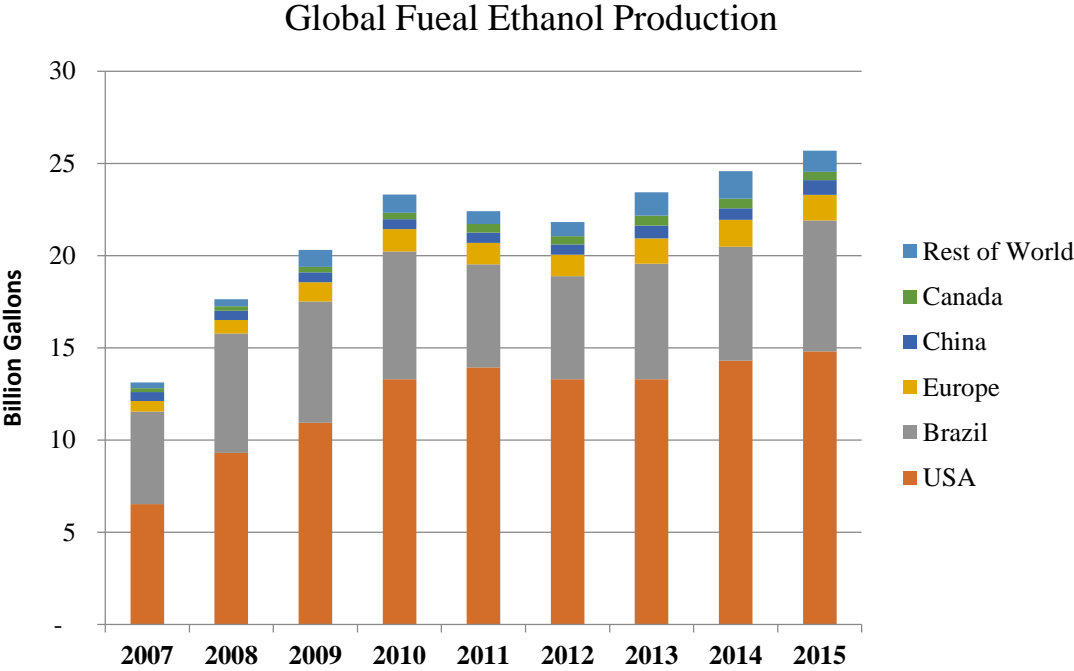


Figure 3.2: Global fuel ethanol production by country/region and year [29].

In the U.S., 90% of the ethanol is produced by corn dry-milling, with the rest being produced by wet-milling. In dry-milling, the whole corn kernel is ground into a flour known as “meal,” which is then mixed with water to a slurry, or *mash*. Enzymes are added to convert starch into sugar, and yeast is used to convert the sugar into ethanol. In wet-milling, the grain is mixed with water containing dilute sulfuric acid, which makes it possible to separate the germ. The remaining fiber, gluten and starch are separated and processed individually. It is common to ferment the starch fraction into ethanol, but can also be sold as purified starch or processed into corn syrup [29].

Research has indicated that cellulosic ethanol offers larger reductions in greenhouse gas emissions compared to the fuel ethanol produced from sugar or starch. It has also become clear that a large-scale use of fuel ethanol will require the use of lignocellulosic feedstocks to a large extent [30]. NREL has long investigated the possibility of producing ethanol from corn



stover or other comparable agricultural residues. The proposed process involves a sulfuric acid pretreatment for hemicellulose hydrolysis followed by a sequential enzymatic hydrolysis and fermentation. A block diagram of the process is shown in figure 3.3.

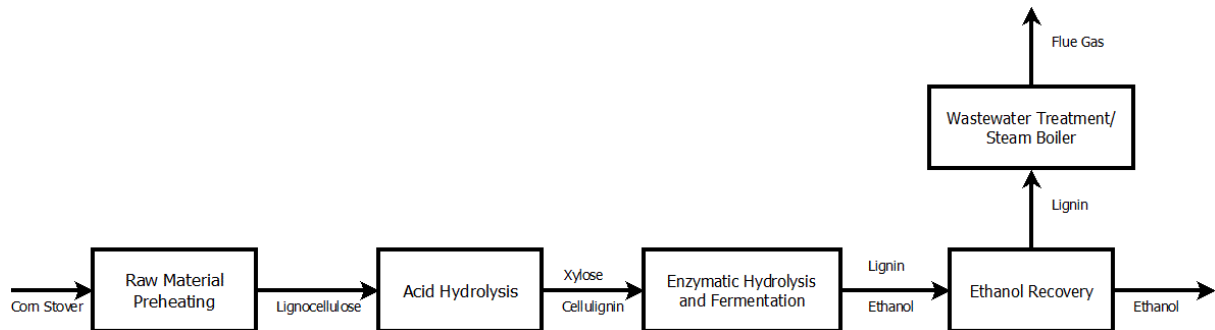


**Figure 3.3:** Block diagram of the NREL ethanol process.

The 2012 study reports a minimum ethanol selling price (MESP) of 2.15 \$/gal, well above the last year average market price of ethanol at 1.5 \$/gal [23, 31].

### 3.3 Furfural Production

Furfural has been produced industrially since 1921, when Quaker Oats started furfural production from oat hulls, corn cobs and sugar cane bagasse. Because of limited demand and high maintenance costs, production technology and product yield has improved little since the 1980s [32]. Current production processes are more or less modified version of the original Quaker Oats process. They mostly consist of steam-injected digesters fed with acid-impregnated biomass. The furfural is drawn as an enriched vapour stream, which subsequently is concentrated in an azeotropic distillation column and rectified via vacuum distillation [4, 33]. The general outline of such process is provided in figure 3.4.

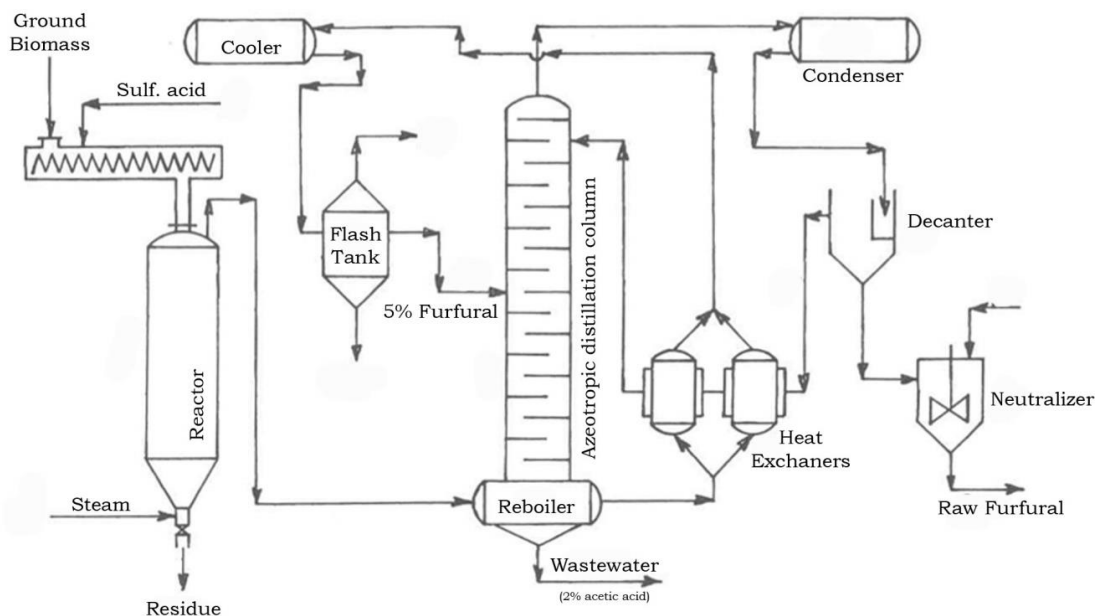


**Figure 3.4:** Schematic of a modern Chinese furfural plant, taken from [4].

The furfural yield is about 11% of initial dry weight of biomass, corresponding to 50% of theoretical yield. The yield will vary with the feedstock and its pentosane content. Other drawbacks include excessive use of sulfuric acid at about 2-2.5 wt% of fed biomass and steam usage in the range of 15-25 times the fed biomass, which makes the overall process very energy intensive.

The global market for furfural is estimated to 300 kton/year, with China as the largest producer and consumer [34, 35]. Production of furfuryl alcohol currently accounts for approximately 60% of the global furfural consumption [36]. Other furfural derived products include furan, tetrahydrofuran, tetrahydrofurfuryl alcohol and furfurylamine. It is also used for production of specialty chemical like pharmaceuticals and food additives.

### 3.4 Proposed Integrated Furfural and Ethanol Production

A number of processes has been proposed for integrated production of furfural with other products. These include the biofine process for production of furfural and levulinic acid and the lignol biorefinery technology, where xylose, furfural, acetic acid and lignin are the main products [3]. There are mainly two strategies for integrating furfural production into a biorefinery concept, based on acid catalyzed pretreatment technology.

The first option is to have a simultaneous production of furfural and pretreatment of the feedstock, based on the current furfural production technology. Having a single unit operation serving multiple purposes is beneficial to both investment- and operating cost. However, this solution suffers from the same drawbacks as the current furfural production technology,

mainly poor yields combined with high steam/energy consumption. It will also require substantial washing and cleaning of the residual cellulose/lignin (cellulignin) for further hydrolysis and fermentation, as it will contain high amounts of fermentation inhibitors.

The second option is to have a dedicated pretreatment process, where hemicellulose is selectively hydrolysed. This pentose-rich liquid stream is then diverted to a dedicated furfural-production area or facility. Having pentose/xylose in a liquid stream could make the production of furfural more cost effective, as both furfural yield and energy consumption could be improved significantly. Further processing of the residual cellulignin is also eased, as the formation of fermentation inhibitors are greatly reduced. The main drawback of this approach is potential high investment costs associated with a dedicated step for fractionating xylose from the feedstock [4].

#### 3.4.1 Marcotullio Process

Marcotullio has proposed an innovative process for the production of furfural [4]. The process is envisioned as an integrated part of a biorefinery, utilizing the dilute aqueous pentose stream resulting from a dedicated pretreatment process. Furfural production is performed in a reactive countercurrent distillation column. As furfural forms, it immediately vapourizes and is separated from the reactive liquid phase [4]. Figure 3.5 shows a simplified process flow diagram of the process proposed by Marcotullio. The furfural product stream can be compared to the raw furfural obtained in the process outlined in figure 3.4. A higher purity is often wanted, and remaining water must be distilled off in a rectification column, analogous to current furfural separation processes [33].

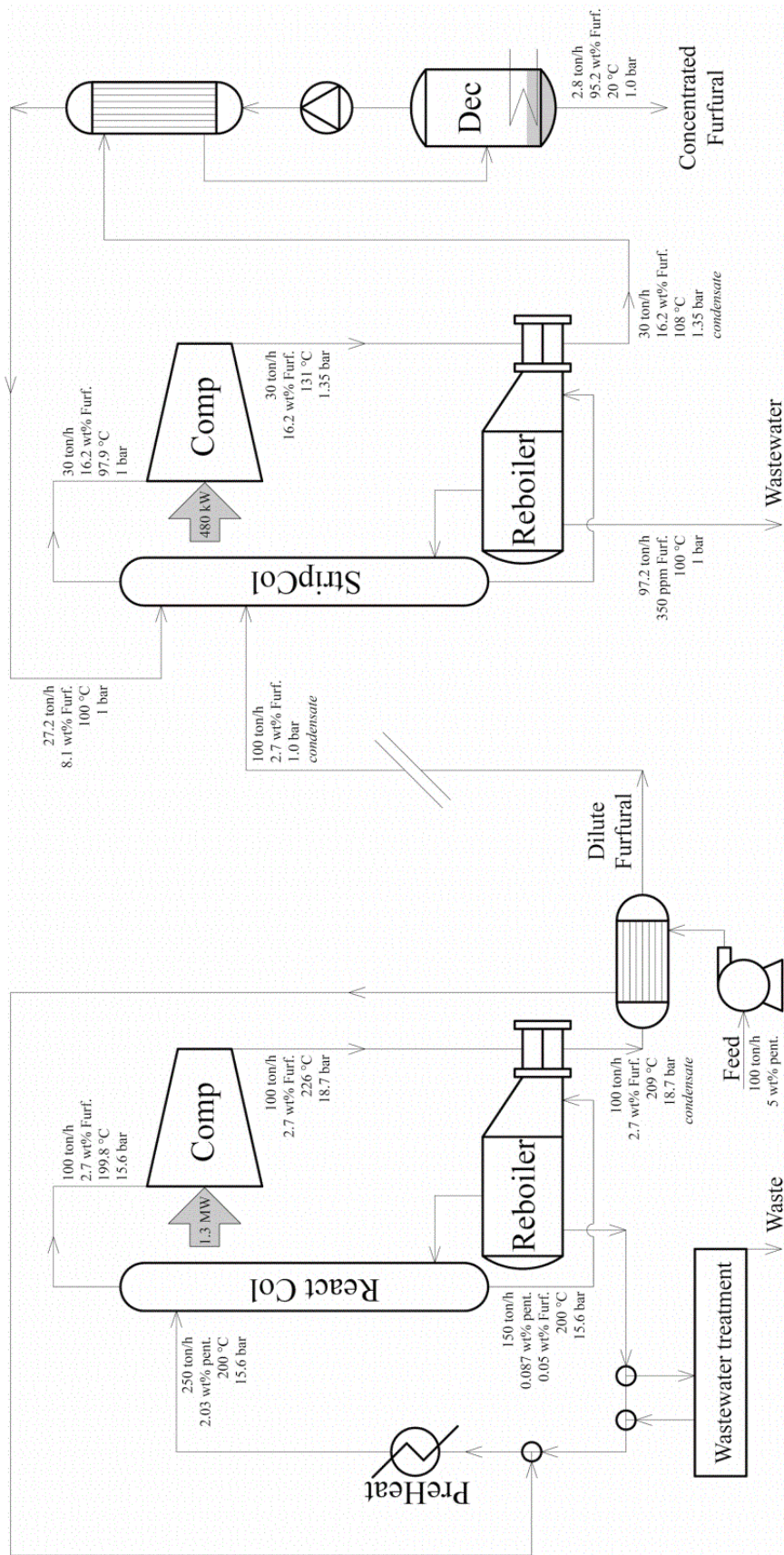


**Figure 3.5:** Simplified process flow diagram of the Marcotullio process with a production rate of 2.8 ton/h 95 wt% furfural [4].

## 4. Process Basis

### 4.1 Process description

The goal of this work has been to get an overall implementation of an integrated process for furfural and ethanol production. Figure 4.1 shows a simple block diagram of the process.

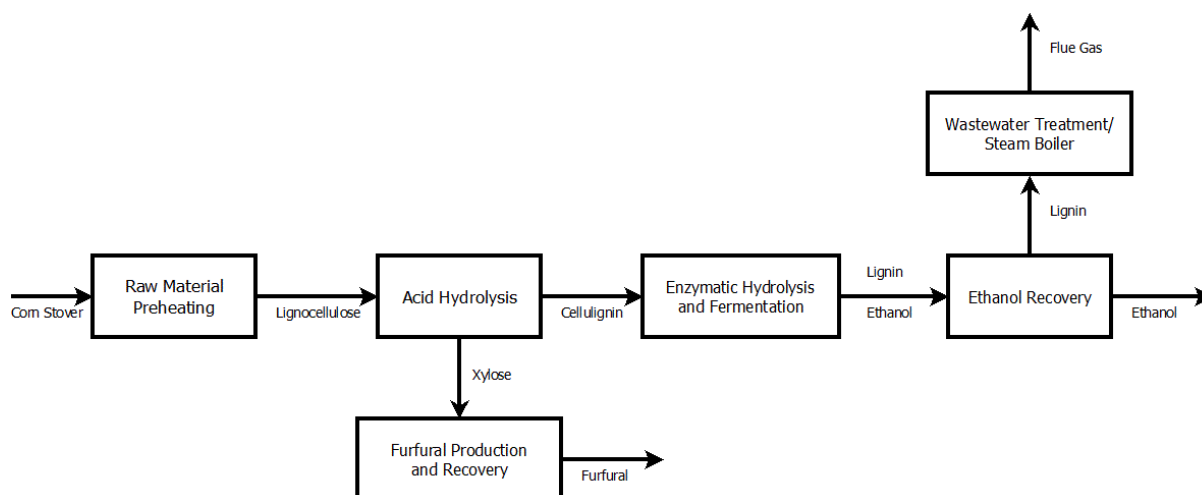


**Figure 4.1:** Block diagram of a process for integrated production of furfural with ethanol.

The process is based on the NREL ethanol process shown in figure 3.3. It differs in that xylose is separated from the slurry after pretreatment and is an example of the two-stage strategy for integrating furfural production with other biorefinery processes. The production of furfural from xylose is based on the Marcotullio process described in section 3.4.

The process has been divided into five main areas, as explained below.

A more thorough discussion of each area is given along with the description of the process implementation in chapter 6. Detailed process flows diagrams for each process area are also included in chapter 6.

#### 4.1.1 Pretreatment and Conditioning

The primary goal of the pretreatment process is to fractionate hemicellulose from the feedstock. This is done by selectively converting hemicellulose into its sugar monomers, most importantly xylose, and then separating the solubilized compounds from the solid phase. The secondary goal is to achieve sufficient pretreatment of the cellulose upon pretreatment. This produces a liquid stream containing xylose and a slurry containing pretreated cellulose and lignin. Dilute sulfuric acid is used as the pretreatment agent.

#### 4.1.2 Enzymatic Hydrolysis and Fermentation

A sequential hydrolysis and fermentation process (SHF) is used to hydrolyse cellulose into glucose, which is then fermented into ethanol. The slurry received from pretreatment is mixed with cellulase enzyme and partially hydrolysed in a continuous reactor. It is then fed to a batch system for final hydrolysis and fermentation. The inoculum used in fermentation is produced by diverting a fraction of the hydrolysed slurry into an inoculum seed train. This stream is then pumped back to the batch system to initiate fermentation.

#### 4.1.3 Ethanol Recovery

The finished beer from fermentation is distilled in two ordinary distillation columns, producing an ethanol azeotrope. Anhydrous ethanol is produced by adsorbing water in a molecular sieve adsorbing system. The beer from fermentation contains residual solids, mainly lignin. The beer is not filtrated prior to distillation, which means that the solids will flow with the beer column bottom stream. This stream is further treated in a wastewater treatment process.

#### 4.1.4 Furfural Production and Recovery

The liquid stream obtained from pretreatment is used to produce furfural. The reaction is catalyzed by sulfuric acid reused from the pretreatment process, and performed in a reactive distillation column. Furfural is recovered by using two distillation columns, called an azeotropic distillation column and a purification column. The azeotropic stream from the first column is split in a decanter. The rich phase is further purified in the purification column.

#### 4.1.5 Wastewater Treatment and Steam Boiler

The wastewater from ethanol recovery contain residual lignin. This is filtrated to produce a stream of combustible solids. Remaining wastewater from ethanol and furfural recovery processes is used to produce methane by anaerobic digestion. This is the first step in wastewater treatment and removes the majority of organic material in the water. Methane and solids are burned in a boiler to produce steam. The steam is used to cover the heating demand of the process and for generating electricity.

## 4.2 Design Basis

The 2011 NREL design report on biochemical conversion of corn stover to ethanol and Marcotullio process for integrated production of furfural constitutes the basis for the plant design described in this report [4, 23].

The feedstock input is 2000 ton/day of dry corn stover, corresponding to an annual feedstock requirement of 700,400 dry ton/year with an anticipated uptime of 96%. The annual production is 120,400 tons of 99.5 wt% ethanol and 93,300 tons of 99.0 wt% furfural. The lignin is used as fuel for a high pressure steam boiler. The steam is used for electricity production and for internal heating purposes.

The type of feedstock and its composition may influence the overall plant design. The amount of cellulose and hemicellulose/xylose in the feedstock will be decisive to the sizing of the ethanol and furfural specific areas of the plant, and may affect design of important process units, such as the pretreatment reactor and solid/liquid separation equipment. In this design, corn stover is chosen as feedstock. The high content of xylan makes it a good choice for integrated furfural production. The feedstock composition and the annual feedstock requirements is equal to that used by NREL, making comparisons of flowsheet calculations and results easy. The assumed composition in this work is shown in table 4.1 [23].

**Table 4.1:** Corn stover feedstock composition on dry-weight basis.

<b>Component</b>	<b>Content [wt%]</b>
<b>Glucan</b>	35.05
<b>Xylan</b>	19.53
<b>Arabinan</b>	2.38
<b>Galactan</b>	1.43
<b>Mannan</b>	0.60
<b>Lignin</b>	15.75
<b>Ash</b>	4.93
<b>Protein</b>	3.10
<b>Acetyl</b>	1.81
<b>Sucrose</b>	0.77
<b>Extractives</b>	14.65
<b>Total</b>	100

### 4.3 Report Conventions

The units used in the report are mainly metric units. One exception is the use of *atm* for pressure, as most of the design data are given in *atm*. Furthermore, *ton* is used for most mass streams, and represent a standard metric ton (1,000 kg).

The process implemented in this work converts solid material into liquid products, and some streams will contain both a liquid and solid phase. The total solid loading is defined as the sum of all soluble solids such as sugars and salts, and insoluble solids such as the structural carbohydrates in the feedstock. To avoid confusion, the terms are used through the discussion of the process implementation and performance.

*Yield* and *conversion* are used to describe the extent of various reactions, and are both a percentage of the maximum theoretical. Conversion is mostly used for a specific reaction, while yield is a measure of the amount of various compounds after reaction.

The numbering of trays/stages in distillation column is top down, with number 1 as the top tray.



# 5. HYSYS Setup

## 5.1 Component List

The component list consist of 28 individual components, of which most is “pure components” retrieved from the native HYSYS source databank. An option to using the HYSYS databank would be to use the Aspen Plus databank, which offers a greater variety of components available for selection. However, when using the Aspen Plus databank, there are some limitations regarding property package set up.

### 5.1.1 Hypotheticals

The HYSYS database is limited, in that it mostly contains components specific to oil and gas processing. Components associated with biomass are therefore created as hypotheticals, and is listed in table 5.1. Most of the properties used to define these are retrieved either from aspen databases using Aspen Properties Manager or from the NREL design report.

**Table 5.1:** Overview of all hypothetical components used, and information about basic properties.

<b>Component Name</b>	<b>Normal Boiling Point [C]</b>	<b>Molecular Mass [g/mol]</b>	<b>Liquid Density [g/L]</b>
<b>Cellulose C</b>	440.37	162.1	1.500
<b>Cellulose A</b>	440.37	162.1	1.500
<b>Xylan</b>	376.63	132.1	1.500
<b>Xylose</b>	343.90	150.1	1.181
<b>Extractives</b>	343.90	180.2	1.181
<b>Ammonium Sulfate</b>	200.0	132.1	1.769
<b>Ammonium Acetate</b>	200.0	77.08	1.170
<b>Diammonium Phosphate (DAP)</b>	200.0	132.1	1.619
<b>Protein</b>	200.0	22.84	1.220
<b>Cell Mass</b>	200.0	24.63	1.200
<b>Ash</b>	200.0	56.08	1.000

Information about normal boiling point, molecular mass and liquid density are essential for estimating unknown properties using native HYSYS functionality. Of the three, at least two must be given. For all hypotheticals, molecular mass and liquid density has been given as the basis for property estimation. The bottom six components have specified the normal boiling point too, as the estimated boiling point was in the range of 0-50 °C for these. As these

components are solids, thermodynamic data related to boiling is assumed to be irrelevant for the energy balance in the simulation. All hypotheticals are solid in reality, but modeled as liquids in HYSYS. The high boiling points is important to keep the components in the liquid phase during simulation. To help with this, the antoine vapour pressure coefficients used to calculate the vapour pressure of components are changed to ensure non-boiling behavior, as explained in the NREL design report. Additional information may also be provided, for example heat of formation, heat of combustion and other property package-specific parameters.

The Cell Mass component are made from ZYMO (*Z. mobilis*) specified in the NREL design report, and is used to represent both *Z. mobilis* and the TRICHO (*T. reesei*) in the NREL design report, as they are comparable both in molecular weight and composition and physical properties.

#### 5.1.2 Modeling of Corn Stover

The corn stover feedstock consist of several different structural carbohydrates. For simplicity, all pentosans are modeled as xylan, and all hexosans are modeled as cellulose, as these two are by far the most abundant components in the feedstock.

Cellulose is modeled as a crystalline component (Cellulose C) and an amorphous component (Cellulose A). Cellulose A is a duplicate of Cellulose C, and meant to represent the amorphous cellulose and the hexosan fraction of hemicellulose. The reason for this is the assumed similarity in physical properties of the two, and that the reaction kinetics will be similar.

The crystallinity of corn stover varies, but usually is between 60-70%. The crystalline fraction as implemented in HYSYS is chosen higher than this, to account for the fact that not all of the amorphous cellulose is available for reaction in untreated feedstock. Specifically, the fraction is adjusted so that the yield of glucose after pretreatment is comparable of that reported by NREL. The motivation for making the duplication of cellulose is not to get an accurate representation of crystallinity, but to account for different reaction kinetics in cellulose and expected yields after acid pretreatment.

Xylan is made as a duplicate of Cellulose C, accounting for different molecular weight, and appropriately scaling the heat of formation property by a factor 5/6 [23]. It represents the total pentosan content in the corn stover.

As mentioned, not all components are available in the native databank. However, some components give good approximations. In accordance with the NREL design report, vanillin is used to represent lignin, as the heat of combustion along with other relevant properties are similar. Other minor components present in the corn stover is modeled as follows:

- Ash is modeled as CaO, based on properties found in the NREL design report and Aspen Properties Managers.
- Sucrose is modeled as dextrose (glucose), and not included as an own component.
- Protein is modeled based on molecular weight and composition of Wheat gliadin, obtained from the NREL design report.
- Acetyl groups present in hemicellulose is modeled as Acetic acid, as it is assumed that it will fully solubilize during acid pretreatment.

## 5.2 Reaction Sets

Eight different reaction sets are made. In the NREL design report, all reactions are described with simple conversion factors. An ambition for this work has been to get an implementation of reaction kinetics. This is done for the acid catalyzed formation and decomposition reactions of glucose and xylose, which means that the sizing of pretreatment equipment and furfural reactor may be done in the simulation case. All kinetic reactions are assumed first order, where the reaction constant  $k$  is described by

$$k = A_0 C^n \exp\left(-\frac{E}{RT}\right), \quad 5.1$$

$A_0$  is the frequency factor at  $C = 0$ ,  $C$  is acid concentration, normally expressed as wt%,  $E$  is the activation energy,  $n$  describe the dependency of acid concentration on the frequency factor,  $T$  is the temperature and  $R$  the universal gas constant. Table 5.2 summarizes the parameters used for formation and decomposition of xylose and glucose.

**Table 5.2:** Overview of kinetic parameters used in the acid catalyzed formation and decomposition of glucose and xylose [17, 37].

Reaction	$A_0$ [ $s^{-1}$ ]	$n$	$E$ [kJ/mol]
<b>Xylan <math>\rightarrow</math> Xylose</b>	$6.13 \cdot 10^{18} (2.08 \cdot c^{-1})$	0	171.6
<b>Xylose <math>\rightarrow</math> Furfural</b>	$3.25 \cdot 10^{12} (2.36 \cdot c^{-1})$	0	133.9
<b>Cellulose <math>\rightarrow</math> Glucose</b>	$4.52 \cdot 10^{17}$	2.74	189.6
<b>Glucose <math>\rightarrow</math> HMF</b>	$3.35 \cdot 10^{12}$	1.86	137.3

The kinetic parameters for the reaction from cellulose to glucose is used for the crystalline fraction of cellulose, while the parameters for the reaction of xylan to xylose is assumed to be valid for the amorphous fraction of cellulose, as the physical and structural properties of these are similar.

HMF is the direct product of glucose degradation, but is highly unstable. In the reaction set, it is modeled as levulinic acid and formic acid, as HMF is assumed to react into these. The validity of this assumption with respect to the furfural reactive distillation column is questionable. HMF has a lower boiling point than furfural, and would be expected to vapourize upon formation, analogously to how furfural is expected to behave. However, experiments show that the yield of levulinic acid and formic acid is higher than for HMF even at a retention time shorter than one minute [38]. This is the main motivation for modeling the reaction products as levulinic acid and formic acid even in the reactive distillation column.

The remaining reaction sets are all described by conversion factors, which will be discussed in chapter 6. A dummy reaction set is also created for use in the continuous enzymatic hydrolysis reactor, which also is discussed in chapter 6.

### 5.3 Choosing Property Package

The property package includes a set of specialized methods for calculating the properties of components and values for properties in the simulation itself. HYSYS includes a range of different property packages for selection.

- Equation of State (EoS) models are used for predicting properties for most hydrocarbons and other non-polar components. These include the Peng-Robinson equation and the Soave-Redlich-Kwong equation, and variations of these.
- Activity models handles highly non-ideal systems, and by nature are more empirical than EoS models. These models are mostly used for non-ideal systems or polar components. It is common to use an EoS model to predict vapour behavior, and use an activity model for the liquid phase. Since activity models are empirical, the application is limited to the data range used to predict its parameters.
- Vapour Pressure models are used at low pressures for ideal mixtures, such as hydrocarbon systems and mixtures of slightly polar ketones and alcohols.

A system consisting of mainly water, furfural and ethanol is considered non-ideal. Mixtures of both water-furfural and water-ethanol forms azeotropes. Both the Non-Random-Two-Liquid

(NRTL) equation and the Universal Quasi Chemical (UNIQUAC) equation have been used to successfully represent such systems. Both models use a combination of temperature- and non-temperature dependent parameters to calculate each component's activity coefficient. They are good choices for representing both vapour-liquid equilibria (VLE) and liquid-liquid equilibria (LLE), although UNIQUAC is more detailed, and applicable for a broader range of components.

For the water/furfural/ethanol system, both NREL and Marcotullio have preferred the use of NRTL. For the purpose of comparability of results, NRTL is chosen for this work.

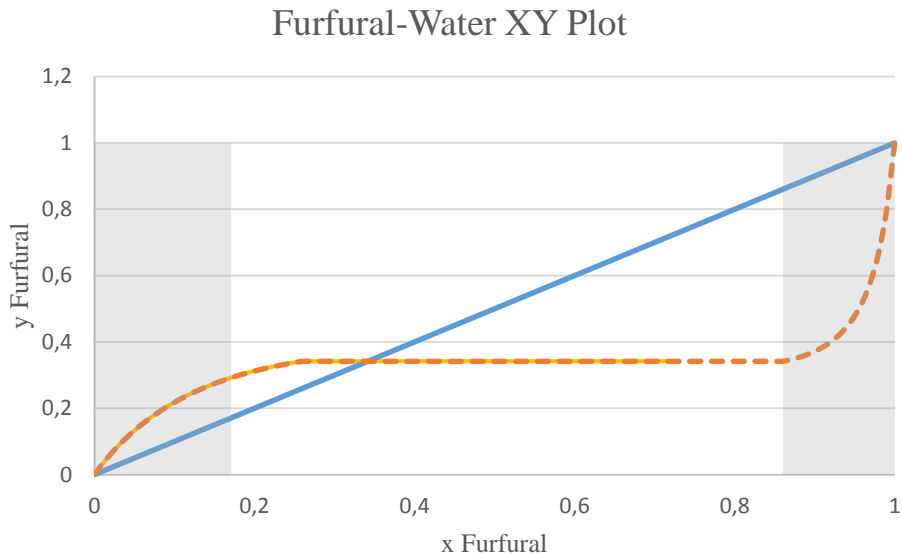
#### 5.4 Estimating Binary Coefficients

Binary coefficients are important for accurate representation of equilibria for both pure components and mixtures. In this work, vapour-liquid equilibria (VLE) of binary and tertiary mixtures containing water, ethanol, furfural and acetic acid is important. The liquid-liquid equilibria (LLE) for water, furfural and acetic acid is also important for the phase separation process described in chapter 3. Binary coefficients for these components are provided natively by the HYSYS database; however, these do not yield good representations of any of the equilibria of interest.

Binary coefficients can either be obtained directly from the literature, or experimental data of equilibrium behavior can be used to calculate the coefficients by regression. HYSYS also provides an automated function for parameter estimation based on the UNIFAC (UNIQUAC Functional-group Activity Coefficients) group-contributing method. It predicts interactions between molecules by applying standardized contributions for functional groups present on the molecules that make up the liquid. The components of special interest in this work, such as water, ethanol, acetic acid and furfural, have well defined values for this method. Furfural as a molecule is specifically defined as its own functional group in the estimation method.

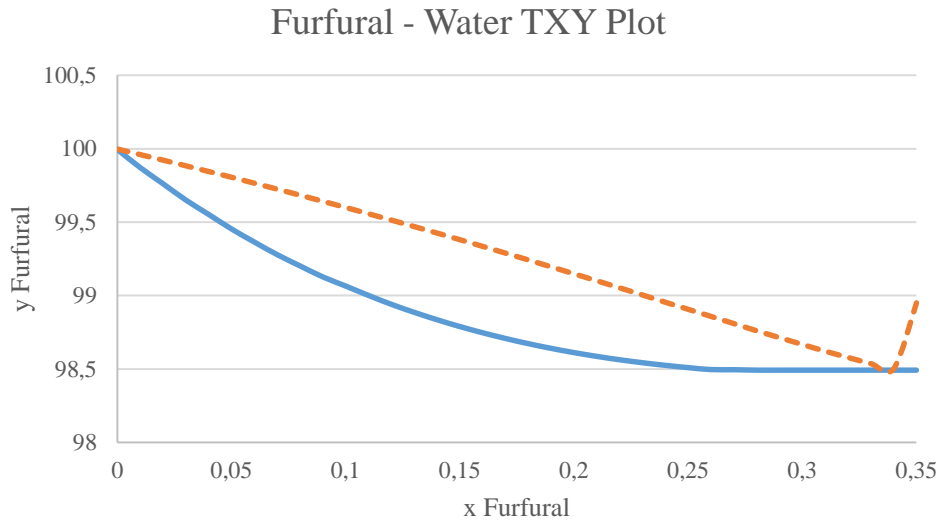
Binary coefficients used in this work are all estimated by using the UNIFAC estimation method with emphasis on representing vapour-liquid equilibria. One drawback of using only one property package based on activity coefficients is that simultaneous representation of VLE and LLE behavior is difficult. The obtained binary coefficients are almost always a compromise between the two. Some properties of the most important mixtures are given in the following figures. All the plots are at atmospheric, as most of the processes are performed at or slightly above 1.0 atm.

Figure 5.1 shows the equilibrium composition of furfural and water in liquid and vapour phase. The estimated azeotropic point is at 34.2 wt% furfural, which is a little under the real composition of 35.0% [39]. The furfural concentration in this work is either far below or above the azeotropic point (shaded area in figure), and the accuracy is considered sufficient.



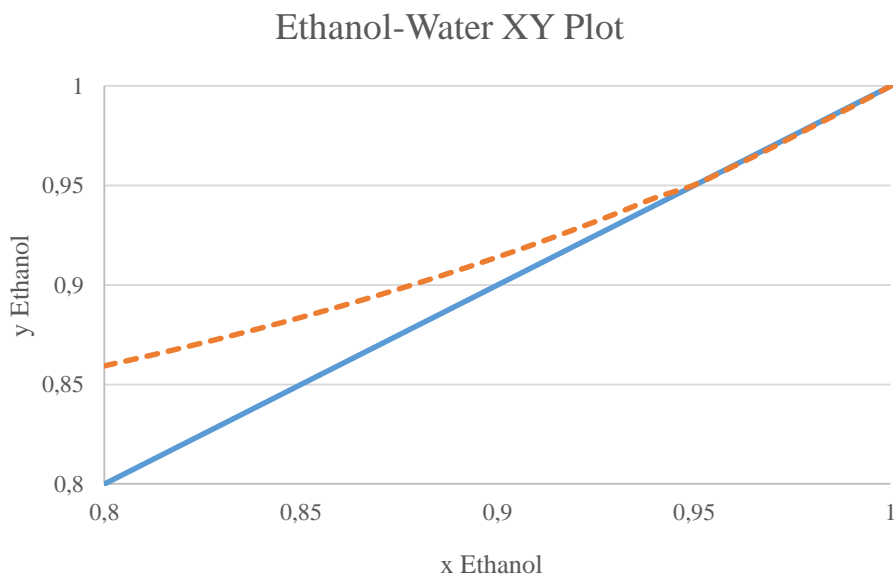
**Figure 5.1:** XY plot of the binary mixture of furfural and water at 1.0 atm. Composition is given in wt%.

Figure 5.2 shows the bubble and dew point curve for the furfural - water mixture up to the azeotropic point. Of special interest is the estimated azeotropic boiling point, which is a rough indication on the validity of both curves. The estimated boiling point is 98.5 C, within 1% of the real boiling point at 97.85 °C [39, 40].



**Figure 5.2:** T-XY plot of the binary mixture of furfural and water at 1.0 atm. Composition is given in wt%.

Figure 5.3 shows the equilibrium composition of ethanol and water in liquid and vapour phase at the ethanol rich end. The estimated azeotropic point is at 95.7 wt%, almost equal to the real composition of 95.5 wt% [41]. The bubble and dew point curves are not shown here, but the azeotropic boiling point is verified to be equal the real boiling point at 78.1 °C [41].



**Figure 5.3:** XY plot of the binary mixture of ethanol and water at 1.0 atm. Composition is given in wt%.

Finally, figure 5.4 shows the LLE plot of the tertiary mixture of water, furfural and acetic acid. It is expected that considerable amounts of acetic acid be present in the furfural specific

part of the plant, and it is chosen as the tertiary component. The plot shows the immiscible area of the tertiary mixture together with the phase separation that is expected. The maximum solubility of furfural in water at 20 °C is estimated to 9.1 wt%, which is lower than the actual solubility at of 8.3 wt% [39]. The furfural rich phase in the binary mixture with water is estimated to 90.0% furfural, which is lower than the real composition of 95.2 wt% [39]. In addition, acetic acid is predicted to have higher solubility in water than furfural.

As expected, the prediction of VLE behavior is closer to reality than the LLE behavior, because of choosing the UNIFAC VLE estimation method. The validity and implications of using somewhat poorly estimated LLE behavior is further discussed in chapter 8.

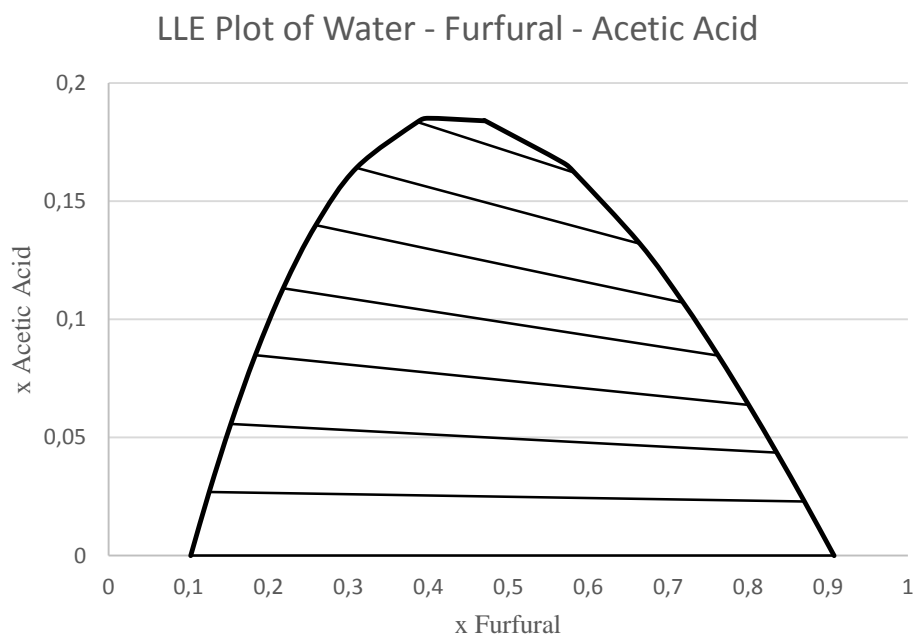


**Figure 5.4:** LLE plot of the tertiary mixture of water, furfural and acetic acid at 1.0 atm and 20.0 C. Composition is given in wt%.



## 6. HYSYS Process Implementation

This chapter gives a thorough description of each process area with special focus on the implementation and modeling HYSYS. An overview of the HYSYS simulation environment highlighting the different process areas are included in appendix A.

Areas concerning feedstock storing and handling, storing and management of finished products and management of utilities are not included in the HYSYS case. In addition, a thorough implementation of wastewater treatment has not been included, which means that the water mass balance is not fully closed.

Production of cellulase for enzymatic hydrolysis is also considered outside the scope of this work. A dedicated process area for this could be included in a later work, or cellulase could be assumed purchased on the market. The previously published design reports by NREL has not included any onsite production of cellulase. The motivation for adding it in their latest design is increased insight and transparency into what drives costs in cellulase production [23].

### 6.1 Area 100: Pretreatment and Conditioning

Process flow diagrams of the process area is show in figure 6.1 and 6.2.

Corn stover is received at a rate of 104.1 ton/h including an assumed water content of 20%. The raw material is mixed with heated process water to a total solid loading of 34%. It is then fed to a plug screw feeder (PS-100), where the pressure is increased to 3.5 atm, and the raw material is physically processed. The plug screw is modeled as a liquid pump, with a specified adiabatic efficiency of 1.0%. The efficiency is back calculated from the NREL design, based on the given pressure difference and energy input. The low efficiency is explained by the high amount of solid matter in the stream. The resulting “mash” is fed into a preheater (MIX-102), where it is heated to 100 °C with direct steam injection. This is to ensure efficient mixing of the acid for pretreatment, and a more homogenous treatment. It is assumed that the preheater only affect physical attributes of the raw material, therefore there is no explicit modeling of the tank. The preheated mash is then fed to a second plug screw feeder (PS-101), raising the pressure to 6.1 atm. Sulfuric acid is mixed in at the reactor inlet. A better solution could be to mix at the discharge of the second plug screw to allow for better mixing, but this makes no difference with regards to modeling.

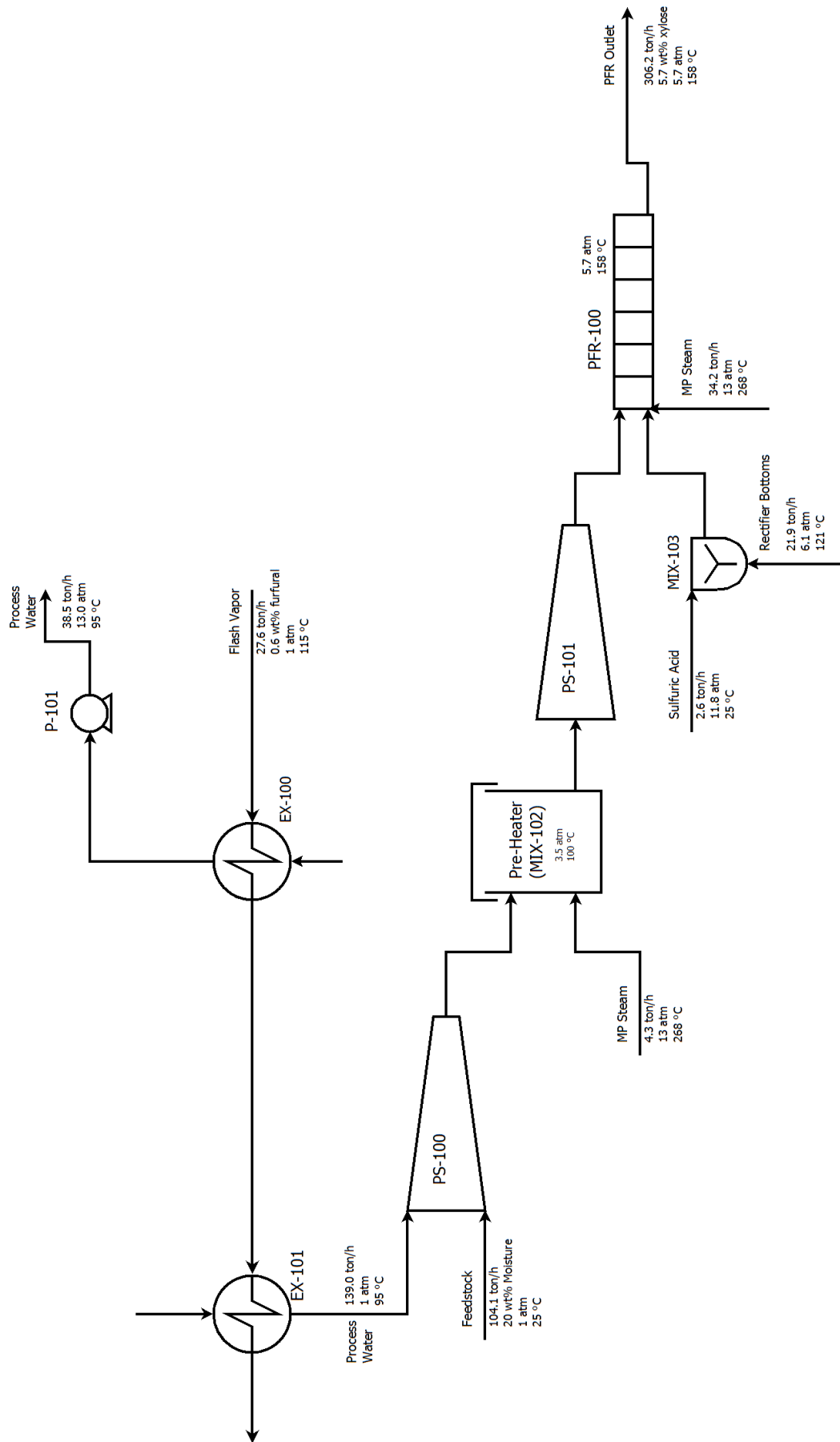


**Figure 6.1:** Process flow diagram of the first part of pretreatment.

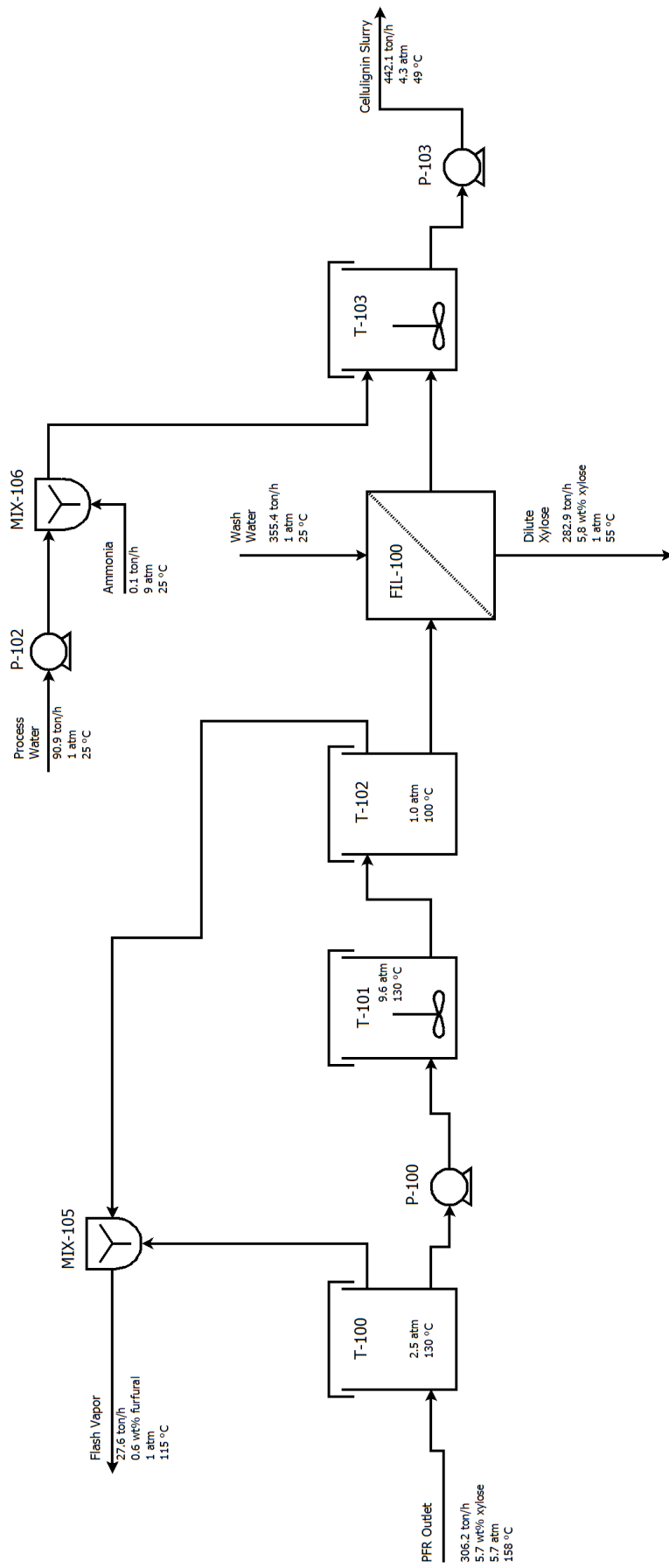


Figure 6.2: Process flow diagram of the second part of pretreatment.

The pretreatment reactor (PFR-100) is modeled as a single PFR tube, and its operating conditions are given in table 6.1. Medium pressure steam at 13.0 atm and 268 °C is used to control the reactor temperature, while the total solid loading is controlled by the process water mixing ratio earlier in the process. The reaction set with its kinetic parameters are outlined in table 5.2.

**Table 6.1:** Pretreatment reactor operating conditions.

<b>Condition</b>	<b>Specification</b>
<b>Sulfuric acid loading [mg/g dry biomass]</b>	30
<b>Residence time [42]</b>	5
<b>Temperature [C]</b>	158
<b>Pressure [atm]</b>	5.7
<b>Total solid loading [wt%]</b>	28
<b>Reactor volume [m<sup>3</sup>]</b>	31.5
<b>Reactor diameter/length [m]</b>	2.0/10.0

The pretreatment reactor is discharged into a flash tank (T-100). The flash pressure is controlled to keep the tank temperature at 130 C. The flash is mainly water with some furfural and acetic acid. The slurry from the flash tank is sent to a secondary oligomer conversion reactor (T-101), modeled as a CSTR reactor with the same reaction set used in the pretreatment reactor. NREL includes oligomers in their modeling of hydrolysis reactions. While this is not done in this work, the oligomer conversion tank has been included to get an accurate representation of the total reaction severity applied to the raw material. The oligomer conversion tank operating conditions are listed in table 6.2.

**Table 6.2:** Oligomer conversion tank operating conditions.

<b>Condition</b>	<b>Specification</b>
<b>Sulfuric acid loading [mg/g dry biomass]</b>	30
<b>Residence time [42]</b>	30
<b>Temperature [°C]</b>	130
<b>Pressure [atm]</b>	9.6
<b>Total solid loading [wt%]</b>	29.5
<b>Tank volume [m<sup>3</sup>]</b>	275
<b>Tank diameter/height [m]</b>	6.1/9.2

The oligomer conversion tank is discharged into a second flash tank (T-102) operating at atmospheric pressure. The flash is combined with the flash from T-100 and used to heat incoming process water. It contains useful amounts of furfural, and is forwarded to area 400 for further processing.

The reaction temperature of the pretreatment reactor and the oligomer conversion reactor is the same as in the NREL design, while the acid loading has been tuned to give comparable conversion of xylan into xylose and further to furfural. The kinetics used indicates a higher acid loading at 30 mg/g compared to 22.1 mg/g used by NREL. The yield of furfural during pretreatment are comparable by that assumed by NREL. The formation of furfural is less important to control in this design compared to NREL, as most of it is either flashed off or washed away in the preceding washing unit. Regardless of this, it is important to limit the formation of furfural, as this is meant to take place in area 400. The acetyl groups present in the hemicellulose is assumed to be completely solubilized into acetic acid. It is therefore modeled as acetic acid in the first place, and the reaction is not included in the pretreatment.

**Table 6.3:** Reaction conversion after pretreatment- and oligomer conversion reactor.

<b>Reaction product</b>	<b>Yield [% of theoretical]</b>
<b>Cellulose C</b>	99.9
<b>Cellulose A</b>	12.2
<b>Glucose</b>	9.2
<b>Xylan</b>	9.0
<b>Xylose</b>	85.5
<b>Furfural</b>	6.0

The use of flash tanks with rapid release of pressure is analogous to a form of steam explosion pretreatment. The raw material is physically broken down and ripped apart, making it more accessible for enzymatic hydrolysis and for general handling (pumping and transportation) of the slurry.

The slurry from the T-102 is sent to a solid/liquid separation unit. The unit uses clean water to wash the slurry from dissolved matter, separating the sugars from the residual cellulignin. The separation and washing is modeled as a simple component splitter. The insoluble solids content is 17.7% for incoming slurry, and 14.0% for washed slurry. Further, the wash yield is assumed to be 0.92, which becomes the split factor for all soluble components. The amount of

wash water is assumed to be 1.2 times the total water content in the washed slurry, corresponding to an excess water consumption of 2.1 m<sup>3</sup> water/ton solid material. No loss of insoluble solids is assumed during the wash. The modeling of the wash unit is based on overall wash parameters, and makes no assumptions regarding type of washing equipment used, or how such equipment would be arranged. It is simply assumed that there exist a combination of washing- and separation equipment capable of the given specifications. The wash filtrate containing sugars is forwarded to area 400.

The washed slurry is sent to a conditioning tank (T-103), where ammonia gas mixed with water is added to neutralize any remaining acid. The insoluble solids content is lowered to 11% and the temperature is lowered to 49 C, both suitable for enzymatic hydrolysis. The slurry is then pressurized and forwarded to area 200.

## 6.2 Area 200: Enzymatic Hydrolysis and Fermentation

A process flow diagram of this process area is shown in figure 6.3.

The washed and neutralized slurry from area 200 is cooled to 48 °C (CL-200), which is the assumed optimum temperature for enzymatic hydrolysis. Cellulase is mixed in at a rate of 20 mg enzyme protein/g cellulose. The insoluble solids content in the resulting slurry is about 11%, making pumping and mixing difficult. Therefore, the hydrolysis is performed in two consecutive steps. The slurry is first fed to a continuous reactor vessel (PFR-200), where the cellulose is partially hydrolysed. This greatly decreases viscosity of the slurry, making it suitable for further hydrolysis in batch reactors (T-200/T-202). The continuous vessel is modeled as a conversion reactor with a dummy reaction set. While no reactions are taking place in the simulation, it has been included to visualize the concept of consecutive hydrolysis. The batch hydrolysis is performed in several tanks, making for a semi-continuous processing of the slurry. It is modeled as a single tank in the simulation. The hydrolysis operating conditions are summarized in table 6.4.

**Table 6.4:** Enzymatic hydrolysis operating conditions.

Condition	Specification
Cellulase loading [mg protein/g cellulose]	20
Temperature [C]	48
Insoluble solid loading [wt%]	11
Cellulose conversion [%]	90

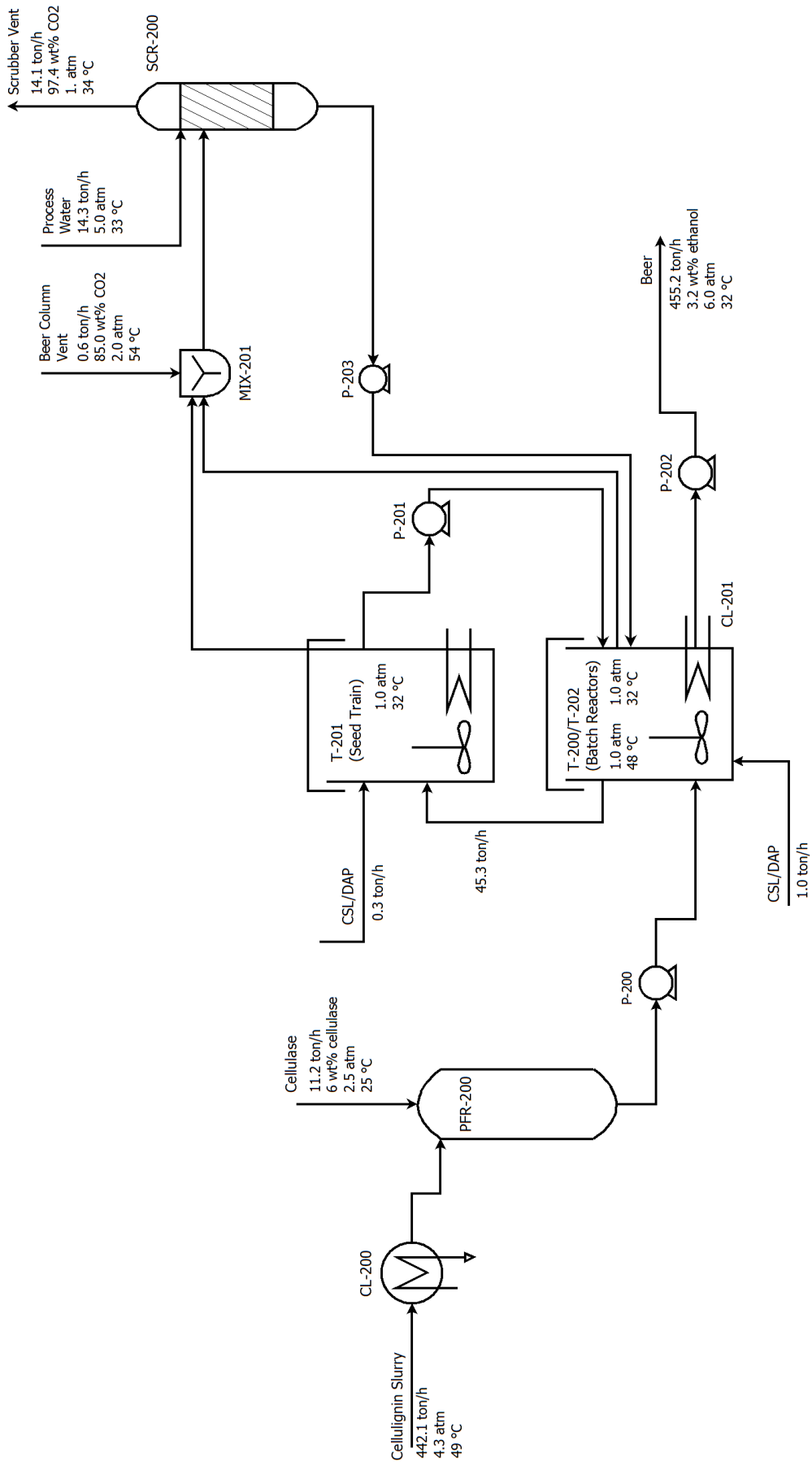


**Figure 6.3:** Process flow diagram of the enzymatic hydrolysis and fermentation.

After hydrolysis, the slurry is cooled to 32 °C for optimum fermentation conditions. The fermentation is carried out in the same batch tanks as the enzymatic hydrolysis, but is modeled as two separate tanks (T-200 and T-202). After the hydrolysed slurry is cooled, a 1/10 fraction is diverted into a seed train (T-201) for production of the ethanologen *Z. mobilis*. Recombinant *Z. mobilis*, capable of fermenting both glucose and xylose, was used by NREL. Although the level of xylose and minor sugar components are much less in this design, *Z. mobilis*, and the associated reaction conversions from the NREL design report, are used in this design. A better option could be to use *S. cerevisiae*, the industry standard for fermenting glucose into ethanol. It gives high yields of ethanol and is more robust, but lack capability of fermenting xylose.

The seed train (T-201) consist of several batch reactors in series, where each tank is successively larger than the former. The smallest tank is inoculated with a laboratory seed culture. The resulting broth is then used to inoculate the next tank. After several iterations, the broth from the largest tank is used as inoculum for fermentation, and is pumped back into the fermentation batch tank. Corn Steep Liquor (water, protein and lactic acid) and Diammonium Phosphate (DAP) are used as nitrogen sources, and is necessary for cell growth. The seed train is modeled as a single batch reactor. CSL loading is assumed to be 0.5 wt% while DAP loading is assumed to be 0.67 g/L broth. The reactions and assumed conversions are listed in table 6.5.

**Table 6.5:** Seed train reactions and assumed conversions.

Reaction	Conversion [%]
Glucose $\rightarrow$ 2 Ethanol + 2 CO <sub>2</sub>	90.0
Glucose + 0.147 Lactic Acid + 0.018 DAP $\rightarrow$ 6 <i>Z. mobilis</i> + 2.4 H <sub>2</sub> O	4.0
3 Xylose $\rightarrow$ 5 Ethanol + 5 CO <sub>2</sub>	80.0
Glucose + 0.122 Lactic Acid + 0.015 DAP $\rightarrow$ 5 <i>Z. mobilis</i> + 2 H <sub>2</sub> O	4.0

After mixing of the inoculum into the hydrolysed slurry, fermentation is initiated. Additional nutritional agents are charged to keep CSL loading at 0.25 wt% and DAP loading at 0.33 g/L broth. Reactions and assumed conversion are listed in table 6.6. Loss reactions, mainly formation of lactic acid from sugars are not included in the reaction set. There is no explicit modeling of inhibitory effects from furans and acetic acid. The assumed conversions are based on actual fermentation experiments, where inhibitors are present, which means that the effects are implicit.



**Table 6.6:** Batch fermentation reactions and assumed conversions.

Reaction	Conversion [%]
Glucose $\rightarrow$ 2 Ethanol + 2 CO <sub>2</sub>	95.0
Glucose + 0.147 Lactic Acid + 0.018 DAP $\rightarrow$ 6 <i>Z. mobilis</i> + 2.4 H <sub>2</sub> O	2.0
3 Xylose $\rightarrow$ 5 Ethanol + 5 CO <sub>2</sub>	85.0
Glucose + 0.122 Lactic Acid + 0.015 DAP $\rightarrow$ 5 <i>Z. mobilis</i> + 2 H <sub>2</sub> O	1.9

The resulting fermentation broth, or beer, are sent to area 300 for ethanol recovery and purification. The CO<sub>2</sub> produced in the seed train and batch reactor are vented and sent to a water scrubber (SCR-200). The CO<sub>2</sub> dissolved in the beer are distilled off in the beer column (COL-300) in area 300, and mixed with the vented CO<sub>2</sub>. The scrubber is modeled as a phase separator. The amount of water used on the scrubber is assumed to be equal to the mass of the combined vent stream into the scrubber. 99.9% of incoming CO<sub>2</sub> are removed. The water from the scrubber contains some ethanol (from the beer column), and gets recycled into the fermentation batch tank.

### 6.3 Area 300: Ethanol Recovery

A process flow diagram of this process area is shown in figure 6.4.

The beer from area 200, containing 3.2 wt% ethanol is fed to the beer column (COL-300) after heat exchange with the beer column liquid bottoms. The beer column is designed to remove all dissolved CO<sub>2</sub> as a top vapour stream, while at the same time removing most of the water (94%) in the bottom stream. The top vapour, containing small amounts of ethanol, are sent to the water scrubber (SCR-200), where most of the ethanol (73%) are recovered and recycled. The bottom stream contains all residual solid material, and are sent to area 500 after heat exchange with the beer column feed stream. The ethanol is removed as a vapour side-stream and is fed directly into the rectification column (COL-301). The rectifier bottoms are almost pure water and are recycled to area 100 as process water. Both columns are modeled using rigorous vapour-liquid distillation column models in HYSYS. The design specifications and operating conditions are outlined in table 6.7.

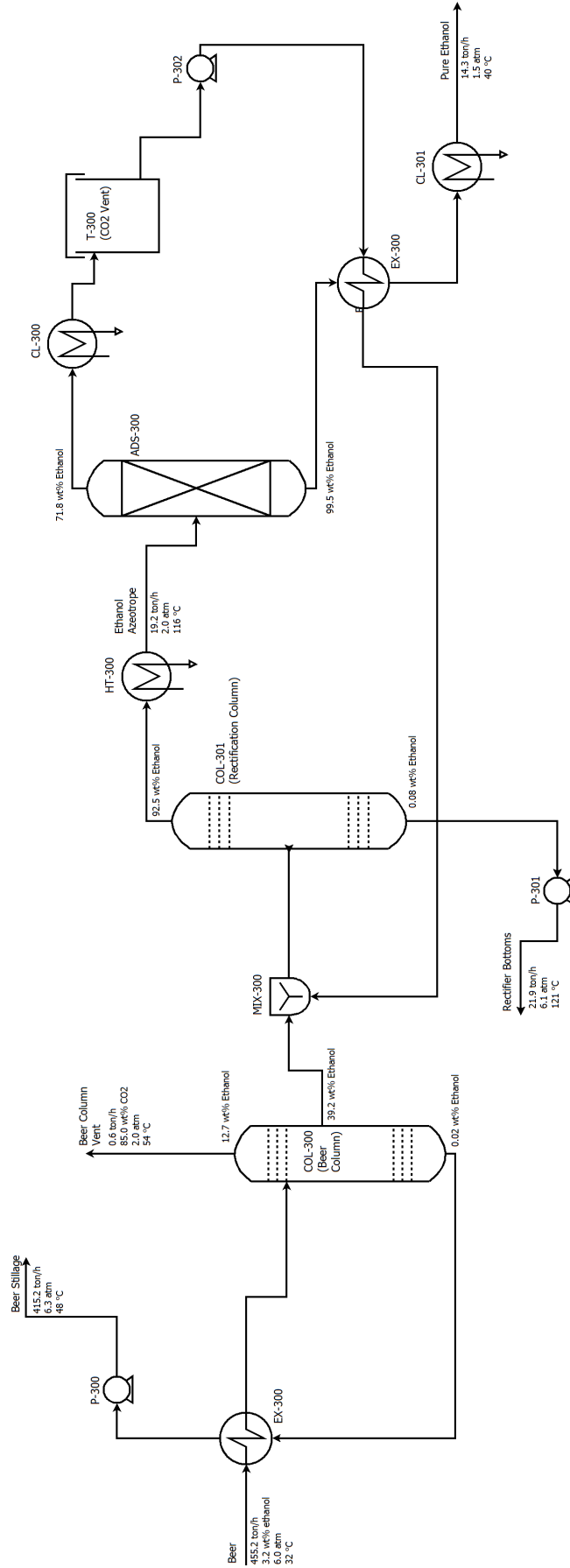


Figure 6.4: Process flow diagram of the ethanol recovery process.

**Table 6.7:** Design specifications and operating conditions of ethanol distillation columns.

Specification	Beer Column	Rectification Column
Trays	32	45
Tray efficiency [%]	48.0	76.0
Feed ethanol composition [wt%]	3.2	43.1
Feed tray	4	22
Draw ethanol composition [wt%]	39.2	92.5
Reboiler duty [kJ/h]	$1.844 \cdot 10^8$	$9.277 \cdot 10^6$
Condenser duty [kJ/h]	$8.600 \cdot 10^7$	$4.887 \cdot 10^7$

The columns are designed based on information in the NREL design report. Tray efficiencies are given in the report, and used in the column design. It is worth noting that the tray efficiency in the beer column is significantly lower than in the rectification column. The reason for this is not explained in the NREL report, but it is assumed that it is meant to account for solid material in the beer column, making for less optimal tray design. Both columns are also designed with appropriate pressure drop obtained from the NREL design report.

The azeotropic ethanol vapour from the rectification column are heated to 116 °C (HT-300) before it enter the molecular sieve adsorption system (ADS-300). The system consist of two columns packed with beds of adsorbent. As the vapour passes through, water is selectively adsorbed in the beds, while ethanol flows through, producing a pure ethanol stream (99.5 wt%). One column is used for adsorption while the other regenerates. The regeneration is accomplished by passing a slip stream of pure ethanol through the water-saturated beds at vacuum pressure. The ethanol strips of the water, producing a 72 wt% ethanol stream. The stream is cooled to 35 °C (CL-300) to remove any dissolved CO<sub>2</sub> (T-300), before it is heated (EX-301) and returned to the rectification column.

The molecular sieve adsorption system is modeled as a simple component splitter. Adjustment blocks are used to obtain the specified compositions in the ethanol products stream (99.5 wt%) and in the ethanol recycle stream (72 wt%).

The initial heat exchanger (EX-300) and the beer column are operated with liquid streams containing residual solid material. The solid material is mainly lignin, with rests of xylan and cellulose. It is assumed that after pretreatment, hydrolysis and fermentation, the remaining

solid is highly porous. In addition, the insoluble solids content is no more than 4 wt%, and nominal liquid flow is assumed.

#### 6.4 Area 400: Furfural Production and Recovery

Process flow diagrams of the furfural production and recovery process are shown in figure 6.5 and 6.6 respectively.

Xylose (5.8 wt%) is pressurized to 15.6 atm and heated to 187 °C (EX-400). The pre-heated xylose stream is mixed with a reactor recycle stream before heated to the final reactor feed temperature of 201 °C (HT-400), just under the bubble point. The reactor feed enters the reactive distillation column (COL-400) at the top tray.

The column is modeled as a rigorous vapour-liquid distillation column with a specified reaction set. The reaction set includes the acid catalyzed reaction of xylose into furfural, and glucose into levulinic acid and formic acid. The reaction kinetics are given in table 5.2. As furfural is formed by xylose dehydration, it immediately vapourizes. As it joins the vapour up-flow, it is no longer in contact with the reactive acidic phase, motivating the exclusion of all furfural loss reactions.

Furfural is drawn as a 5.0 wt% vapour stream at the column top. The dilute furfural is pressurized to 19.7 atm (COMP-400), and is heat exchanged in the column reboiler. The energy invested in compressing the top vapour is small (~ 3%) compared to column reboiler duty. The remaining vapour is condensed in EX-400, where the pressure is lowered to atmospheric pressure. Further, the column bottom stream is controlled by the furfural concentration in the column top vapour. The bottom and top stream is almost equal in this design. The bottom is split (SPLIT-400) in a recycle stream and a wastewater stream. The recycle ratio is set to give a column acid loading of 1.75 wt%, which is appropriate for furfural production. Marcotullio [4] suggested the use of halide salts such as NaCl or KCl for increased selectivity in furfural formation. As the reaction kinetics do not reflect the use of such salts, the addition of such compounds is excluded from the simulation.

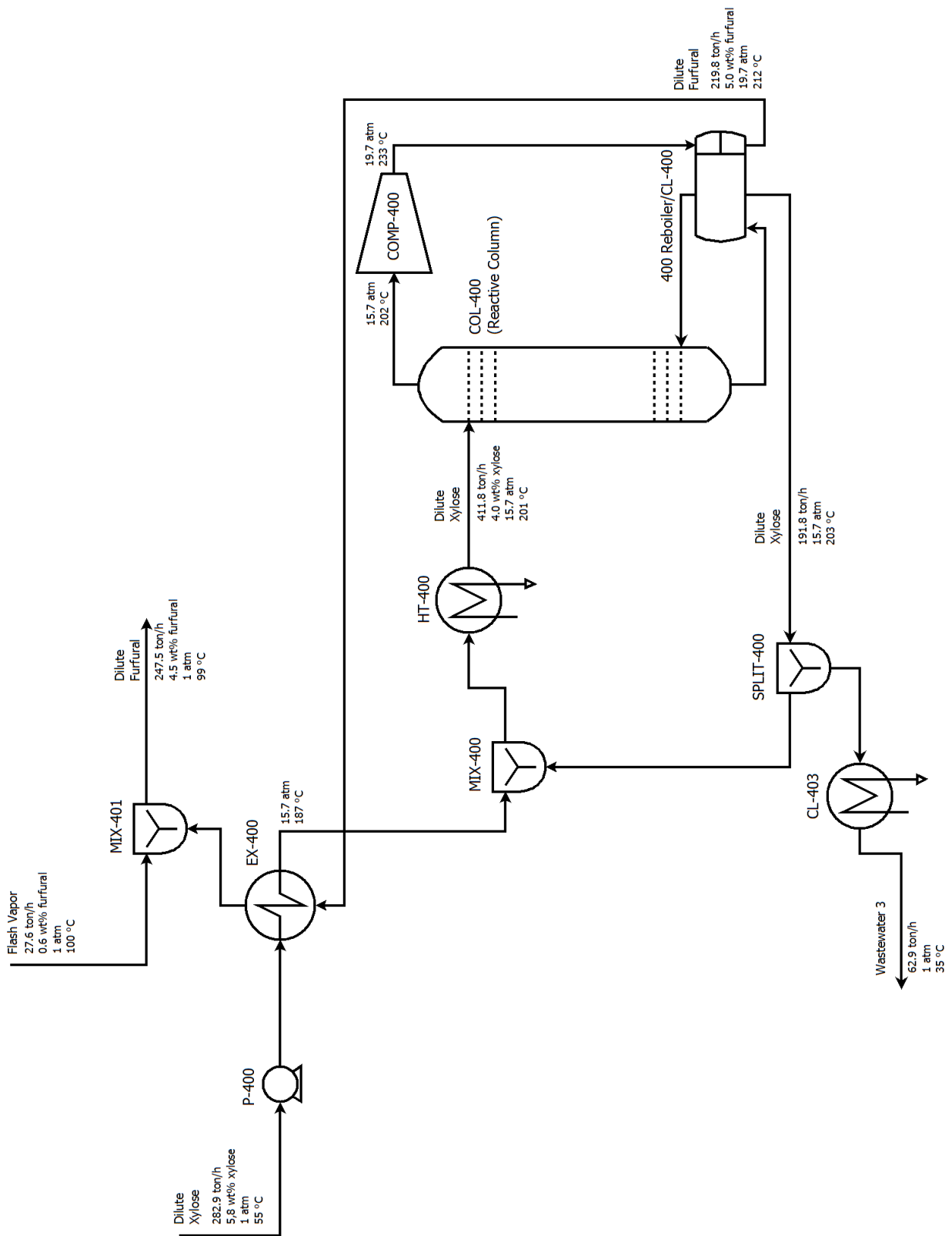


**Figure 6.5:** Process flow diagram of the furfural production process.

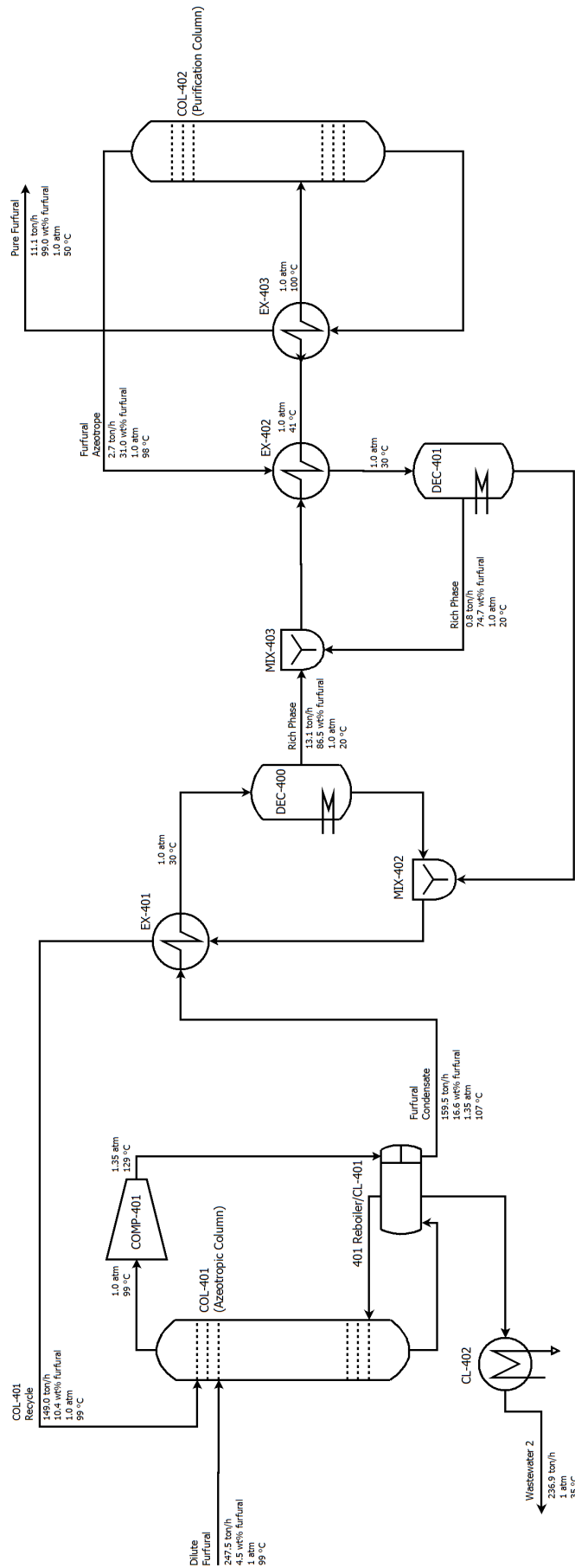


Figure 6.6: Process flow diagram of the furfural recovery process.

The dilute furfural is mixed with the combined flash stream from area 100, and fed to the azeotropic distillation column (COL-401). Volatiles, mainly ethanol, are removed as a vapour top stream, while furfural is drawn as a vapour side stream at 16.6 wt%. The furfural vapour stream is compressed (COMP-401) to 1.35 atm, and condensed in the reboiler of the COL-401 reboiler. The furfural condensate is further cooled in EX-402, before entering the primary decanter (DEC-400). The decanter liquid content is cooled to 20 °C to promote phase separation. The decanter separates the two liquid phases to a furfural weak and rich phase. The weak phase (10.4 wt%) is heated in EX-402 and recycled to the azeotropic column. The recycle is fed at stage 5, slightly higher than the dilute furfural feed, as it is richer in furfural. The rich phase (86.5 wt%) is recovered for further purification.

The furfural rich phase is heated to 100 °C in EX-403 and EX-404 and fed to the furfural purification column. This is a small distillation column with few stages, designed to boil off the remaining water. The water is removed at a near azeotropic composition at the top of the column, while pure furfural (99%) is removed as a liquid, and cooled in EX-404. The top azeotrope stream is cooled in EX-403 before entering the secondary decanter. The liquid content is cooled to 20 °C to promote phase separation as in the primary decanter. The furfural rich phase is directed to the purification column, while the furfural weak phase is recycled back to the azeotropic column. The design specifications and operating conditions for the two distillation columns are outlined in table 6.8.

**Table 6.8:** Design specifications and operating conditions of furfural distillation columns.

<b>Specification</b>	<b>Azeotropic Column</b>	<b>Purification Column</b>
<b>Trays</b>	30	12
<b>Tray efficiency [%]</b>	100.0	100.0
<b>Feed furfural composition [wt%]</b>	4.5	85.8
<b>Feed tray</b>	8	10
<b>Draw furfural composition [wt%]</b>	16.6	99.0
<b>Reboiler duty [kJ/h]</b>	$3.06 \cdot 10^8$	$5.19 \cdot 10^6$
<b>Condenser duty [kJ/h]</b>	$1.19 \cdot 10^7$	$4.48 \cdot 10^6$

The number of trays in the azeotropic column is based on the Marcotullio design, while the trays in the purification is a pure estimate based on observed energy consumption. The reboiler duty is below 2% of the azeotropic column reboiler duty, so further optimization of this is considered unnecessary at this point. As there is no information on tray efficiency for

neither of the columns, 100.0% is used as a first assumption. Pressure drop is also assumed negligible in all three columns as an initial approximation.

An important aspect of the furfural production process presented in this area is the immediate separation of furfural from the reactive liquid phase in the reactive distillation column. While the sulfuric acid is left in the liquid phase, considerable amounts of organic acids, mainly acetic acid, is boiled off the top of the column with the furfural. The total acid content in the dilute furfural stream is about 0.5 wt%. Considerable amounts of this acid is present in the vapour stream from the azeotropic distillation column, and some of it ultimately ends up in the 99 wt% furfural product stream. As acidity has a negative impact on furfural loss reactions, the industrial solution would be to neutralize the azeotropic column feed stream. The acids would then leave the aqueous bottom stream in the azeotropic column as soluble salts. This would in turn have a positive effect on separation performance and energy consumption, as acetic acid would no longer be present in the recycle streams.

Finally, the two wastewater streams from the reactive distillation column and the azeotropic column are cooled to 35 °C in CL-403 and CL-402 respectively, and sent to wastewater treatment in area 500.

## 6.5 Area 500: Wastewater Treatment and Steam Boiler

A process flow diagram of this area is shown in figure 6.7.

The cooled liquid bottom stream from the beer column (COL-300) is pressurized to 6.3 atm and fed to a pressure filter (FIL-500) for solid-liquid separation. The separation is performed by filtration only, without any washing of the solids. The solid cake is dried with air to 40-45% moisture. The separation unit is modeled as a simple component splitter. Explicit modeling of air consumption is not included. The split factors are simply set to achieve the given performance of the filtration unit. This is analogous to the approach used in the washing unit in area 100. Here to, it is assumed that no solids are lost to the liquid stream. The dried lignin is sent to a burner (BUR-500), while the wastewater is cooled (CL-500) to 35 °C for anaerobic digestion, and mixed with the two wastewater streams from area 300. This mixing is not included in the model.



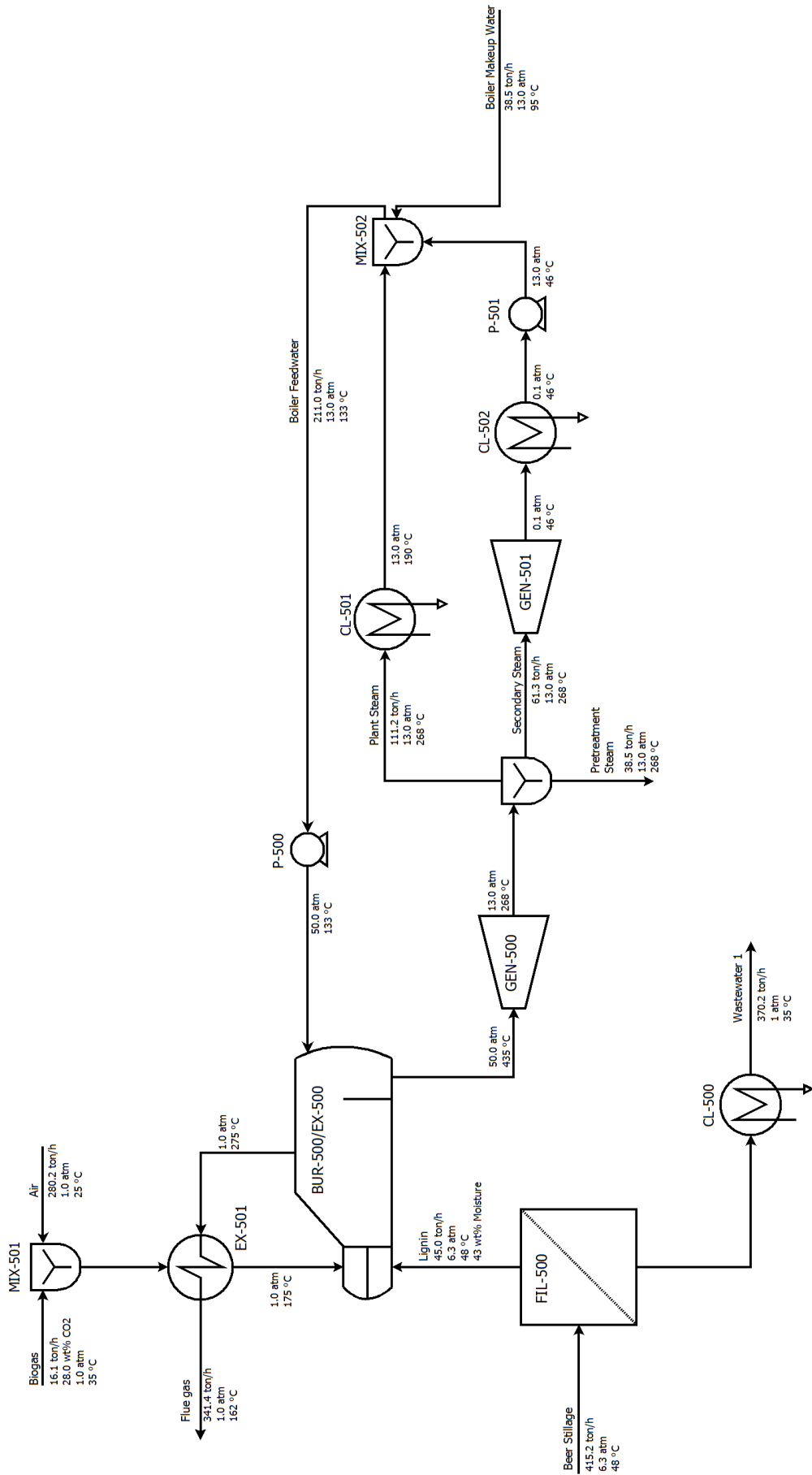


Figure 6.7: Process flow diagram of the steam boiler process.

The motivation for including treatment of wastewater is to get an estimate of the electricity and heat that can be produced by burning lignin and methane produced by anaerobic digestion. Therefore, a rigorous model of the actual water treatment has not been included. In reality, wastewater treatment is a combination of anaerobic digestion, aerobic digestion, clarification and evaporation to produce useful process water. A spreadsheet (S:Anaerobic Digester) has been used to calculate the amount of methane and CO<sub>2</sub> produced by anaerobic digestion of organic material in the wastewater. The basis for the calculation is the combined chemical oxygen demand (COD) for the organic matter present in the wastewater. COD is defined as the oxygen needed for complete oxidation of organic material.

The methane production rate is calculated as 228 g/kg COD removed, based on design specifications from NREL. It is assumed that 91% of the organic matter is utilized for anaerobic digestion. CO<sub>2</sub> is also produced at a near equimolar rate to methane, forming a 51% methane/49% CO<sub>2</sub> mixture on a dry molar basis.

An important aspect in anaerobic digestion is to have a reasonable concentration of organic matter to get an efficient production of methane. The COD loading of the combined wastewater streams for this process is in the range of 30 g/L wastewater. The loading in the NREL wastewater treatment process is 67 g/L. 30 g/L is still sufficient for methane production, but it is questionable if the efficiency is comparable to NREL.

The resulting methane/CO<sub>2</sub> biogas is mixed with air, and preheated with the flue gas to about 175 °C in EX-501. It is then fed into the burner (BUR-500), where methane is burned together with solid material from the pressure filter. The burner is modeled as a conversion reactor. All combustible material is assumed burned with oxygen at 100.0% conversion. Excess air is used to get an outlet temperature of 1500 C. The conversion reactor forces the use of a liquid outlet in addition to the gas outlet. This stream mostly consist of incombustible solid ash. The two outlet streams are combined to one stream in MIX-500, as the ash is assumed to flow with the flue gas in a real burner. The combined flue gas is heat exchanged with high pressure steam in a boiler (EX-500) and further cooled in EX-501. The heat transfer relative to the heat of combustion is 84%. Choosing a lower combustion temperature would bring this closer to 80%, which is the heat transfer reported by NREL for their steam boiler.

The steam boiler is modeled as a rankine cycle consisting of the actual boiler, two steam turbines, two steam condensers and two liquid pumps. Pre heated makeup water (95 C) is received from area 100, and mixed with the condensed steam from the condensers. The

combined water is pressurized to 50.0 atm (P-500) and fed to the boiler. The boiler produces superheated high pressure steam at 435 °C. The high pressure steam is used to drive the primary turbine (GEN-500), which produces electricity at an assumed adiabatic efficiency of 85%. The outlet medium pressure steam is split (SPLIT-500) into three streams. Most of the steam is used as either direct steam injection heating in area 100, or for indirect steam heating in the plant (CL-501). The remainder is used to drive the secondary turbine (GEN-501), which also produced electricity at an assumed adiabatic efficiency of 85%. The outlet vacuum steam is condensed with cooling water (CL-502) and then pressurized to 13.0 atm (P-501).

The split is adjusted so that the heat of condensation of medium pressure plant steam (CL-501) equals the heating demand, which is further discussed in chapter 7. The two generators produces almost 30 MW electricity, which corresponds to a cycle energy efficiency of 15.6%. The cycle is tuned towards production of high-grade medium pressure steam used for heating. As this is considered useful energy for the plant, the combined energy efficiency exceeds 65%.



## 7. Heat Integration

Information about heat exchangers and heat integration are given in both the NREL design report and the Marcotullio process design, and implemented in HYSYS as described in chapter 6. Heat exchangers, heaters and coolers in area 100, 200, 300 and 500 are all based on the NREL design, while area 400 is based on the Marcotullio design. The reactive distillation column (COL-400) is fully heat integrated with the top vapour by equalizing the duties of the COL-400 Reboiler and CL-400. The azeotropic distillation column is also fully heat integrated with the top vapour by equalizing the duties of the COL-401 Reboiler and CL-401.

Additional cooling and heating requirements are summarized in table 7.1 and 7.2. These includes reboilers, condenser, heaters and coolers that are yet not integrated in any way in the HYSYS implementation.

From table 7.2, we see that the only stream useful for further heat integration is from CL-403, which is the wastewater from the reactive distillation column (COL-400). This stream could be used for heating of T-200. Assuming constant heat capacity, a match between these two would give an outlet temperature of 65.9 C, and a minimum temperature difference of 17.9 C, which is sufficient. Cooling water are used for cooling the remainder of CL-403 along with all other units listed in table 7.2.

**Table 7.1:** Heating requirements for the plant. Start and end temperatures for the stream to be heated are given. These are set equal for the reboilers.

Unit Operation	Energy [kJ/h]	Start Temp. [C]	End Temp. [C]
<b>T-200 (Enzymatic Hydrolysis)</b>	$3.19 \cdot 10^7$	48.0	48.0
<b>COL-300 Reboiler</b>	$1.85 \cdot 10^8$	125.7	125.7
<b>COL-301 Reboiler</b>	$9.33 \cdot 10^6$	120.6	120.6
<b>COL-402 Reboiler</b>	$4.19 \cdot 10^6$	156.7	156.7
<b>HT-300</b>	$8.98 \cdot 10^5$	88.8	116.0
<b>HT-400</b>	$1.56 \cdot 10^7$	191.1	201.0
<b>Total Heating Requirement</b>	<b><math>2.69 \cdot 10^8</math></b>	-	-

**Table 7.2:** Cooling requirements for the plant. Start and end temperatures for the stream to be cooled are given. These are set equal for the condenser.

Unit Operation	Energy [kJ/h]	Start Temp. [C]	End Temp. [C]
<b>COL-300 Condenser</b>	$8.59 \cdot 10^7$	54.3	54.3
<b>COL-301 Condenser</b>	$4.94 \cdot 10^7$	88.8	88.8
<b>COL-401 Condenser</b>	$1.19 \cdot 10^7$	96.3	96.3
<b>COL-402 Condenser</b>	$4.48 \cdot 10^6$	97.9	97.9
<b>CL-200</b>	$1.28 \cdot 10^6$	48.7	48.0
<b>CL-201</b>	$2.85 \cdot 10^7$	48.0	32.0
<b>T-201 (Seed train)</b>	$2.40 \cdot 10^6$	32.0	32.0
<b>T-202 (Fermentation)</b>	$2.16 \cdot 10^7$	32.0	32.0
<b>CL-300</b>	$7.14 \cdot 10^6$	116.0	35.0
<b>CL-301</b>	$1.36 \cdot 10^7$	88.8	40.0
<b>CL-402</b>	$6.44 \cdot 10^7$	100.0	35.0
<b>CL-403</b>	$3.91 \cdot 10^7$	202.7	35.0
<b>DEC-400</b>	$6.00 \cdot 10^6$	20.0	20.0
<b>DEC-401</b>	$8.84 \cdot 10^4$	20.0	20.0
<b>CL-502</b>	$1.26 \cdot 10^8$	46.1	46.0
<b>Total Cooling Requirement</b>	<b><math>4.62 \cdot 10^8</math></b>	-	-
<i>CL-501 (Steam Boiler Cycle)</i>	$2.37 \cdot 10^8$	268	190

After integration of T-200, there is still an unmet heating demand of over  $2.37 \cdot 10^8$  kJ/h. This is supposed covered by the medium pressure steam from area 500 (CL-501). The HT-400 has an outlet temperature slightly higher than the condensing temperature of the medium pressure steam. The steam, however, is superheated to 268 °C, and carries approximately  $1.7 \cdot 10^7$  kJ/h beyond the saturation point. This just covers the HT-400 Heating demand. A better solution would be to have an additional steam level with slightly higher pressure for HT-400 heating, but this is omitted for simplicity. As a final clarification; the electricity and heat production as implemented in HYSYS relies on the match of T-200 with CL-403, although it is not implemented in the simulation. It is also assumed that the medium pressure steam can cover the HT-400 heating demand.

The incoming process water streams are set to 25 °C. This is based on the assumption that the water source is recycled water from wastewater treatment. However, there will be a significant makeup stream of fresh water at a temperature closer to 5-15 °C, depending on the

location of the plant. Initial heating of this water to 25 °C is assumed covered by the streams mentioned in table 7.2, as the excess heat available at this temperature range is abundant.

### 7.1 Alternative Heat Integration

An alternative to the heat integration implemented in this design is to use medium pressure steam produced in area 500 to heat the reactive distillation column (COL-400), and use the top vapour from this column to heat the other column reboilers. This would eliminate the need of compression of the column top vapour (COMP-400). However, this would require implementation of one additional steam level in the steam boiler cycle, as the bubble point temperature at 13.0 atm is below the reboiler temperature of the reactive column. This would in turn decrease the electricity production from the cycle, as the pressure in the additional steam level would be raised from 13.0 atm to about 20.0 atm. This would offset the electricity savings of eliminating the compressor, and additional investment costs are also required. Heat integration and energy optimization is further discussed in chapter 8.





## 8. Analysis and Discussion

Many of the results obtained from the flowsheet calculations performed in HYSYS will be discussed and compared to the NREL ethanol plant and the Marcotullio process. The results are directly comparable, as the feedstock rate and composition is equal to that used by NREL. In addition, the xylose stream formed in the pretreatment process is similar to the liquid feedstock assumed by Marcotullio.

### 8.1 Carbon and Energy Balance

The overall carbon mole balance for the plant is presented in table 8.1. Included are all carbon inlets and the major carbon outlets. As seen in the table, over 98% of the carbon enters as corn stover feedstock. Other carbon sources include corn steep liquor used as fermentation nutrition and cellulase enzyme for cellulose hydrolysis. The carbon balance is not fully closed, as carbon outlets totals to about 96% of total incoming carbon. The reason for this is the simplified modeling of wastewater treatment, where only 91% of the COD is removed in anaerobic digestion. In addition, some soluble organics is found in the filtrated lignin (FIL-500), that is not accounted for. The reaction set for the burner (BUR-500) only includes reactions for combustion of solid material and methane, neglecting the minor organic components. Only carbon in the form of CO<sub>2</sub> is accounted for in the flue gas stream.

**Table 8.1:** Overall Carbon Mole Balance.

Stream	Carbon Flow [kmol/h]	% of Total Carbon Inlet
<b>Carbon Inlets</b>		
<b>Corn Stover Feedstock</b>	3,116	98.6
<i>Useful Carbon</i>	1856	-
<b>Corn Steep Liquor (CSL)</b>	16	0.5
<b>Cellulase</b>	29	0.9
<b>Total</b>	3160	100.0
<b>Carbon Outlets</b>		
<b>Ethanol</b>	619	19.6
<b>Furfural</b>	577	18.3
<b>Scrubber Vent</b>	315	9.9
<b>Flue Gas</b>	1,552	48.7
<b>Total</b>	3,048	96.4

Of the total carbon input to the process, 19.6% leaves as ethanol and 18.3% as furfural. The remaining carbon exits the plant as CO<sub>2</sub> formed during fermentation or combustion. The useful carbon listed in the table 8.1 represents cellulose and xylan present in the feedstock, which is available for conversion into either ethanol or furfural. Of this carbon, 928 kmol/h is converted by the ethanol-route, including CO<sub>2</sub> released in the scrubber vent. 577 kmol/h is converted by the furfural-route and recovered as furfural, resulting in a combined carbon utilization of 81.1% of the theoretical. This is slightly higher than the 76% obtained by NREL in its ethanol plant [23]. The formation of furfural from xylose in the reactive distillation column in area 400 has a conversion approaching 100%, as no loss or side reactions are considered. The losses during product recovery is also negligible, making the efficiency of furfural production very high, which explains the higher utilization of carbon in this plant.

**Table 8.2:** Lower heating value (LHV) of corn stover feedstock and products. Excess electricity is also included.

<b>Stream</b>	<b>LHV [GJ/h]</b>
<b>Corn Stover</b>	1,369
<i>Useful Carbon</i>	802
<b>Ethanol</b>	381
<b>Furfural</b>	260
<i>Electricity</i>	67

Table 8.2 shows the lower heating value of the feedstock and the products, including the excess electricity produced. The combined energy of ethanol, furfural and excess electricity is 52% of the energy content in the corn stover, which is a little higher than the 48% obtained by NREL. However, as will be discussed in section 8.4, a reasonable assumption may be that the excess electricity of the plant is close to zero. This reduces the energy content of the products to 47% of the corn stover. If only the carbohydrate fraction of the corn stover is considered, the energy content of the products is 80%, similar to the carbon efficiency.

The utilization of carbon may be somewhat overestimated, as all pentosans are modeled as xylan and all hexosans are modeled as cellulose. It is uncertain to what degree monosaccharides such as mannose, galactose and arabinose may be fermented into ethanol. The error of doing this, however, is assumed to be small, as these sugars are directed into area 400 for furfural production. In this area, all hexoses, including glucose from cellulose, is

assumed lost to by-products. Further, all pentoses (mainly arabinose) are assumed to dehydrate into furfural in the same way as xylose.

## 8.2 Ethanol Recovery Performance

Important process parameters related to ethanol recovery in area 300 are compared to the corresponding process area in the NREL ethanol plant, and presented in table 8.3.

**Table 8.3:** Comparison of data for ethanol recovery. The data is given as specific values relative to the given ethanol production rate, for easy comparison. Data for comparison is taken from [23].

	<b>This Work</b>	<b>NREL</b>	<b>Change [%]</b>
<b>Ethanol Production [ton/h]</b>	14.3	21.8	-34
<b>Beer Column Feed Composition [wt%]</b>	3.2	4.9	-35
<b>Beer Column Draw Composition [wt%]</b>	39.2	37.0	6
<b>Heating Demand [GJ/ton]</b>	13.7	7.47	83
<i>COL-300 Reboiler [GJ/ton]</i>	12.9	6.33	104
<i>COL-301 Reboiler [GJ/ton]</i>	0.65	1.08	-40
<i>HT-300 [GJ/ton]</i>	0.06	0.06	9

As the majority of xylose formed during pretreatment are recovered for furfural production, the ethanol production rate scales correspondingly. The specific heating demand however is over 80% higher, which is related to increased specific reboiler duty in the beer column (COL-300). The ethanol content in the beer fed to the beer column is 3.2 wt%, compared to 4.9 wt% in the NREL process, which explains the increased specific heating demand of the reboiler. The ethanol content in the beer column vapour draw is also slightly higher. A more efficient design may be to lower the vapour draw composition, shifting separation to the rectification column.

## 8.3 Furfural Production and Recovery Performance

The furfural production and recovery process in area 400 is somewhat altered to the original process proposed by Marcotullio. The reactive distillation column (COL-400) bottoms is split into a recycle stream and a purge stream. The recycle stream is about 70% of the column bottoms, and is used to increase the concentration of sulfuric acid in the column from 0.8 wt% to 1.75 wt%. The purge is sent to wastewater treatment and is *not* recycled back to the column. This increases the furfural content in the column top vapour from 2.7 wt% to 5.0

wt%. A purifying column (COL-402) is also included to increase the purity of the produced furfural to 99.0 wt%.

Table 8.4 summarizes some important performance data of the process area compared to the Marcotullio process. The xylose content in the liquid stream received from area 100 is 5.8 wt%, slightly higher than the 5.0 wt% assumed by Marcotullio. 0.7 ton/h furfural also flows into area 400 along with the pretreatment flash and the xylose feed. This explains the specific xylose feed of 1.49 ton xylose/ton furfural, which implies a furfural yield greater than 100%. If the extra furfural produced in area 100 is accounted for, the furfural yield is still over 99%. A major premise for excluding side and loss reactions is the assumption of instantaneous separation of furfural from the reactive liquid phase. Figure 8.1 shows the actual flow of furfural in the reactive column.

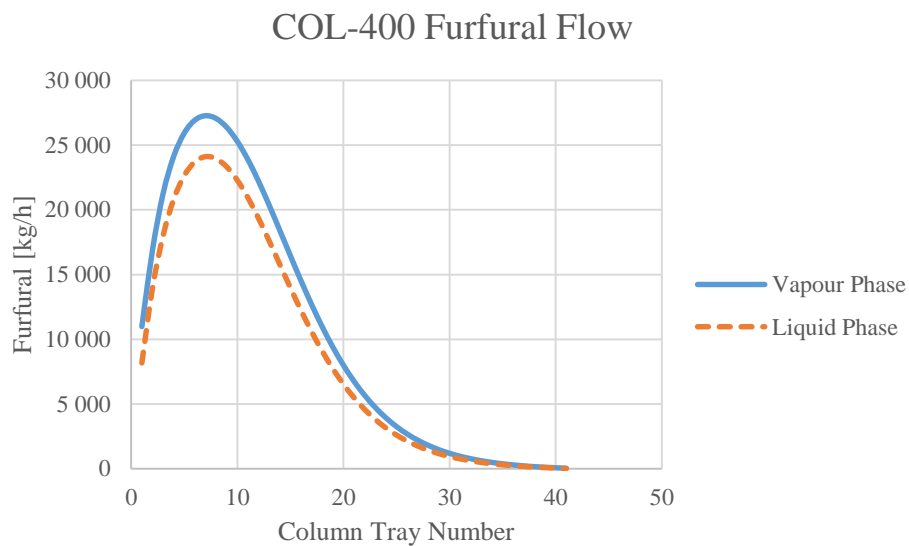


**Figure 8.1:** Total flow of furfural in vapour and liquid phase as a function of column tray number.

Approximately 40-50% of the total furfural at each state is present in the liquid phase. This shows the yield of furfural obtained in this process is overestimated, as there will be acid catalyzed loss reactions in the reactive column. Loss and side reactions with appropriate reaction kinetics could be implemented for increased accuracy.

**Table 8.4:** Comparison of main performance data for production and recovery of furfural. The data are given as specific values relative to the given furfural production rate, for easy comparison. The COL-401 Recycle Factor described the ratio of the recycle stream into the azeotropic distillation column relative to the main feed into the same column. Data for comparison are taken from [4].

	<b>This Work</b>	<b>Marcotullio</b>	<b>Change [%]</b>
<b>Furfural Production [ton/h]</b>	11.0	2.67	312
<b>Xylose Feed [ton/ton]</b>	1.49	1.88	-20
<b>COL-401 Recycle Factor</b>	0.60	0.27	122
<b>Heating Demand [GJ/ton]</b>	1.89	-	-
<b>Total Electricity Demand [kWh/ton]</b>	524	668	-22
<i>COMP-400 [kWh/ton]</i>	<i>319</i>	<i>488</i>	<i>-35</i>
<i>COMP-401 [kWh/ton]</i>	<i>215</i>	<i>180</i>	<i>20</i>

The COL-401 Recycle Factor describes the ratio of the recycle stream received from the primary decanter (DEC-400) relative to the main furfural feed into the column. The relative recycle is more than doubled in this design, compared to Marcotullio. The increased recycle factor is mostly a result of the higher concentration of xylose and furfural used in this process. The somewhat inaccurate prediction of LLE behavior in the decanter also contributes to this. The calculated rich phase furfural composition at 20 °C and atmospheric pressure is in the range off 86-87 wt% , while it is closer to 95% in reality [4, 39]. The phase separation model could be substituted with a simple component splitter. The decanter feed however contains considerable amounts of acetic acid, making the implementation less trivial. Acetic acid and other carboxylic acids is normally neutralized before the recovery process, as acidity has negative impact on furfural yields. If this were added to the model, the acetic acid would leave the process with the wastewater stream in the azeotropic column as a soluble salt, making the implementation of the decanter as a component splitter easier.

The effect of inaccurate LLE behavior is assumed to be negligible for the overall performance of the furfural recovery. The calculated furfural content in the rich phase is assumed to have negligible impact on the purification column (COL-402). It is a small column compared to the other, and has a correspondingly low reboiler duty.

The other consideration is how the LLE behavior affects the separation of the phases. While the rich phase furfural concentration is underestimated, the weak phase furfural concentration is overestimated correspondingly, as shown in chapter 5. By assuming an incoming decanter

feed of 16.6 wt% furfural in pure water, the ratio of weak phase relative to the rich phase is only 3.5% larger than in the real case. This shows that the inaccurate LLE behavior has little influence on the amount of recycle to the azeotropic column, and hence its performance and eventual sizing. The error however increases with increasing concentration of acetic acid, as it increases the mutual solubility of water and furfural, which is indicated in figure 5.4.

The maximum composition for maintaining complete integration is found to be 16.6 wt % furfural, which is a little higher than that used by Marcotullio. This may be explained by the higher furfural content in the column main feed. By increasing the furfural content in the vapour draw towards the azeotropic composition (35 wt%), the heat of condensation of the vapour draw no longer meet the heating demand of the column reboiler, and additional heat must be provided by steam. The reason for choosing a lower furfural concentration is that separation of furfural from water is weighted towards the decanter, where separation occurs spontaneously without the use of energy. The main objective of the column is therefore to increase the furfural concentration for effective phase separation in the decanter, while using as little energy as possible.

The total specific heating demand is calculated to 1.89 GJ/ton furfural. Marcotullio do not report this figure, so no comparison is done. In addition to this, there is also the implicit heating demand of the steam injection in the pretreatment area, necessary to produce the liquid xylose feed. The pretreatment steam usage is 3.5 ton steam/ton furfural. The theoretical energy requirement of producing steam at 13.0 atm is 2.83 GJ/ton, which corresponds to a theoretical heating demand of 11.8 GJ/ton furfural. Steam usage in pretreatment, however, is a prerequisite for the production of ethanol, whether the resulting xylose is used to produce furfural or not. Because of this, the implied heating demand of the pretreatment steam is not included in the calculated heating demand given in table 8.4.

The specific heating demand in existing furfural plants varies, but a conservative estimate is 40 GJ/h [4], assuming a steam consumption of 15 ton/ton furfural. This illustrates the remarkable advantage of integrating furfural production with ethanol production, enabling the use of a liquid xylose feed.

The total specific electricity demand is reduced compared with Marcotullio, due to the changes made in the implementation of the reactive column, and the higher xylose concentration in the feed.

## 8.4 Heat Recovery and Electricity Production

The steam boiler cycle is somewhat simplified compared to the corresponding modeling done by NREL. An overview of the produced electricity and steam is given in table 8.5. As discussed in section 8.1, the utilization of useful carbon is higher in this work, and this decreases the amount of carbon converted to methane in the anaerobic digestion system. This explains the slightly reduced boiler duty and cycle water flow.

**Table 8.5:** Steam boiler cycle performance data, and data from the NREL ethanol plant for comparison [23]. The amount of wastewater, and the produced methane from anaerobic digestion, is also included. These are given as absolute values, while the rest are given as specific values relative to the boiler duty.

	<b>This Work</b>	<b>NREL</b>	<b>Change [%]</b>
<b>Wastewater Loading [ton/h]</b>	670.0	376.3	78
<b>Methane Production [kg/h]</b>	4052	5378	-25
<b>Boiler Duty [GJ/h]</b>	565.8	604.6	-6
<b>Cycle Makeup [kg/GJ]</b>	68.0	58.4	9
<b>Cycle Flow [kg/GJ]</b>	372.9	388.4	-10
<i>Plant Steam Heating [kg/GJ]</i>	<i>196.5</i>	<i>124.4</i>	<i>48</i>
<i>Pretreatment Steam Heating [kg/GJ]</i>	<i>68.0</i>	<i>46.4</i>	<i>37</i>
<i>Vacuum Steam [kg/GJ]</i>	<i>108.3</i>	<i>167.8</i>	<i>-40</i>
<i>Boiler Preheating [kg/GJ]</i>	<i>-</i>	<i>49.8</i>	<i>-</i>
<b>Electricity Generated [kWh/GJ]</b>	52.2	68.4	-29

As seen in table 8.5, the generated steam is either used for plant heating, direct steam injection in the pretreatment area or used for electricity production in the secondary steam turbine (GEN-501). NREL also includes a dedicated fraction for economizing preheating of the boiler water, but this is excluded in this design. The steam used for plant heating is 48% larger in this design. This is due to the increased heating demand in the beer column (COL-300), and the added heating demand that comes with the integration of furfural production. The steam used for direct steam injection in the pretreatment area is also increased, mainly due to increased steam use in the pretreatment reactor (PFR-100). NREL has neglected the heat of reaction for all reactions in their design. As the hydrolysis of cellulose and hemicellulose is endothermic, the steam demand suggested in this work is assumed more accurate, as heat of reaction is included in the simulation.

The increased demand for steam heating reduces the electricity produced in the secondary steam turbine (GEN-501). This in turn reduced the total amount of produced electricity by 29%. A summary of electricity production and plant consumption is given in table 8.6.

**Table 8.6:** Overall electricity production and consumption for the plant.

<b>Process Unit</b>	<b>Power [kW]</b>
<b>Electricity Production</b>	
<b>GEN-500</b>	17850
<b>GEN-501</b>	11660
<b>Total</b>	29510
<b>Electricity Consumption</b>	
<b>Area 100</b>	4377
<b>Area 200</b>	146
<b>Area 300</b>	73
<b>Area 400</b>	5904
<b>Area 500</b>	364
<b>Total</b>	10864
<b>Excess Electricity</b>	18646

The electricity consumption is the sum of all electricity streams in the simulation, and do not accurately represent the electricity demand in an actual plant. NREL reports an electricity consumption related to wastewater treatment of 7.5 MW in their design. The amount of wastewater in this plant is almost 80% higher, mainly due to increased usage of process water because of integrated furfural production. If is electricity consumption is assumed directly proportional to wastewater loading, the electricity demand associated to wastewater treatment would be 13.3 MW in this plant. This reduced the excess electricity to 5.4 MW. Electricity for mixing, agitation and circulation in tanks, batch reactors and distillation columns are also neglected in the design, and it is unclear if the plant would be self sufficient with electricity. NREL report a total electricity consumption of 28.5 MW. The estimated electricity consumption related to furfural production is just below 6 MW, which indicates that there would be a small deficiency of electricity. A detailed model of the wastewater treatment is needed for more certain estimates on the electricity balance.



## 8.5 Process Optimization

A lot of the process parameters used in this work are retrieved from the NREL ethanol plant design, and the Marcotullio process, which is assumed individually optimized. However, the integration of the two process changes some important process parameters, such as the beer ethanol concentration and the overall ethanol production rate. A lot of the process optimization requires sizing of process equipment, and implementation of a rigorous economical model for the overall process. An example of this is related to the sizing and operation of the batch reactors used for hydrolysis and fermentation, along with the seed train batch reactors. The economic optimum is a complex relation between reaction kinetics, enzyme loading, conversion ratios and equipment sizing. While a complete economic model of the plant is considered outside the scope of this work, some general remarks can be made.

Most of the possible optimization is related to heat integration and possible reduction in energy demand. As seen in section 8.2, the amount of water introduced in the process, and hence the ethanol concentration in the beer, has great impact on the heating demand of the ethanol recovery process. Reducing water consumption is a general optimization target in most industrial aqueous process, such as the pulping industry, and will be important for further energy optimization in this process.

### 8.5.1 Area 400 Column Integration

Heat exchanger design, and selection of minimum temperature difference, is also important for process economics. Higher energy recovery must be traded off over increased investment costs related to installed heat exchanger area. An example of this is the heat integration of the two larger columns in area 400.

Figure 8.2 and 8.3 shows how installed heat exchanger area and compressor duty varies with the pressure used for vapour compression in COMP-400 and COMP-401 respectively. The combined purchase cost of the reboiler and corresponding compressor is also included. Purchase cost is estimated based on cost equations given in [22]. The cost is on a U.S. Gulf Coast basis, as of January 2010. The cost are not adjusted to present value, because it is meant to give insight into the confined design choice.

### COL-400 Heat Integration

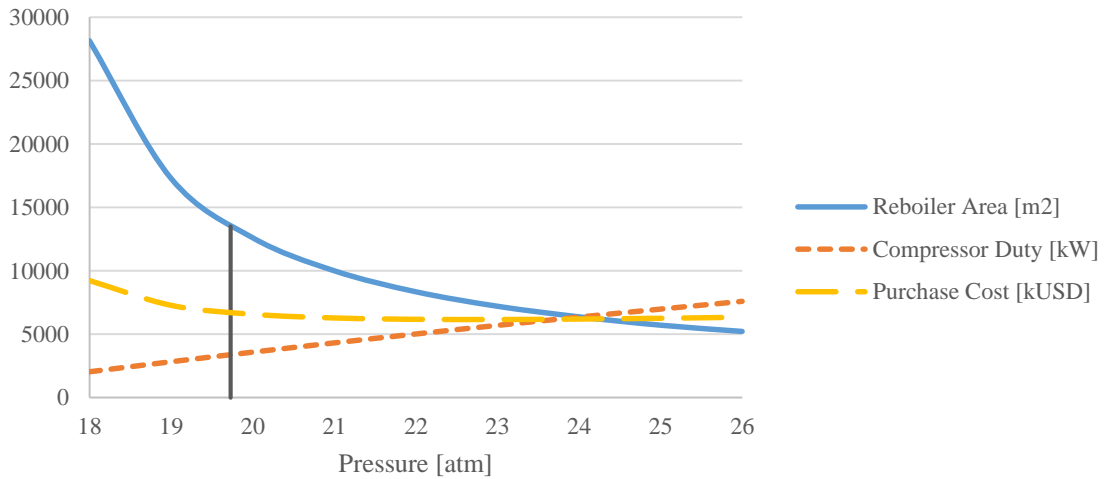


**Figure 8.2:** Installed reboiler heat exchanger area and compressor duty as a function of outlet pressure in the compressor [COMP-400]. Purchase cost of reboiler and compressor is included. The vertical line indicates the design pressure.

### COL-401 Heat Integration

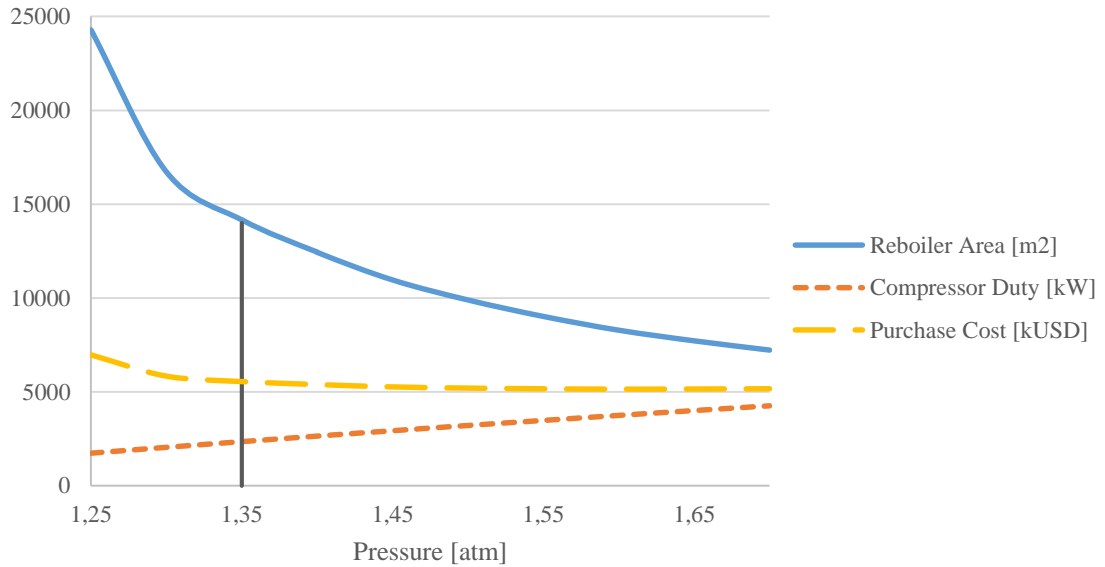


**Figure 8.3:** Installed reboiler heat exchanger area and compressor duty as a function of outlet pressure in the compressor [COMP-401]. Purchase cost of reboiler and compressor is included. The vertical line indicates the design pressure.

The total purchase cost of the equipment for COL-400 integration reaches a minimum at 23 atm. The heat exchanger cost drives the cost at lower pressure, while the compressor cost drives the cost at increased pressures. By choosing the design pressure at 19.7 atm, the

compressor duty is reduced by 33%, at the expense of an 8.8% increase in purchase cost relative to the minimum.

A similar trend is observed for COL-401, where the total purchase cost reaches a minimum at 1.6 atm. Here to, reboiler cost drives the cost at decreased pressure, while the compressor cost drives the cost at increased pressure. The purchase cost at the design pressure is 7.8% higher than the minimum, while the compressor duty is decreased by 37%. The true optimum design pressure will be a function of the price of electricity at the plant location. The change in pressure in the two vapour streams also has slight effect on the overall performance in area 400. This in turn will make for minor differences in steam heating demand and produced electricity in area 500. This must also be accounted for when designing the heat integration.

### 8.5.2 COL-401 Vapour Draw Composition

Another consideration already discussed in section 8.4 is the azeotropic column vapour draw composition. Figure 8.4 shows how the composition affects the performance of the furfural recovery.

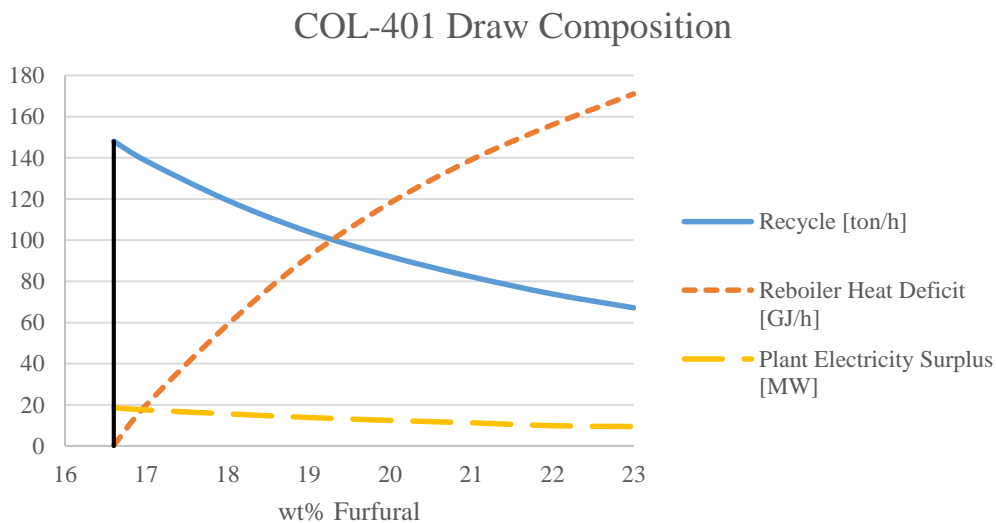


**Figure 8.4:** Column recycle inlet, reboiler heat deficit and overall plant electricity surplus as a function of varying composition in the column vapour draw. The vertical line indicates the design composition.

By increasing the concentration of furfural beyond 16.6 wt% and towards the azeotropic point, the reboiler is no more fully heat integrated with the vapour stream. The higher purity reduces the recycle and the power consumption of vapour compression. The reduced power consumption do not make up for the increased heating demand, and the overall plant electricity surplus decreases from 18.6 MW at 16.6 wt% to 9.5 MW at 23.0 wt%. Beyond this

point, the secondary turbine [GEN-501] stops producing electricity. To be able to deliver enough heating, the steam boiler cycle design must be changed. Calculations from 23.0 wt% towards the azeotropic point is therefore not investigated.

### 8.5.3 COL-300 Vapour Draw Composition

The specific heating demand of ethanol recovery is shown to be over 80% higher compared to the NREL ethanol recovery process. The reason for this is the decrease in ethanol concentration in the initial beer. As the beer composition has changed, the design of the recovery process may be suboptimal. Figure 8.5 shows how the beer column vapour draw composition affects the reboiler duties of the beer column and rectification column.

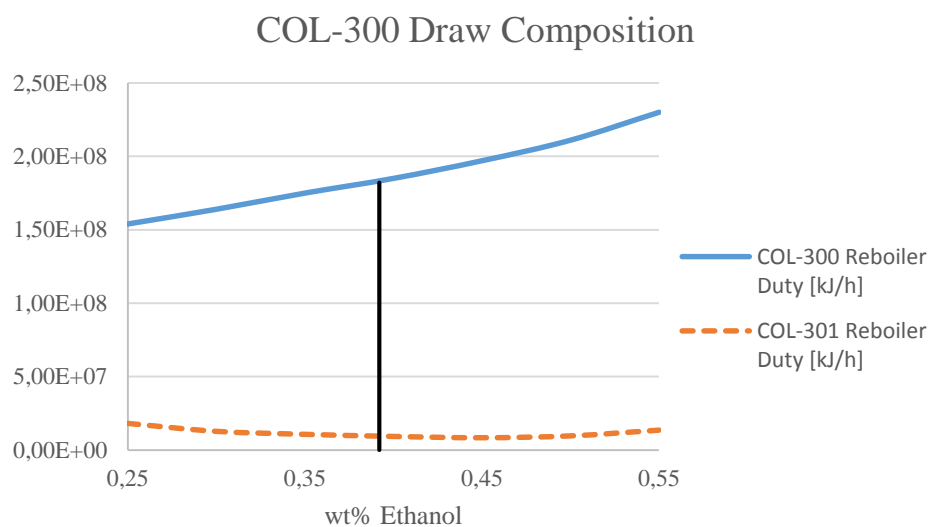


**Figure 8.5:** Reboiler duty in beer column and rectification column as a function of varying composition in the beer column vapour draw. The vertical line indicates the design composition.

The figure suggest that a more optimal design could be achieved by lowering the ethanol content in the vapour draw from the beer column. This means that more water must be separated in the rectifying column. However, the calculations are based on the assumption that the number of stages and the size of the two columns are unchanged. The implied saving of lowering the ethanol content is therefore most likely overestimated. The design composition is actually in the lower end of what is common in industrial distillation processes. Ethanol content in the beer column vapour draw usually range from 40-60 wt%. [43]. The design composition is therefore assumed close to the optimal design.

### 8.5.4 Steam Boiler Cycle Pressure

The steam boiler cycle electricity production is highly influence by the choice of pressure in the boiler heat exchanger. Figure 8.6 shows how the produced electricity in the two steam

turbines vary with the cycle pressure, while at the same time producing the specified amount of medium pressure steam for heating.

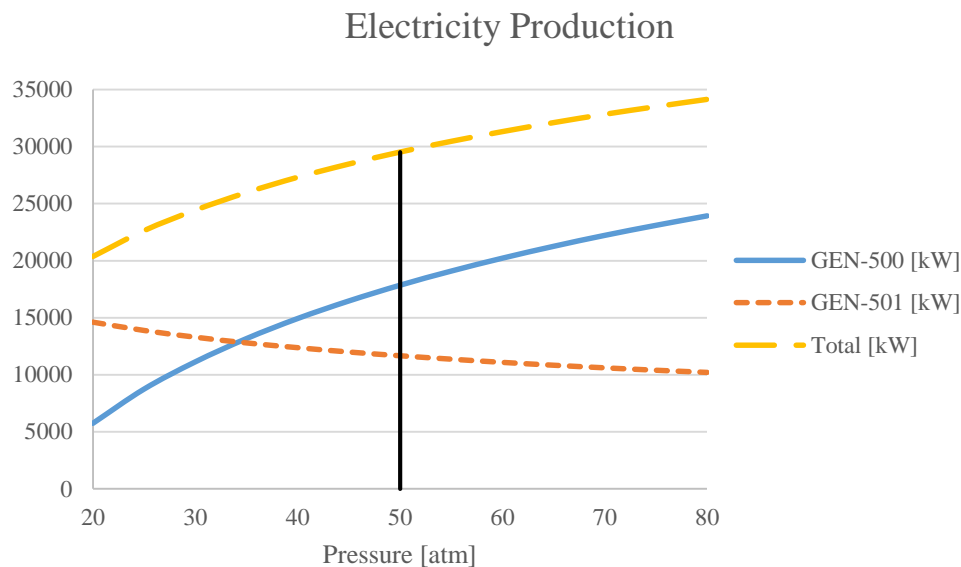


**Figure 8.6:** Produced electricity in the two steam turbines in the steam boiler cycle as a function of the cycle pressure in the boiler.

The electricity production would increase by choosing a higher design pressure. However, as the pressure increases, so does the temperature at which the majority of heat exchange occur. Pressures exceeding 100 atm is common in real boilers used for heat recovery in combined cycle power plants. This however requires two or more steam levels, such that heat transfer is spread over a broader temperature range. For processes where the main goal is heat production, it is generally considered sufficient to use one steam level, and that a lower than optimal pressure is used. The steam boiler design used by NREL is quoted as an “off-the-shelf-technology,” which means that design considerations such as pressure and temperature already are accounted for. The design pressure of 50 atm is a little lower than the 62 atm used by NREL, and the calculated electricity production is most likely in the conservative end.

## 8.6 Market Considerations

As mentioned earlier, a rigorous economic model including detailed estimates on investment cost, production cost and revenues are considered outside the scope of this work. Some general information on raw material and product prices are given in table 8.7. Additional cost related to ash disposal, purchase of sulfuric acid catalyst and fermentation nutrition is not considered at this point.

The most certain price is that of ethanol, as there is a well-established market for it, especially in the U.S. The cost of cellulase is quoted based on estimations from one of the major enzyme producers, Novozymes. The price estimate however is from 2007, and is here used more as a guideline. The price of corn stover is also an estimate, as the market is yet to be established at a large scale. Further, the price of furfural is quoted from a market report on the Chinese furfural market. The price has seen a steady decline from over 1500 USD/ton in March, 2013 to 1000 USD/ton in April, 2016, and is expected to further decrease [35]. The same trend is observed for ethanol.

**Table 8.7:** Overview of main feedstock costs and products revenue [27, 31, 35, 44].

	<b>Flow [ton/year]</b>	<b>Price [USD/ton]</b>	<b>Cash Flow [MUSD/year]</b>
<b>Corn Stover (20 wt% H<sub>2</sub>O)</b>	875,400	50	-43.8
<b>Cellulase</b>	4,700	6270	-29.5
<b>Ethanol [99.5%]</b>	120,400	500	60.2
<b>Furfural [99.0%]</b>	93,300	1000	93.3
<b>Total</b>	-	-	80.2

For furfural, decline in market demand combined with increased competition and struggle for market shares makes the future production of it uncertain. The market size is estimated to 300 kton/year [34]. The proposed use of furfural as a platform chemical with numerous new areas of applications is yet to be materialized in the market. In addition, recent declines in oil prices has made petroleum based chemicals even more attractive. The proposed integrated production of furfural presented in this work has a production rate of over 93 kton/year, which is almost one third of the current market demand. Construction of such a plant would greatly influence the market price negatively, and it is uncertain if it would be economically feasible. However, the acid pretreatment process with subsequent washing allows for high adaptability. Figure 8.7 shows how the washing yield (the extent of washing) can be tuned to vary the production of ethanol and furfural. The prerequisite for such adaptability is appropriate sizing of the ethanol specific part of the plant, which would increase the initial investment costs.

### Washing Yield Influence on Production

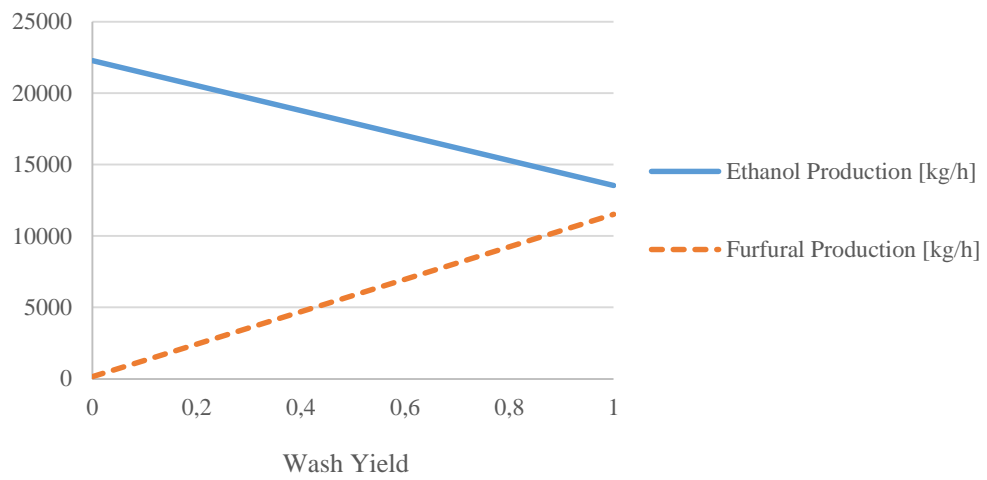


**Figure 8.7:** Ethanol and furfural production rate as a function of pretreatment washing yield.





## 9. Conclusion

An integrated process for production of ethanol and furfural from corn stover was successfully implemented in HYSYS. The design was based on the NREL ethanol process and the Marcotullio furfural process. The plant uses 875,400 ton/year of corn stover as feedstock, and produces 120,400 ton/year 99.5 wt% ethanol and 93,300 ton/year 99.0 wt% furfural. The combined carbon utilization of the process was found to be 81.1%, which is slightly higher than comparable processes. This is in part explained by lossless formation of furfural assumed in the reactive distillation. The simulation of the column shows that loss reactions could be implemented for increased accuracy in prediction of furfural yield, and that the obtained carbon utilization may be overestimated.

The furfural production and recovery process was slightly altered compared to the Marcotullio process. The xylose feed concentration was increased from 5.0 to 5.8 wt%. A purge stream in the reactive distillation recycle was also added. Specific heating demand was found to be 1.89 GJ/ton furfural, while the specific electricity demand was reduced from 668 to 524 kWh/ton furfural.

A specific plant area was implemented to estimate energy and electricity production from combustion of residual solid material and methane produced by anaerobic digestion of wastewater. A steam boiler cycle was used to produce steam for direct steam injection in the pretreatment process and medium pressure steam for plant heating. The steam turbines generates a total of 29.5 MW of electricity, with a calculated plant excess of 18.6 MW. Electricity consumption associated with wastewater treatment was not accounted for, and the excess electricity is assumed to be close to zero.

The plant electricity production is 28.6% lower in the NREL ethanol process, due to reduced performance in the ethanol recovery process. The specific reboiler heating demand in ethanol recovery is found to be 83% higher, mainly due to a more dilute fermentation broth. Heating associated with integrated furfural production also reduces the production of electricity.

A rigorous economic model was considered outside the scope of this work. The HYSYS model is a good basis for further assessment of the economic viability of the process. Better accuracy could be achieved by adding furfural loss reactions. It is also recommended to include an additional fluid package with binary coefficients optimized for LLE behaviour. Poor estimation of LLE behaviour is found to have negligible effect on performance, but

would be a prerequisite for appropriate equipment sizing. A further ambition could be the addition of kinetic reaction sets for the enzymatic hydrolysis and fermentation. This would enable the use of HYSYS for all equipment sizing, including continuous reactors, batch reactors and distillation columns, and would simplify optimization with regards to equipment sizing and investment costs.

# References

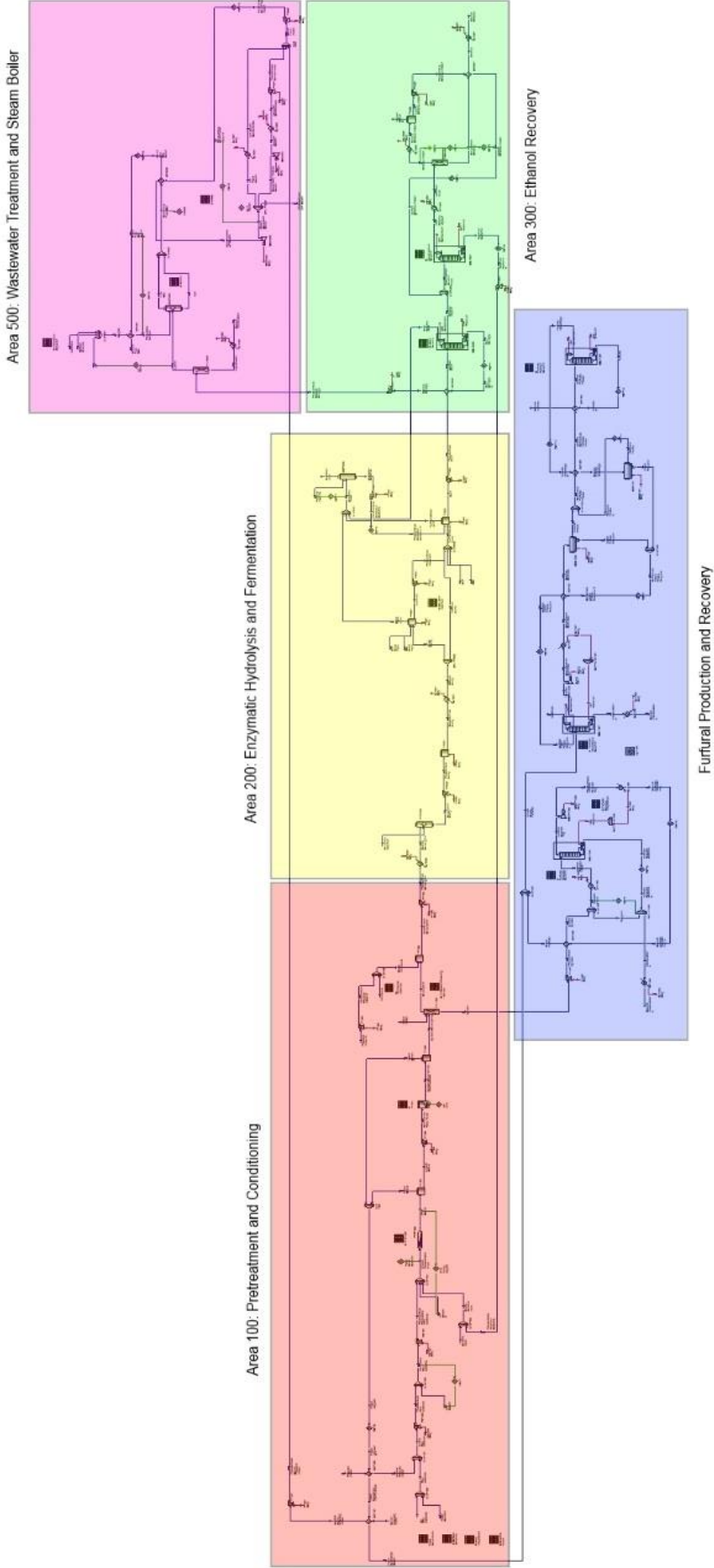
1. Kamm, B., et al., *Biorefinery Systems – An Overview*, in *Biorefineries-Industrial Processes and Products*. 2008, Wiley-VCH Verlag GmbH. p. 1-40.
2. *US Biofuels: Climate Change and Policies*. [cited 2016 2 June]; Available from: <http://www.worldwatch.org/files/pdf/Biofuels%20Issue%20Brief.pdf>.
3. De Jong, W. and G. Marcotullio, *Overview of biorefineries based on co-production of furfural, existing concepts and novel developments*. *International journal of chemical reactor engineering*, 2010. **8**(1).
4. Marcotullio, G., *The chemistry and technology of furfural production in modern lignocellulose-feedstock biorefineries*. 2011: TU Delft, Delft University of Technology.
5. Stokke, D.D., Q. Wu, and G. Han, *Lignocellulosic Materials*, in *Introduction to Wood and Natural Fiber Composites*. 2013, John Wiley & Sons Ltd. p. 19-59.
6. Wyman, C.E., *Special issue: Biotechnology for the conversion of lignocellulosics Ethanol from lignocellulosic biomass: Technology, economics, and opportunities*. *Bioresource Technology*, 1994. **50**(1): p. 3-15.
7. Haghghi Mood, S., et al., *Lignocellulosic biomass to bioethanol, a comprehensive review with a focus on pretreatment*. *Renewable and Sustainable Energy Reviews*, 2013. **27**: p. 77-93.
8. Rowell, R.M., *Handbook of Wood Chemistry and Wood Composites*. 2005: CRC Press.
9. Vassilev, S.V., et al., *An overview of the organic and inorganic phase composition of biomass*. *Fuel*, 2012. **94**: p. 1-33.
10. Agarwal, U.P., R.R. Reiner, and S.A. Ralph, *Cellulose crystallinity of woods, wood pulps, and agricultural fibers by FT-Raman Spectroscopy*. *Red*, 2011. **19**(60.7): p. 67.9.
11. Zhao, X., L. Zhang, and D. Liu, *Biomass recalcitrance. Part I: the chemical compositions and physical structures affecting the enzymatic hydrolysis of lignocellulose*. *Biofuels, Bioproducts and Biorefining*, 2012. **6**(4): p. 465-482.
12. Clements, L.D. and D.L. Van Dyne, *The Lignocellulosic Biorefinery- A Strategy for Returning to a Sustainable Source of Fuels and Industrial Organic Chemicals*, in *Biorefineries-Industrial Processes and Products*. 2008, Wiley-VCH Verlag GmbH. p. 115-128.
13. Hayes, D.J., et al., *The biofine process—production of levulinic acid, furfural, and formic acid from lignocellulosic feedstocks*. *Biorefineries—Industrial Processes and Product*, 2006. **1**: p. 139-164.
14. Van Dyne, D.L., M.G. Blase, and L.D. Clements, *A strategy for returning agriculture and rural America to long-term full employment using biomass refineries. Perspectives on new crops and new uses*. ASHS Press, Alexandria, Va, 1999: p. 114-123.
15. Mosier, N., et al., *Features of promising technologies for pretreatment of lignocellulosic biomass*. *Bioresource Technology*, 2005. **96**(6): p. 673-686.
16. Sun, Y. and J. Cheng, *Hydrolysis of lignocellulosic materials for ethanol production: a review*. *Bioresource Technology*, 2002. **83**(1): p. 1-11.
17. Carrasco, F. and C. Roy, *Kinetic study of dilute-acid prehydrolysis of xylan-containing biomass*. *Wood Science and Technology*, 1992. **26**(3): p. 189-208.
18. Drapcho, C.M., N.P. Nhuan, and T.H. Walker, *Biofuels Engineering Process Technology*. 2008.

19. Saeman, J.F., *Kinetics of Wood Saccharification - Hydrolysis of Cellulose and Decomposition of Sugars in Dilute Acid at High Temperature*. Industrial & Engineering Chemistry, 1945. **37**(1): p. 43-52.
20. Lavarack, B.P., G.J. Griffin, and D. Rodman, *The acid hydrolysis of sugarcane bagasse hemicellulose to produce xylose, arabinose, glucose and other products*. Biomass and Bioenergy, 2002. **23**(5): p. 367-380.
21. *Washing*. 2005 [cited 2016 28 April]; Available from: [https://noppa.lut.fi/noppa/opintojakso/bj60a1400/materiaali/6\\_washing.pdf](https://noppa.lut.fi/noppa/opintojakso/bj60a1400/materiaali/6_washing.pdf).
22. Towler, G. and R.K. Sinnott, *Chemical Engineering Design - Principles, Practice and Economics of Plant and Process Design (2nd Edition)*. Elsevier.
23. Humbird, D., et al., *Process design and economics for biochemical conversion of lignocellulosic biomass to ethanol: dilute-acid pretreatment and enzymatic hydrolysis of corn stover*. 2011, National Renewable Energy Laboratory (NREL), Golden, CO.
24. Montague, L., A. Slayton, and J. Lukas, A. Aden, M. Ruth, K. Ibsen, J. Jechura, K. Nieves, J. Sheehan, and B. Wallace.
25. *World Agricultural Production*. [cited 2016 20 may]; Available from: <http://apps.fas.usda.gov/psdonline/circulars/production.pdf>.
26. *World of Corn*. 2015 [cited 2016 16 May]; Available from: <http://www.worldofcorn.com/pdf/WOC%20Metric.pdf>.
27. Ertl, D., *Sustainable corn stover harvest*. Iowa Corn Promot Board, 2013: p. 1-8.
28. *Commercial-scale cellulosic ethanol plant opens*. [cited 2016 4 May]; Available from: <https://www.eia.gov/todayinenergy/detail.cfm?id=17851>.
29. *World Fuel Ethanol Production*. [cited 2016 5 May]; Available from: <http://www.ethanolrfa.org/resources/industry/statistics/#1459794955504-26451131-8a1b>.
30. Öhgren, K., et al., *A comparison between simultaneous saccharification and fermentation and separate hydrolysis and fermentation using steam-pretreated corn stover*. Process Biochemistry, 2007. **42**(5): p. 834-839.
31. *Ethanol Price*. [cited 2016 25 May]; Available from: <http://www.tradingeconomics.com/commodity/ethanol>.
32. Cai, C.M., et al., *Integrated furfural production as a renewable fuel and chemical platform from lignocellulosic biomass*. Journal of Chemical Technology and Biotechnology, 2014. **89**(1): p. 2-10.
33. Zeitsch, K.J., *The chemistry and technology of furfural and its many by-products*. Vol. 13. 2000: Elsevier.
34. Machado, G., et al., *Literature Review on Furfural Production from Lignocellulosic Biomass*. Natural Resources, 2016. **7**(03): p. 115.
35. *Furfural Market Comment*. [cited 2016 27 May]; Available from: <http://www.cnchemicals.com/Press/86385-CCM:%20China's%20market%20price%20of%20furfural%20bounces%20back%20in%20April.html>.
36. Peleteiro, S., et al., *Furfural production using ionic liquids: A review*. Bioresource Technology, 2016. **202**: p. 181-191.
37. Bhandari, N., D.G. Macdonald, and N.N. Bakhshi, *Kinetic studies of corn stover saccharification using sulphuric acid*. Biotechnology and Bioengineering, 1984. **26**(4): p. 320-327.
38. Chang, C., X. Ma, and P. Cen, *Kinetics of Levulinic Acid Formation from Glucose Decomposition at High Temperature I*. Chinese Journal of Chemical Engineering, 2006. **14**(5): p. 708-712.
39. A. *Properties of furfural*, in *Sugar Series*, J.Z. Karl, Editor. 2000, Elsevier. p. 234-239.

40. *Furfural Properties*. [cited 2016 18 May]; Available from: [http://www.furan.com/\\_resources/downloads/Physical\\_Properties\\_of\\_Furfural.pdf](http://www.furan.com/_resources/downloads/Physical_Properties_of_Furfural.pdf).
41. Speight, J.G., *Lange's handbook of chemistry*. McGraw Hill Standard Handbook, New York Table, 2005. **4**: p. 4.41-4.51.
42. Garrote, G., H. Dominguez, and J. Parajo, *Hydrothermal processing of lignocellulosic materials*. European Journal of Wood and Wood Products, 1999. **57**(3): p. 191-202.
43. Amarasekara, A.S., *Handbook of Cellulosic Ethanol*. 2013, Somerset, US: Wiley-Scrivener.
44. Zhuang, J., et al., *Economic analysis of cellulase production methods for bio-ethanol*. Applied Engineering in Agriculture, 2007. **23**(5): p. 679-687.




# A HYSYS Simulation Flowsheet










# B HYSYS Workbook


1	 NORWEGIAN UNIV OF Burlington, MA USA		Case Name: Biorefinery.hsc			
2			Unit Set: SI			
3			Date/Time: Mon Jun 06 13:32:03 2016			
4						
5	<b>Workbook: Case (Main)</b>					
6	<b>Material Streams</b> <span style="float: right;">Fluid Pkg: All</span>					
7						
8						
9						
10						
11	Name	Flash Outlet	Dry Raw Material	Xylose/Cellulignin	Wash Water	Cellulignin
12	Vapour Fraction	1.0000	0.0000	0.0000	0.0000	0.0000
13	Temperature (C)	130.1	25.00 *	101.4	25.00 *	54.61
14	Pressure (kPa)	257.4	101.3 *	101.3 *	101.3	101.3
15	Molar Flow (kgmole/h)	796.9	697.8	1.132e+004	1.973e+004	1.705e+004
16	Mass Flow (kg/h)	1.450e+004	8.331e+004 *	2.786e+005	3.554e+005	3.511e+005
17	Liquid Volume Flow (m3/h)	14.51	62.79	260.5	356.1	339.2
18	Heat Flow (kJ/h)	-1.902e+008	-5.383e+008	-3.506e+009	-5.620e+009	-5.013e+009
19	Name	Xylose	PFR Outlet	Liquid Outlet	Conversion Tank Feed	Xylose/Cellulignin Int
20	Vapour Fraction	0.0000	0.0000	0.0000	0.0000	0.0000
21	Temperature (C)	54.60	158.0	130.1	130.3	129.5
22	Pressure (kPa)	101.3	577.6	257.4 *	972.7 *	577.6 *
23	Molar Flow (kgmole/h)	1.399e+004	1.283e+004	1.203e+004	1.203e+004	1.204e+004
24	Mass Flow (kg/h)	2.829e+005	3.062e+005	2.917e+005	2.917e+005	2.917e+005
25	Liquid Volume Flow (m3/h)	277.4	288.0	273.5	273.5	273.6
26	Heat Flow (kJ/h)	-4.113e+009	-3.869e+009	-3.679e+009	-3.679e+009	-3.679e+009
27	Name	Flash Outlet 2	Pressurized Cellulignin	Mixed Raw Material	MP Steam 2	Preheated Raw Mater
28	Vapour Fraction	1.0000	0.0000	0.0000	1.0000	0.0000
29	Temperature (C)	101.4	48.71	77.09	268.0 *	99.97
30	Pressure (kPa)	101.3 *	435.7 *	101.3	1317 *	359.7
31	Molar Flow (kgmole/h)	718.6	2.210e+004	9572	1898	9809
32	Mass Flow (kg/h)	1.310e+004	4.421e+005	2.432e+005	3.419e+004 *	2.475e+005
33	Liquid Volume Flow (m3/h)	13.11	430.4	223.0	34.26	227.3
34	Heat Flow (kJ/h)	-1.722e+008	-6.451e+009	-3.026e+009	-4.438e+008	-3.074e+009
35	Name	Mixed Pressurized Fe	Water Content	Raw Material	Pressurized Raw Mate	Pressurized Preheate
36	Vapour Fraction	0.0597	0.0000	0.0000	0.0000	0.0000
37	Temperature (C)	162.0	25.00 *	25.00	86.40	109.4
38	Pressure (kPa)	618.1	101.3 *	101.3	359.7 *	618.1 *
39	Molar Flow (kgmole/h)	1.295e+004	1156	1854	9572	9809
40	Mass Flow (kg/h)	3.062e+005	2.083e+004	1.041e+005	2.432e+005	2.475e+005
41	Liquid Volume Flow (m3/h)	285.0	20.87	83.66	223.0	227.3
42	Heat Flow (kJ/h)	-3.869e+009	-3.294e+008	-8.677e+008	-3.018e+009	-3.066e+009
43	Name	Pressurized Rectifier	Dilute Sulfuric Acid	Neutralized Cellulignin	Cooled Cellulignin	Cellulignin Slurry
44	Vapour Fraction	0.0000	0.0000	0.0000	0.0000	0.0000
45	Temperature (C)	120.6	116.6	48.65	48.00 *	47.42
46	Pressure (kPa)	618.1 *	618.1	101.3	253.3 *	253.3
47	Molar Flow (kgmole/h)	1214	1247	2.210e+004	2.210e+004	2.271e+004
48	Mass Flow (kg/h)	2.191e+004	2.454e+004	4.421e+005	4.421e+005	4.533e+005
49	Liquid Volume Flow (m3/h)	21.95	23.44	430.4	430.4	441.5
50	Heat Flow (kJ/h)	-3.370e+008	-3.595e+008	-6.451e+009	-6.452e+009	-6.623e+009
51	Name	Saccharified Slurry	Pressurized Slurry	Seed Slurry	Fermentation Feed	Fermentation Vent
52	Vapour Fraction	0.0000	0.0000	0.0000	0.0000	1.0000
53	Temperature (C)	48.00 *	47.47	32.00	32.00	32.00
54	Pressure (kPa)	101.3 *	516.8 *	101.3	101.3	101.3
55	Molar Flow (kgmole/h)	2.256e+004	2.271e+004	2256	2.262e+004	288.6
56	Mass Flow (kg/h)	4.533e+005	4.533e+005	4.533e+004	4.533e+005	1.236e+004
57	Liquid Volume Flow (m3/h)	445.6	441.5	44.56	446.2	14.93
58	Heat Flow (kJ/h)	-6.591e+009	-6.622e+009	-6.619e+008	-6.623e+009	-1.111e+008
59	Name	Beer	Seed Train Vent	Inoculum	Pressurized Inoculum	Transfer Slurry
60	Vapour Fraction	0.0000	1.0000	0.0000	0.0000	0.0000
61	Temperature (C)	32.00 *	32.00	32.00 *	32.06	32.00
62	Pressure (kPa)	101.3	101.3	101.3	506.6 *	101.3
63	Molar Flow (kgmole/h)	2.357e+004	30.05	2284	2284	2.030e+004
64	Mass Flow (kg/h)	4.552e+005	1287	4.430e+004	4.430e+004	4.080e+005
65	Liquid Volume Flow (m3/h)	455.5	1.555	44.26	44.26	401.0
66	Heat Flow (kJ/h)	-6.757e+009	-1.157e+007	-6.553e+008	-6.553e+008	-5.957e+009
67						
68						
69	Aspen Technology Inc.		Aspen HYSYS Version 8.6 (32.0.0.8628)		Page 1 of 5	

1	 NORWEGIAN UNIV OF Burlington, MA USA		Case Name: Biorefinery.hsc			
2			Unit Set: SI			
3			Date/Time: Mon Jun 06 13:32:03 2016			
4						
5						
6	<b>Workbook: Case (Main) (continued)</b>					
7						
8						
9	<b>Material Streams (continued)</b>				Fluid Pkg:	All
10						
11	Name	Cooled Slurry	Heated Beer	Beer Column Vent	Beer Stillage	Cooled Stillage
12	Vapour Fraction	0.0000	0.0000	1.0000	0.0000	0.0000
13	Temperature (C)	32.00 *	103.0 *	54.26	125.7	48.23
14	Pressure (kPa)	101.3	607.9	202.6	233.0	233.0
15	Molar Flow (kgmole/h)	2.256e+004	2.357e+004	14.23	2.201e+004	2.185e+004
16	Mass Flow (kg/h)	4.533e+005	4.552e+005	609.3	4.182e+005	4.152e+005
17	Liquid Volume Flow (m3/h)	445.6	455.5	0.7387	414.6	411.7
18	Heat Flow (kJ/h)	-6.619e+009	-6.626e+009	-5.201e+006	-6.158e+009	-6.242e+009
19	Name	Pressurized Beer	Rectifier Bottoms	Pure Ethanol Vapour	Scrubber Feed	Process Water
20	Vapour Fraction	0.0000	0.0000	1.0000	1.0000	0.0000
21	Temperature (C)	32.07	120.6	88.83	32.99	25.00 *
22	Pressure (kPa)	607.9 *	202.6	152.0	101.3	101.3 *
23	Molar Flow (kgmole/h)	2.357e+004	1224	466.0	332.9	7718
24	Mass Flow (kg/h)	4.552e+005	2.207e+004	1.922e+004	1.426e+004	1.390e+005
25	Liquid Volume Flow (m3/h)	455.5	22.12	23.78	17.23	139.3
26	Heat Flow (kJ/h)	-6.756e+009	-3.399e+008	-1.082e+008	-1.279e+008	-2.199e+009
27	Name	Process Water-3	Scrubber Vent	Scrubber Bottoms	Pressurized Scrubber	Adsorber Feed
28	Vapour Fraction	0.0000	1.0000	0.0000	0.0000	1.0000
29	Temperature (C)	33.00 *	33.94	33.94	33.98	116.0 *
30	Pressure (kPa)	506.6 *	101.3 *	101.3 *	435.7 *	152.0
31	Molar Flow (kgmole/h)	791.4	331.1	793.2	793.2	466.0
32	Mass Flow (kg/h)	1.426e+004	1.412e+004	1.439e+004	1.439e+004	1.922e+004
33	Liquid Volume Flow (m3/h)	14.29	17.04	14.47	14.47	23.78
34	Heat Flow (kJ/h)	-2.250e+008	-1.274e+008	-2.255e+008	-2.255e+008	-1.073e+008
35	Name	Dehydrated Ethanol	Ethanol/Water	Ethanol	Heated Ethanol/Water	Cooled Ethanol/Water
36	Vapour Fraction	1.0000	1.0000	0.9511	0.0077	0.0000
37	Temperature (C)	116.0	116.0	88.77	101.0	35.00 *
38	Pressure (kPa)	152.0	152.0	152.0	253.3	152.0
39	Molar Flow (kgmole/h)	313.1	152.9	313.1	152.9	152.9
40	Mass Flow (kg/h)	1.432e+004	4905	1.432e+004	4905	4905
41	Liquid Volume Flow (m3/h)	17.97	5.813	17.97	5.813	5.813
42	Heat Flow (kJ/h)	-7.160e+007	-3.575e+007	-7.283e+007	-4.165e+007	-4.288e+007
43	Name	Pressurized Ethanol/W	Rectification Column	Reactor Feed	Dilute Furfural	Pressurized Xylose
44	Vapour Fraction	0.0000	0.1238	0.0000	0.0000	0.0000
45	Temperature (C)	35.04	452.7	191.8	99.00 *	54.82
46	Pressure (kPa)	253.3 *	209.5	1581	101.3 *	1581 *
47	Molar Flow (kgmole/h)	152.9	1690	1.956e+004	1.164e+004	1.399e+004
48	Mass Flow (kg/h)	4905	4.129e+004	4.118e+005	2.198e+005	2.829e+005
49	Liquid Volume Flow (m3/h)	5.813	45.90	400.2	218.6	277.4
50	Heat Flow (kJ/h)	-4.288e+007	-4.081e+008	-5.621e+009	-3.246e+009	-4.113e+009
51	Name	Heated Xylose	Heated Reactor Feed	Furfural Reactor Botto	Furfural Reactor Top	Wastewater 2
52	Vapour Fraction	0.0000	0.0000	0.0000	1.0000	0.0000
53	Temperature (C)	187.2	201.0 *	202.8	201.6	99.97
54	Pressure (kPa)	1581	1581	1581	1581	101.3
55	Molar Flow (kgmole/h)	1.399e+004	1.956e+004	8279	1.164e+004	1.308e+004
56	Mass Flow (kg/h)	2.829e+005	4.118e+005	1.920e+005	2.198e+005	2.369e+005
57	Liquid Volume Flow (m3/h)	277.4	400.2	182.9	218.6	237.2
58	Heat Flow (kJ/h)	-3.963e+009	-5.605e+009	-2.468e+009	-2.745e+009	-3.657e+009
59	Name	Furfural Distillate	Cooled Furfural React	Condensed Distillate	Compressed Distillate	Combined Water Pha
60	Vapour Fraction	1.0000	0.1130	0.0021	1.0000	0.0000
61	Temperature (C)	99.23	211.7	107.2	129.3	20.00
62	Pressure (kPa)	101.3	2000 *	136.8	136.8 *	101.3
63	Molar Flow (kgmole/h)	7550	1.164e+004	7550	7550	7432
64	Mass Flow (kg/h)	1.595e+005	2.198e+005 *	1.595e+005	1.595e+005	1.483e+005
65	Liquid Volume Flow (m3/h)	156.2	218.6	156.2	156.2	146.5
66	Heat Flow (kJ/h)	-1.789e+009	-3.097e+009	-2.086e+009	-1.780e+009	-2.114e+009
67						
68						
69	Aspen Technology Inc.		Aspen HYSYS Version 8.6 (32.0.0.8628)			Page 2 of 5

1	 NORWEGIAN UNIV OF Burlington, MA USA		Case Name: Biorefinery.hsc			
2			Unit Set: SI			
3			Date/Time: Mon Jun 06 13:32:03 2016			
4						
5						
6	<b>Workbook: Case (Main) (continued)</b>					
7						
8						
9	<b>Material Streams (continued)</b>				Fluid Pkg:	All
10						
11	Name	Furfural Phase	Heated Water Phase	Pressurized Furfural R	Lignin	Wastewater
12	Vapour Fraction	0.0000	0.0036	1.0000	0.0000	0.0000
13	Temperature (C)	20.00	98.82	233.2	48.30	48.30
14	Pressure (kPa)	101.3	101.3 *	2000 *	638.3	638.3
15	Molar Flow (kgmole/h)	207.9	7469	1.164e+004	1438	2.041e+004
16	Mass Flow (kg/h)	1.313e+004	1.490e+005	2.198e+005	4.503e+004	3.702e+005
17	Liquid Volume Flow (m3/h)	11.62	147.2	218.6	41.27	370.4
18	Heat Flow (kJ/h)	-5.048e+007	-2.078e+009	-2.733e+009	-4.496e+008	-5.792e+009
19	Name	Cooled Distillate	Cooled Furfural React	Liquid Ethanol/Water	DAP Seed Train	CSL Seed Train
20	Vapour Fraction	0.0000	0.1128	0.0000	0.0000	0.0000
21	Temperature (C)	30.00 *	211.7	35.00	25.00 *	25.00 *
22	Pressure (kPa)	101.3 *	2000	152.0	101.3 *	101.3 *
23	Molar Flow (kgmole/h)	7550	1.164e+004	152.9	0.2300	9.401
24	Mass Flow (kg/h)	1.595e+005	2.198e+005	4905	30.37	226.7
25	Liquid Volume Flow (m3/h)	156.2	218.6	5.813	1.876e-002	0.2064
26	Heat Flow (kJ/h)	-2.133e+009	-3.096e+009	-4.288e+007	-4.695e+004	-2.535e+006
27	Name	DAP	CSL	Ethanol Vapour	Ammonia	Process Water 2
28	Vapour Fraction	0.0000	0.0000	0.0402	1.0000	0.0000
29	Temperature (C)	25.00 *	25.00 *	497.5	25.00 *	25.00 *
30	Pressure (kPa)	101.3 *	101.3 *	209.5	911.9 *	101.3 *
31	Molar Flow (kgmole/h)	0.9028	37.60	1537	5.797	5047
32	Mass Flow (kg/h)	119.2	906.6	3.638e+004	98.72	9.092e+004
33	Liquid Volume Flow (m3/h)	7.364e-002	0.8257	40.08	0.1602	91.10
34	Heat Flow (kJ/h)	-1.843e+005	-1.014e+007	-3.664e+008	-2.677e+005	-1.438e+009
35	Name	Dilute Ammonia	Flash Vapour	Heated Process Water	Flash Exchange Intern	Cooled Wastewater 3
36	Vapour Fraction	0.0000	1.0000	0.0000	0.3368	0.0000
37	Temperature (C)	25.34	115.3	95.00 *	99.92	35.00 *
38	Pressure (kPa)	506.6	101.3	101.3	101.3	101.3 *
39	Molar Flow (kgmole/h)	5053	1515	7718	1520	2714
40	Mass Flow (kg/h)	9.102e+004	2.759e+004	1.390e+005	2.767e+004	6.291e+004
41	Liquid Volume Flow (m3/h)	91.26	27.62	139.3	27.69	59.92
42	Heat Flow (kJ/h)	-1.438e+009	-3.624e+008	-2.158e+009	-4.044e+008	-8.480e+008
43	Name	Cooled Wastewater 2	Cooled Wastewater	Air	Combined Flue Gas	Ash
44	Vapour Fraction	0.0000	0.0000	1.0000	0.9839	0.0000
45	Temperature (C)	35.00 *	35.00 *	25.00 *	1500	1500
46	Pressure (kPa)	101.3 *	101.3 *	101.3 *	101.3	101.3
47	Molar Flow (kgmole/h)	1.308e+004	2.041e+004	9711	1.189e+004	191.9
48	Mass Flow (kg/h)	2.369e+005	3.702e+005	2.802e+005	3.408e+005	9279
49	Liquid Volume Flow (m3/h)	237.2	370.4	323.9	404.3	7.993
50	Heat Flow (kJ/h)	-3.721e+009	-5.813e+009	-6.617e+004	-5.261e+008	-2.675e+007
51	Name	Pressurized Cooled S	Preheated Biogas	Cooled Flue Gas	Superheated HP Stea	Boiler Flue Gas Outlet
52	Vapour Fraction	0.0000	1.0000	0.9923	1.0000	0.9938
53	Temperature (C)	48.30	175.0	161.6	435.1	275.0 *
54	Pressure (kPa)	638.3 *	101.3	101.3	5066	101.3
55	Molar Flow (kgmole/h)	2.185e+004	1.023e+004	1.191e+004	1.171e+004	1.189e+004
56	Mass Flow (kg/h)	4.152e+005	2.958e+005	3.414e+005	2.110e+005	3.408e+005
57	Liquid Volume Flow (m3/h)	411.7	351.5	404.9	211.4	404.3
58	Heat Flow (kJ/h)	-6.242e+009	-7.648e+007	-1.139e+009	-2.674e+009	-1.092e+009
59	Name	Flue Gas	Methane	Biogas	Carbon Dioxide	Pretreatment MP Stea
60	Vapour Fraction	1.0000	1.0000	1.0000	1.0000	1.0000
61	Temperature (C)	1500	35.00 *	25.63	35.00 *	268.0
62	Pressure (kPa)	101.3	101.3 *	101.3	101.3 *	1317
63	Molar Flow (kgmole/h)	1.170e+004	252.6	1.023e+004	263.5	2135
64	Mass Flow (kg/h)	3.316e+005	4052	2.958e+005	1.160e+004	3.847e+004
65	Liquid Volume Flow (m3/h)	396.3	13.53	351.5	14.05	38.54
66	Heat Flow (kJ/h)	-4.993e+008	-1.883e+007	-1.226e+008	-1.037e+008	-4.993e+008
67						
68						
69	Aspen Technology Inc.		Aspen HYSYS Version 8.6 (32.0.0.8628)			Page 3 of 5



1	 NORWEGIAN UNIV OF Burlington, MA USA		Case Name: Biorefinery.hsc			
2			Unit Set: SI			
3			Date/Time: Mon Jun 06 13:32:03 2016			
4						
5						
6	<b>Workbook: Case (Main) (continued)</b>					
7						
8						
9	<b>Material Streams (continued)</b>				Fluid Pkg: All	
10						
11	Name	Flash Exchange Outle	MP Plant Steam	MP Steam Condensat	Boiler Makeup Water	Heated Boiler Makeup
12	Vapour Fraction	0.1496	1.0000	0.0000	0.0000	0.0000
13	Temperature (C)	99.89	268.0	190.0 *	25.00 *	95.00 *
14	Pressure (kPa)	101.3	1317	1317	101.3 *	101.3
15	Molar Flow (kgmole/h)	1520	6174	6174	2135	2135
16	Mass Flow (kg/h)	2.767e+004	1.112e+005	1.112e+005	3.847e+004	3.847e+004
17	Liquid Volume Flow (m3/h)	27.69	111.5	111.5	38.54	38.54
18	Heat Flow (kJ/h)	-4.158e+008	-1.444e+009	-1.681e+009	-6.083e+008	-5.970e+008
19	Name	Boiler Feed Water	Pressurized Boiler Pro	Pressurized Boiler Fec	Steam Generator Outl	Cellulase Addition
20	Vapour Fraction	0.0000	0.0000	0.0000	1.0000	0.0000
21	Temperature (C)	132.0	95.20	132.7	268.0	25.00 *
22	Pressure (kPa)	1317	1317 *	5066 *	1317 *	253.3 *
23	Molar Flow (kgmole/h)	1.171e+004	2135	1.171e+004	1.171e+004	613.6
24	Mass Flow (kg/h)	2.110e+005	3.847e+004	2.110e+005	2.110e+005	1.120e+004
25	Liquid Volume Flow (m3/h)	211.4	38.54	211.4	211.4	11.10
26	Heat Flow (kJ/h)	-3.241e+009	-5.969e+008	-3.240e+009	-2.739e+009	-1.703e+008
27	Name	Sulfuric Acid	Wastewater 3	Recycle	MP Steam	Pressurized Process V
28	Vapour Fraction	0.0000	0.0000	0.0000	1.0000	0.0000
29	Temperature (C)	25.00 *	202.7	202.7	268.0 *	25.04
30	Pressure (kPa)	1196 *	1581	1581	1317 *	506.6 *
31	Molar Flow (kgmole/h)	32.79	2714	5562	237.6	5047
32	Mass Flow (kg/h)	2631	6.291e+004	1.289e+005	4280 *	9.092e+004
33	Liquid Volume Flow (m3/h)	1.482	59.92	122.8	4.289	91.10
34	Heat Flow (kJ/h)	-2.244e+007	-8.090e+008	-1.658e+009	-5.556e+007	-1.438e+009
35	Name	Furfural	Furfural Azeotrope	Heated Furfural Phase	Cooled Furfural Azeot	Recycle Phase
36	Vapour Fraction	0.0000	0.0000	0.0602	0.0000	0.0000
37	Temperature (C)	156.7	97.87	100.2	30.00 *	20.00
38	Pressure (kPa)	101.3	101.3	101.3	101.3 *	101.3
39	Molar Flow (kgmole/h)	117.5	104.8	222.3	104.7	14.38
40	Mass Flow (kg/h)	1.120e+004	2696	1.390e+004	2692	764.6
41	Liquid Volume Flow (m3/h)	9.718	2.586	12.30	2.582	0.6876
42	Heat Flow (kJ/h)	-2.167e+007	-2.898e+007	-5.136e+007	-2.954e+007	-3.781e+006
43	Name	Water Recycle	Combined Furfural Ph	Water Phase Recycle	Mixed Dilute Furfural	Volatiles
44	Vapour Fraction	0.0000	0.0000	0.0000	0.0164	0.9997
45	Temperature (C)	20.00 *	20.00	20.00 *	99.50	96.12
46	Pressure (kPa)	101.3	101.3	101.3	101.3	101.3
47	Molar Flow (kgmole/h)	90.28	222.3	7342	1.316e+004	2.526
48	Mass Flow (kg/h)	1927	1.390e+004	1.464e+005	2.475e+005	68.83
49	Liquid Volume Flow (m3/h)	1.894	12.30	144.6	246.3	6.958e-002
50	Heat Flow (kJ/h)	-2.584e+007	-5.426e+007	-2.089e+009	-3.662e+009	-5.841e+005
51	Name	Heated Combined Fur	Cooled Furfural	Cooled Ethanol	Secondary Turbine St	Vacuum Steam
52	Vapour Fraction	0.0000	0.0000	0.0000	1.0000	0.8796
53	Temperature (C)	41.14	50.00 *	40.00 *	268.0	46.07
54	Pressure (kPa)	101.3	101.3	152.0	1317	10.13 *
55	Molar Flow (kgmole/h)	222.3	116.4	313.1	3402	3402
56	Mass Flow (kg/h)	1.390e+004	1.109e+004	1.432e+004	6.129e+004	6.129e+004
57	Liquid Volume Flow (m3/h)	12.30	9.623	17.97	61.41	61.41
58	Heat Flow (kJ/h)	-5.366e+007	-2.376e+007	-8.640e+007	-7.955e+008	-8.375e+008
59	Name	Vacuum Condensate	Pressurized Condensa			
60	Vapour Fraction	0.0000	0.0000			
61	Temperature (C)	46.00 *	46.15			
62	Pressure (kPa)	10.13	1317 *			
63	Molar Flow (kgmole/h)	3402	3402			
64	Mass Flow (kg/h)	6.129e+004	6.129e+004			
65	Liquid Volume Flow (m3/h)	61.41	61.41			
66	Heat Flow (kJ/h)	-9.638e+008	-9.637e+008			
67						
68						
69	Aspen Technology Inc.		Aspen HYSYS Version 8.6 (32.0.0.8628)		Page 4 of 5	

1	 NORWEGIAN UNIV OF Burlington, MA USA		Case Name: Biorefinery.hsc			
2			Unit Set: SI			
3			Date/Time: Mon Jun 06 13:32:03 2016			
4						
5						
6	<b>Workbook: Case (Main) (continued)</b>					
7						
8	<b>Energy Streams</b>					
9						Fluid Pkg: All
10						
11	Name	P-100 Duty	P-103 Duty	PS-100 Duty	PS-101 Duty	CL-200 Duty
12	Heat Flow (kJ/h)	3.276e+005	2.144e+005	7.397e+006	7.697e+006	1.281e+006
13	Name	T-200 Duty	T-202 Duty	P-201 Duty	CL-201 Duty	T-201 Duty
14	Heat Flow (kJ/h)	3.188e+007	-2.163e+007	2.559e+004	2.849e+007	-2.403e+006
15	Name	300 Reboiler	300 Condenser	P-202 Duty	301 Condenser	301 Reboiler
16	Heat Flow (kJ/h)	1.852e+008	8.589e+007	3.275e+005	4.935e+007	9.331e+006
17	Name	P-203 Duty	HT-300 Duty	CL-300 Duty	P 302 Duty	P-301 Duty
18	Heat Flow (kJ/h)	6513	8.975e+005	7.135e+006	790.0	1.351e+004
19	Name	P-400 Duty	HT-400 Duty	400 Reboiler	401 Reboiler	401 Condenser
20	Heat Flow (kJ/h)	5.564e+005	1.558e+007	3.633e+008	3.059e+008	1.193e+007
21	Name	COMP-401 Duty	DEC-400 Duty	CL-401 Duty	COMP-400 Duty	CL-402 Duty
22	Heat Flow (kJ/h)	8.465e+006	-6.003e+006	3.059e+008	1.223e+007	6.444e+007
23	Name	CL-500 Duty	P 300 Duty	GEN-500 Duty	CL-501 Duty	P-101 Duty
24	Heat Flow (kJ/h)	2.088e+007	2.423e+005	6.426e+007	2.369e+008	6.735e+004
25	Name	P-500 Duty	P-102 Duty	402 Condenser	402 Reboiler	CL-400 Duty
26	Heat Flow (kJ/h)	1.191e+006	4.932e+004	4.480e+006	5.189e+006	3.633e+008
27	Name	DEC-401 Duty	CL-403 Duty	P-200 Duty	CL-301 Duty	GEN-501 Duty
28	Heat Flow (kJ/h)	-8.837e+004	3.908e+007	1.734e+005	1.357e+007	4.199e+007
29	Name	CL-502 Duty	P-501 Duty			
30	Heat Flow (kJ/h)	1.263e+008	1.095e+005			
31						
32						
33						
34						
35						
36						
37						
38						
39						
40						
41						
42						
43						
44						
45						
46						
47						
48						
49						
50						
51						
52						
53						
54						
55						
56						
57						
58						
59						
60						
61						
62						
63						
64						
65						
66						
67						
68						
69	Aspen Technology Inc.		Aspen HYSYS Version 8.6 (32.0.0.8628)		Page 5 of 5	



## C Equipment Sizing and Cost Estimation

The reboilers of the reactive distillation column (COL-400) and azeotropic distillation column (COL-401) along with the corresponding vapour compressors (COMP-400 and COMP-401) has been sized and cost estimated.

The reboilers are sized by equation C.1 [22]:

$$Q = UA\Delta T_{lm}F_t \quad (\text{C.1})$$

Where  $Q$  is the transferred heat,  $U$  is the overall heat transfer coefficient,  $A$  is the heat transfer area,  $\Delta T_{lm}$  is the logarithmic mean temperature and  $F_t$  is the correction factor. The transferred heat and stream temperatures were collected from HYSYS.  $U$  is assumed 3000 kJ/(h·m<sup>2</sup>·K) and  $F_t$  is assumed 1 [22]. The reboilers are not modeled as heat exchangers, hence there is no readout of the correction factor.

Equipment cost is determined by equation C.2 [22]:

$$C_e = a + bS^n \quad (\text{C.2})$$

Where  $C_e$  is the equipment cost (Jan 2010, U.S.Gulf coast USD),  $a$ ,  $b$ , and  $n$  are equipment specific cost constants and  $S$  is the sizing parameter.

**Table C.1:** Cost parameters for sizing, including sizing parameter range.

Equipment	$S$ Bound	$a$	$b$	$n$
Reboiler	10-500 m <sup>2</sup>	29000	400	0.9
Compressor	75-30,000 kW	580000	20000	0.6

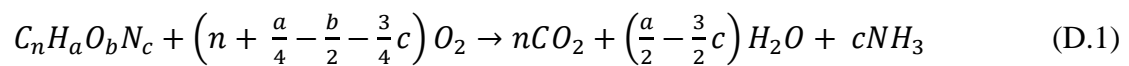
The reboiler has an upper sizing bound of 500 m<sup>2</sup>. The size of the reboiler exceed this, but extrapolation is assumed valid for this purpose. The final purchase cost of equipment is calculated by multiplying with a material factor,  $f_m$ . The compressors are assumed made of carbon steel, with  $f_m$  equal to 1. The COL-400 reboiler is assumed made of titanium while the COL-401 reboiler is assumed made of stainless steel (SS304). The material factor is assumed 1.65 and 1.3 respectively [4, 22].





## D Chemical Oxygen Demand

Chemical Oxygen Demand (COD) of the wastewater stream is required to estimate the production of methane by anaerobic digestion. Equation D.1 shows the oxidation of an arbitrary organic compound.



The mass-specific COD factor is then calculated by equation D.2.

$$COD_m = \left(n + \frac{a}{4} - \frac{b}{2} - \frac{3}{4}c\right) \frac{M_w(O_2)}{M_w(C_nH_aO_bN_c)} \quad (D.2)$$

**Table D.1:** Calculated mass-specific COD for compounds present in the wastewater.

Compound	Chemical Formula	COD <sub>m</sub>
Extractives	C <sub>6</sub> H <sub>12</sub> O <sub>6</sub>	1.0655
Glucose	C <sub>6</sub> H <sub>12</sub> O <sub>6</sub>	1.0655
Xylose	C <sub>5</sub> H <sub>10</sub> O <sub>5</sub>	1.0670
Lactic Acid	C <sub>3</sub> H <sub>6</sub> O <sub>3</sub>	1.0655
Levulinic Acid	C <sub>5</sub> H <sub>8</sub> O <sub>3</sub>	1.5159
Furfural	C <sub>5</sub> H <sub>4</sub> O <sub>2</sub>	1.6649
Acetic Acid	C <sub>2</sub> H <sub>4</sub> O <sub>2</sub>	1.0667
Formic Acid	CH <sub>2</sub> O <sub>2</sub>	0.3478

Some components are present only in trace amounts in the wastewater, and has been neglected from the calculation. The total COD is calculated by multiplying the mass stream of each component with its COD factor, and then summarizing all to get the total COD for the wastewater.